



UNIVERSITY OF
BIRMINGHAM

**DUAL-BAND AND SWITCHED-BAND
HIGHLY EFFICIENT POWER
AMPLIFIERS**

By

Fatemeh Norouzian

A thesis submitted to

University of Birmingham

for the degree of

DOCTOR OF PHILOSOPHY

School of Electronic, Electrical and Computer Engineering

University of Birmingham

October 2014

UNIVERSITY OF
BIRMINGHAM

University of Birmingham Research Archive

e-theses repository

This unpublished thesis/dissertation is copyright of the author and/or third parties. The intellectual property rights of the author or third parties in respect of this work are as defined by The Copyright Designs and Patents Act 1988 or as modified by any successor legislation.

Any use made of information contained in this thesis/dissertation must be in accordance with that legislation and must be properly acknowledged. Further distribution or reproduction in any format is prohibited without the permission of the copyright holder.

Abstract

The Power Amplifier is the most challenging module of a wireless network to design and it is the highest power consumer. Lots of research has been dedicated to design highly efficient and linear power amplifiers in the last decades. The high demand for wireless communication systems creates the requirement for multiband transmitters and receivers. Providing high efficiency for power amplifiers in multiband applications is even more challenging. The work presented in this thesis is focused on designing high efficiency frequency adaptive power amplifiers. Frequency adaptive power amplifiers are categorized in three groups: broadband, multi-band and switched-band power amplifiers.

Two main design methodologies of frequency adaptive power amplifiers are proposed in this thesis. They are dual-band and switched-band power amplifiers. The advantages and limitations of their output performances are evaluated. The main goals in this thesis are achieving high efficiency and required output power over all working bands and maintaining consistent performance over the bandwidth. In the dual-band power amplifiers, the distributed matching network is designed without any switches. For the dual-band power amplifier, output power of 34.2 and 35.8dBm and efficiency of 67% and 81.3% have been obtained in 782 MHz and 1745 MHz, respectively. Switched-band power amplifiers include a number of possible configurations. Both of the switched-band Class-E power amplifiers have switched shunt capacitor values. One uses a dual-band matching network with the efficiency of about 72% in both bands while the other uses a novel switched-band matching network and provide 60% drain efficiency in both working band. The results demonstrate the tradeoffs between achieving consistent high performance in each band and introducing losses and complexity in the switching design.

*I would like to dedicate this thesis to my Parents
and my lovely Auntie (Hengameh)*

Acknowledgment

Last four years of hard work toward Ph.D. degree was enjoyable and wonderful experience to me; thanks God for giving me this opportunity and support me all the way through. Here, I would like to take a moment and express my gratitude to all the people who helped me in this way.

First of all, I would like to thank my brilliant supervisor, Dr. Peter Gardner, for all his valuable support and encouragement. This research would not have been possible without his knowledge, experience and him keeping me on the right track. I would also like to thank him for understanding and encouraging me, when life and research were tough.

All the staff in the Communication Engineering Group at University of Birmingham has helped me in various ways and thanks to them all. I would like to thank my mentor Dr. Edward Tarte for his help and time he spent for me through my whole study experience.

A big thanks to Mr Alan Yates for his support and help in fabricating PCBs, using equipment and assisting with the practical side of my research as well as being a good friend.

I have made several good friends during my PhD and my special thanks go to them for providing pleasant environment and their support inside and outside the University. I would like to thanks Dr. Oluwabunmi Tade, Dr. Yuri Nechayev, Fatemeh Tahavori, Jin Tang, Farzad Hayati, Ghazal Tanhaei, Donya Jasteh, Roozbeh Nabiei, Alhassan Almahroug, Mohammad Milani and Sanaz Roshanmanesh.

Finally, I would like to give a very special thank to the best parents in a world. They always love me and support me in every way possible. Thank you for believing in me and being next to me. I cannot find words to thank my lovely parents. I am grateful to my brothers, Ali, Mehdi, Hossein, for their love, support and advice. I also want to thank my

Auntie, Hengameh, for encouraging me to start a PhD, May her soul rest in peace. A big thank you to my wonderful partner, who always supports me, encourages me and makes me smile. Thank you.

Publications

Published:

- 1) F. Norouzian, P. Gardner, "Concurrent Dual-Band High Efficiency Class-E Power Amplifier", *Microwave Integrated Circuits Conference (EuMIC)*, pp.332-335, 6-8 October 2013.
- 2) F. Norouzian, P. Gardner, "Analytical Solution for Switched-Band Matching Networks", *Passive RF and Microwave Components, 3rd Annual Seminar*, pp.43-52, 26-26 March 2012.

In preparation:

- 1) F. Norouzian, P. Gardner, "The Dual-Band and Switched-Band Class-E Power Amplifier", Journal paper
- 2) F. Norouzian, P. Gardner, "Switched-Band Harmonic Terminated Matching Networks with Derived Analytical Solution", Conference paper
- 3) F. Norouzian, P. Gardner, "Reported Multiband and Switched-Band Power Amplifiers", Review paper

List of Abbreviations

PA - Power Amplifier

MB-PA – Multiband Power Amplifier

SB-PA – Switched-Band Power Amplifier

MN – Matching Network

OMN – Output Matching Network

IMN – Input Matching Network

MB-MN – Multiband Matching Network

SB-MN – Switched-Band Matching Network

OTS MN – Open to Short Matching Network

STS MN – Stub to Short Matching Network

SMPA – Switchable Matching Power Amplifier

FMPA – Fixed Matching Power Amplifier

DOMN – Distributed Output Matching Network

HT – Harmonic Termination

LNA – Low Noise Amplifier

GaAs – Gallium Arsenide

GaN – Gallium Nitride

HEMT – High Electron Mobility Transistor

HFET – Heterojunction Field-Effect Transistor

LTE – Long Term Evolution

RF – Radio Frequency

RFPA – Radio Frequency Power Amplifier

VNA – Vector Network Analyser

DUT – Device Under Test

1G – First Generation

Table of Content

1. Chapter 1 - Introduction	1
1.1 Motivation.....	2
1.2 Radio Frequency Power Amplifier (RFPA).....	3
1.3 Outline of Work and Structure of Thesis.....	5
2. Chapter 2 - Power Amplifier Theory	9
2.1 Specification of Power Amplifier.....	9
2.1.1 Output Power and Gain.....	9
2.1.2 Efficiency.....	10
2.1.3 Linearity.....	11
2.2 Classes of Power Amplifiers.....	13
2.2.1 Class-E Power Amplifier.....	17
2.2.1.1 Class-E Design Equations.....	19
2.3 Active Devices.....	20
2.3.1 MEMS.....	21
2.3.2 Varactors.....	21
2.3.3 PIN Diode.....	22
2.3.4 FET Switches.....	24
2.3.5 Performance Comparison.....	24
2.4 Linearization Techniques.....	25
2.4.1 Feedback.....	26
2.4.2 Feed-Forward.....	27
2.4.3 Pre-Distortion.....	28
2.4.4 Envelope Elimination and Restoration.....	29
2.5 Discussion.....	30

3. Chapter 3 - Multiband and Switched-Band Power Amplifiers-A Literature Review	31
3.1 Adaptive Power Amplifiers.....	33
3.1.1 Multiband Power Amplifiers.....	34
3.1.2 Switched-Band Power Amplifiers.....	41
3.2 Discussion.....	49
4. Chapter 4 - Analysis and Design of Switched-Band Matching Networks for Power Amplifiers	51
4.1 Detach Stub Matching Network.....	52
4.1.1 Analytical solution.....	53
4.1.2 Numerical Example.....	55
4.1.2.1 Ideal Transmission Line.....	56
4.1.2.2 Physical Transmission Line.....	57
4.1.3 Experimental.....	59
4.2 Open to Short Stub (OTS) Matching Network.....	60
4.2.1 Design.....	61
4.2.2 Analytical Solution.....	61
4.2.3 Numerical Example.....	68
4.2.4 Experimental.....	72
4.3 Short to Stub (STS) Matching Network.....	73
4.3.1 Design.....	73
4.3.2 Analytical Solution.....	74
4.3.3 Numerical Example.....	78
4.3.4 Experimental.....	81
4.4 Comparison of Matching Networks.....	81
4.5 Harmonic Termination Network.....	82

4.5.1	Theory of Harmonic Termination Network.....	83
4.5.2	Simulation.....	83
4.5.3	Implementation of Harmonic Termination and Matching Network....	84
4.6	Discussion.....	85
5.	<i>Chapter 5 - Design and Simulation of Dual-Band Class-E Power Amplifiers.....</i>	86
5.1	Single-Band Class-E Power Amplifier.....	86
5.1.1	Theory.....	87
5.1.2	Simulation of Single-Band Power Amplifiers.....	89
5.2	Dual-Band Class-E Power Amplifier with GaAs HFET.....	94
5.2.1	Theory.....	96
5.2.2	Simulation.....	97
5.2.3	Measurement.....	97
5.2.4	Measurement with Different Shunt Capacitor Values.....	100
5.3	Dual-Band Class-E Power Amplifier with GaN HEMT.....	102
5.3.1	Simulation.....	103
5.3.2	Measurement with Different Shunt Capacitor Values.....	105
5.4	Discussion.....	106
6.	<i>Chapter 6 - Design and Simulation of Switched-Band Class-E Power Amplifiers.....</i>	107
6.1	Switchable Matching Power Amplifier.....	108
6.1.1	Theory.....	108
6.1.2	Simulation.....	111
6.1.3	Measurement.....	112
6.2	Fixed Matching Power Amplifier.....	113
6.2.1	Theory.....	115

6.2.2 Simulation.....	115
6.3 Discussion.....	118
7. Chapter 7 - Conclusion.....	119
7.1 Thesis summary.....	120
7.2 Conclusion.....	122
7.3 Future Work.....	123
References.....	124
Appendix A.....	137
Appendix B.....	138
B.1 Vector Network Analyser.....	138
B.2 Spectrum Analyser.....	139
Appendix C.....	140

List of Figures

Figure 1.1 Basic topology of RFPA.....	3
Figure 1.2 Matching Network Topology.....	4
Figure 1.3 Compression characteristics for conjugate and power match [44].....	5
Figure 1.4 Overview of the thesis chapters.....	6
Figure 2.1 Power in PA.....	10
Figure 2.2 Input and output signal of (a) linear PA and (b) Non-linear PA.....	11
Figure 2.3 Error Vector.....	13
Figure 2.4 Class E Amplifier [24].....	17
Figure 2.5 Transistor I-V characteristic and Class-E load line.....	19
Figure 2.6 Varactor diode equivalent circuit.....	22
Figure 2.7 Lumped element model of PIN diode (a) forward bias and (b) reverse bias.....	22
Figure 2.8 Comparison between PAE and output power of switches used in multiband matching network techniques.....	25
Figure 2.9 Linearization Techniques.....	26
Figure 2.10 Feedforward Linearization Technique.....	28
Figure 2.11 Concept of Pre-distortion [40].....	29
Figure 2.12 Envelope Elimination and Restoration.....	30
Figure 3.1 Frequency response of an ideal broadband PA.....	32

Figure 3.2 Balanced amplifier.....	32
Figure 3.3 Distributed Amplifier.....	33
Figure 3.4 Frequency response of an ideal dual-band PA.....	34
Figure 3.5 Gain performance of an ideal SB-PA over frequency.....	41
Figure 3.6 SB-PA (a) switching between numbers of narrow band PAs (b) switched-band matching network (SB-MN).....	42
Figure 3.7 Summary of adaptive PAs.....	50
Figure 4.1 Detached stub matching network.....	53
Figure 4.2 Simulation result of detach stub MN with ideal transmission line.....	56
Figure 4.3 Simulation result of detach stub MN with physical transmission line.....	57
Figure 4.4 Simulation result after adjustments at the first band.....	58
Figure 4.5 Total loss factor of the detach stub MN in OFF (blue) and ON (pink) state with PIN diode (a) Infineon and (b) Skyworks.....	59
Figure 4.6 Simulated and measured S_{11} in (a) OFF and (b) ON state.....	60
Figure 4.7 Simulated and measured input impedance of detach stub MN in (a) OFF state and (b) ON state.....	60
Figure 4.8 Open to Short MN.....	61
Figure 4.9 Coverage region of OTS in case 1(a) capacitive load and (b) inductive load.....	65
Figure 4.10 Coverage region for OTS in case 2.....	66

Figure 4.11 Coverage region for OTS in third case.....	67
Figure 4.12 Physical length of the stub with different characteristics impedance.....	69
Figure 4.13 Simulation result of OTS in case 1 (a) OFF and (b) ON state of the switch.....	69
Figure 4.14 Physical length of the stub for different characteristics impedance of the stub....	70
Figure 4.15 Simulation result of OTS MN in case 2 (a) ON state and (b) OFF state.....	70
Figure 4.16 Physical length of the stub for different characteristics impedance of the stub....	71
Figure 4.17 Simulation result of OTS MN in case 3 (a) ON state and (b) OFF state.....	71
Figure 4.18 Total loss factor of the switch in the OTS MN in OFF state (blue) and ON state (pink).....	72
Figure 4.19 Photograph of OTS MN (switch end of the stub).....	72
Figure 4.20 Simulated and measured input impedance of OTS MN at (a) ON state and (b) OFF state.....	73
Figure 4.21 Stub to Short MN.....	73
Figure 4.22 Coverage region for STS MN in case 1.....	76
Figure 4.23 Coverage region for STS MN in case 2.....	77
Figure 4.24 Coverage region of the STS MN in case 3.....	78
Figure 4.25 Total loss factor analysis of the switch in STS MN in OFF state (blue) and ON state (pink).....	79
Figure 4.26 Simulation result of the STS MN in case 1 (a) OFF and (b) ON state of the	

switch.....	80
Figure 4.27 Simulation result of the STS MN in case 2 (a) OFF and (b) ON state of the switch.....	80
Figure 4.28 Simulation result of the STS MN in case 3 (a) OFF and (b) ON state of the switch.....	80
Figure 4.29 Photographs of the fabricated STS MN in case 1 (switch in the middle of the stub).....	81
Figure 4.30 Simulated and measured input impedance of STS MN (a) OFF state and (b) ON state.....	81
Figure 4.31 Harmonic termination circuit.....	83
Figure 4.32 HT simulation result.....	84
Figure 4.33 Implementation of HT and MN (a) OFF state (b) ON state.....	85
Figure 5.1 Topology of the design.....	87
Figure 5.2 OMN (a) basic OMN for Class-E (b) distributed OMN.....	88
Figure 5.3 Simulation result of implemented OMN and HT circuit (a) first band and (b) second band.....	90
Figure 5.4 Output power and efficiency of the single-band PAs over the whole band of operation (a) first PA and (b)second PA.....	91
Figure 5.5 The Package model.....	93
Figure 5.6 De-embedding package of the transistor with mirrored negative the package	

model.....	93
Figure 5.7 Simulated voltage and current waveform for the first PA at (a) the device plane and (b) package plane.....	94
Figure 5.8 Simulated voltage and current waveform for the second PA at (a) the device plane and (b) package plane.....	94
Figure 5.9 Fabricated prototype of dual-band Class-E PA.....	98
Figure 5.10 Gain versus input power with different gate voltages (lower band) and (b) higher band.....	98
Figure 5.11 Measured efficiency and output power of the dual-band PA with GaAs transistor versus input power (a) first band (b) second band.....	100
Figure 5.12 Efficiency with different shunt capacitor in (a) lower band and (b) higher band. Legend shows the shunt capacitor values.....	101
Figure 5.13 Output Power with different shunt capacitor in (a) lower band and (b) higher band. Legend shows the shunt capacitor values.....	102
Figure 5.14 Output power and efficiency of the dual-band PA with GaN transistor over frequency in (a) lower and (b) higher band.....	104
Figure 5.15 Voltage and current waveforms in (a) lower and (b) higher band.....	104
Figure 5.16 Efficiency with different shunt capacitor in (a) lower band and (b) higher band. Legend shows the shunt capacitor values.....	105
Figure 6.1 Different method of switching capacitors (a) switching between stubs (b)	

series capacitors (b) parallel capacitors.....	110
Figure 6.2 Proposed method for shunt capacitance (a) with a stub (b) with a capacitor.....	111
Figure 6.3 SMPA schematic.....	111
Figure 6.4 Voltage and current waveform of SMPA in (a) the lower and (b) the higher band.....	112
Figure 6.5 Fabricated prototype of switched-band Class-E PA.....	113
Figure 6.6 Output power and efficiency of simulation and measurement of SMPA in (a) the lower and (b) the higher band.....	114
Figure 6.7 FMPA schematic.....	115
Figure 6.8 Voltage and current waveforms of FMPA in (a) ON and (b) OFF state.....	116
Figure 6.9 Output power and efficiency of FMPA over frequency in (a) OFF state and (b) ON state.....	117

List of Tables

Table 2.1 Possible losses in PA with the possible solutions.....	11
Table 2.2 Classes of amplifiers.....	14
Table 3.1 Multiband Power Amplifiers.....	37
Table 3.2 Switched-band Power Amplifiers.....	45
Table 4.1 Selected frequencies and their required impedances for all the cases.....	78
Table 4.2 Calculated length and width of the transmission line and stubs for STS MN in all the cases.....	79
Table 4.3 OTS and STS MN comparison.....	82
Table 5.1 Calculated lumped component values.....	90
Table 5.2 Output performances of the single-band Class-E PAs.....	91
Table 5.3 Substrate properties.....	99
Table 5.4 Dual-band PA with GaAs transistor performance.....	99
Table 5.5 Dual-band Class-E PA with GaN transistor performances.....	103
Table 6.1 SMPA output performances.....	113
Table 6.2 Dual-band OMN and switched shunt capacitance Class-E PA (FMPA) performances.....	116
Table 6.3 Switched-band Class-E PAs.....	118
Table 7.1 Simulation performance comparison between all designed Class-E PAs.....	122

Chapter 1

Introduction

Wireless communication systems transfer data between two points without physical connection (cable). Smoke signals, torch signalling and mirror flashing are examples of very early wireless communication system. Today, wireless communication has been playing an important role in people's daily life; cellular system, Bluetooth and satellite are a few examples of the wireless systems that have been used daily by humans. The population of internet users is increasing everyday as the Internet can be accessed in coffee shops, airports and almost anywhere. The current communication system is congested. Therefore, the communication world requires reliable, cost effective communication system everywhere and always available. To meet this requirement, efficient use of radio spectrum is essential by using unused spectrum [1]. In order to make people lives easier, the wireless communication systems need to be more cost effective, faster and provide longer battery life. To meet these demands, adaptable, multiband, highly efficient and linear transmitters are required.

Mobile communication system usage grows faster than other wireless communication systems. The mobile communication system started in 1978 with first generation (1G) cellular phone. 1G was mainly transmitting voice data. Whereas, mobile communication systems are multifunctional now; they are able to provide lots of services to their users such as: text, video message, video call and connecting to the internet everywhere [2]. Mobile handsets improve everyday to offer more features to their users, improve battery life, reduce their size and weight while maintaining the same price.

In this chapter, the motivation of this research will be discussed and followed by a brief introduction of the most challenging and power consuming component of the transmitter (power amplifier). The last section presents the outline of the work and structure of the thesis.

1.1 Motivation

The significant increase in demand for wireless communication systems and the proliferation of communication standards has created interest in more efficient ways of sharing the spectrum in the last few years. A system using the multiple radio channels and applying intelligent decision making to optimise their deployment is called a *Cognitive Radio System*. This system is an intelligent wireless communication system and uses intelligent processing to produce flexible and reconfigurable radio network adapted to the environment and user's requirements [1] and [3]. This action requires three steps as follows [3]:

- Perception: use sensors to collect data from external and internal factors
- Conception: manage information from the sensors to adapt a system
- Execution: it is an optimization and adaptation mechanism.

By incoming Radio Frequency (RF) stimuli, some changes are applied to the parameters such as: transmitter-power, carrier frequency and modulation strategy. Cognitive radio system tries to work in frequency ranges without causing and suffering interference with other communication systems. This task is done by scanning and detecting the unoccupied spectra and shifts the user to those bands of frequencies. Enabling hardware to satisfy cognitive radio system requirement is a subject undergoing intense study. The Power Amplifier (PA) is the most difficult component of the transmitter to design for cognitive radio

systems. Tackling this challenge motivates the author to develop PA design method to meet this requirement with high efficiency and a particular level of output power. One possible topology for meeting this requirement is a wideband PA, but this involves a performance compromise. The other possibilities are multiband or switched-band PAs. All of these topologies will be discussed more in Chapter 3.

1.2 Radio Frequency Power Amplifier (RFPA)

A Power Amplifier (PA) is used in the last stage of the transmit path. The radio frequency PA (RFPA) converts input DC power to the sufficient level of RF energy to transmit through an antenna. The basic topology of the RFPA is shown in Fig 1.1. It consists of an active device (transistor). DC power feeds the transistor via the drain and passes through a large inductor. The RF input signal connects to the gate of the transistor via a matching network (MN) to provide matching at the fundamental frequency. This MN is called the input matching network, shown by IMN in Fig. 1.1. The signal is transferred from the drain of the transistor to the output port via the output matching network (shown by OMN in Fig.1.1) which OMN provides matching at fundamental and harmonic frequencies.

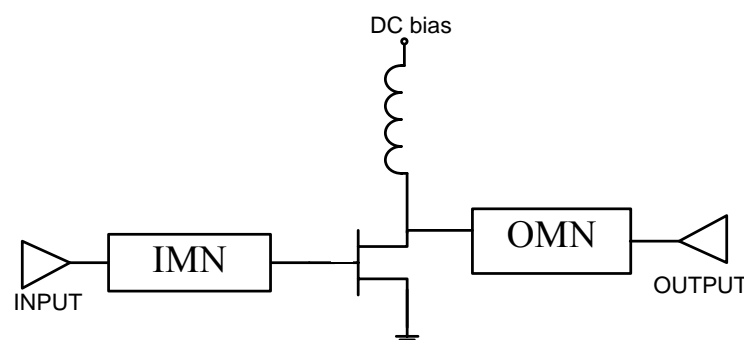


Figure 1.1-Basic topology of RFPA

The basic idea of MNs is illustrated in Fig. 1.2, which shows a MN placed between load impedance and a transmission line to maximize the power transferred to the load. The MN

can be designed by transmission line or lumped elements. Conjugate matching theory sets the value of the load impedances equal to the real part of the generator's impedance and opposite sign of the imaginary part. The transistor conducts less current than it can handle in this technique, because it is based on small signal impedance concept and takes no account of the optimum load line. Therefore, the transistor does not operate in its fully power capacity. The transistors are the most expensive component of the PAs and it is not cost effective to waste their power capacity. Using load-line matching in designing PA OMNs allows the designer to use most of the devices' power capacity and maximize the power. Fig. 1.3 is a graph of the theoretical power characteristic of a PA which has been designed with conjugate matching (solid line) and power matching (dashed line). Points 'A' and 'A'' refer to the maximum linear power of a PA with conjugate match and power match, respectively. Beyond these points, the dotted lines show the extrapolated linear characteristic which the solid and dashed lines show the actual nonlinear characteristic. 1dB compression power is also shown by 'B' for conjugate match and 'B'' for power match. At these points, the actual powers are 1 dB below those given by the extrapolated linear characteristics. As it is shown in Fig.1.3, conjugate match provides higher small signal gain and power match is able to provide more output power [4].



Figure 1.2-Matching Network Topology

As mentioned earlier, the PA in a mobile handset is the most power consuming component [5] and [6]; therefore, designing high efficiency PAs has to date been a critical research area. Higher PA efficiency results in decreasing the heat (cooler operation) and also increasing lifetime and reliability of the device. Switched-mode PAs such as Class-F, Class-E and their

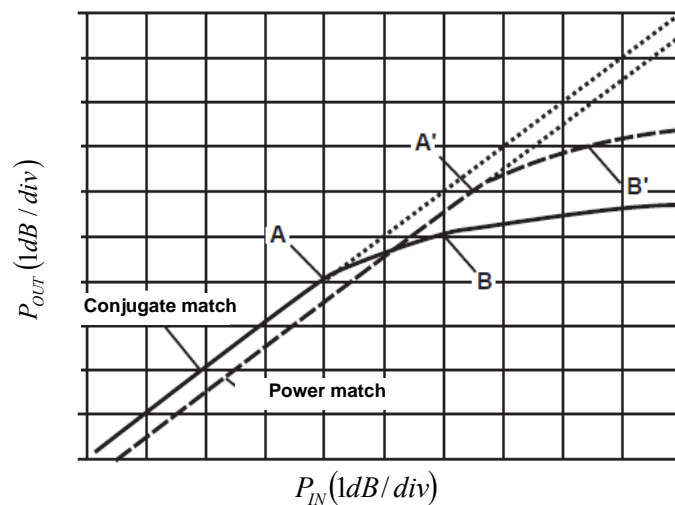


Figure 1.3-Compression characteristics for conjugate and power match [4]

many variants, theoretically can provide high efficiency performances. Achieving high efficiency in multiband applications is even more complex and difficult. Providing the same performance and high efficiency in all working bands is a challenging task, because their performances are frequency dependent due to requiring optimum output termination and harmonic elimination in all bands at the same time. Due to this difficulty and high demand of multiband high efficiency PAs, the research covered in this thesis explores the design of PAs to operate with high efficiency in all frequency bands of multiband applications.

1.3 Outline of Work and Structure of Thesis

This research is mainly concentrated on developing a methodology to design highly efficient multiband PA which can meet the requirement of cognitive radio systems. As mentioned earlier, switched-mode PAs are good candidates to provide high efficiency performances and in this work, Class-E PA is chosen due to its design simplicity, requirement of slower devices compared to other switched-mode PAs and less sensitivity to parameter variations [7]-[8]. The objectives of this work are:

- Proposing a new methodology of designing a switched-band MN to reduce the loss and nonlinearity of switches along with an analytical solution for them, to prove the validity and observe the coverage region of the MNs and shorten the design time.
- A methodology of designing high efficiency single-band Class-E PA with distributed MN has been discovered.
- A dual-band Class-E PA based on the proposed single-band PAs has been designed and delivers high efficiency performances.
- One of the proposed switched-band MN has been used to design a switched-band Class-E PA.
- The effect of shunt capacitance across the transistor in a Class-E PA topology on engineering the waveform and accordingly on the efficiency, has been studied.

The research and objective of this work is explained in the next six chapters. The content of each chapter is discussed briefly here. An overview of all the chapters is shown in Fig. 1.4.

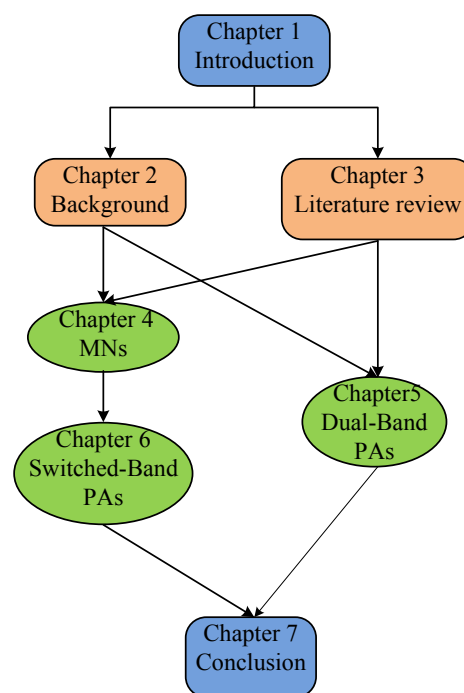


Figure 1.4-Overview of the thesis chapters

Chapter 2 presents all of the basic criteria to design a PA, such as: some important specifications (output power, gain, efficiency and linearity), classes of PAs and linearization techniques. Also, different available switches are presented in this chapter to find the appropriate switch for the application of this work.

Chapter 3 is a literature review on frequency adaptive PAs. This chapter starts with studying all the possible approaches to design frequency adaptive PA: multiband and switched-band PAs. All the reported multiband and switched-band PAs, to the author's knowledge, are included and discussed in this chapter. The performance and circuit diagram of all the reported multiband and switched-band PAs are summarized in two tables.

Design, techniques and equations for the proposed switched-band MNs are discussed in **Chapter 4**. Three techniques to design switched-band MNs are presented in this work. These MNs provide the required impedances for two different frequencies by means of a detachable stub and switching between open and short circuit stubs. Through this technique, the MNs are capable of providing a match for more than two frequency bands. Analytical solution for all the MNs have been derived to investigate range of frequencies and impedances achievable, give more precise results and shorten the design stage. These MNs can be applied for many applications (e.g. PAs, LNAs, Antennas etc). The MNs are compared in terms of their accuracy and size. To apply the selected MN to design a PA, a dual-band harmonic tuned MN is presented. The network is composed of a fundamental matching circuit and a second harmonic termination circuit. The example demonstrates accurate matching capability at the fundamental and open circuit at the second harmonic frequencies. The MNs are designed, fabricated and tested.

The proposed technique of designing a high efficiency single-band and dual-band Class-E PA is described in **Chapter 5**. Initially, the technique is applied to design single-band PAs to prove the validity of technique and also have it as a reference design to compare the

performance of the technique in dual-band application. After that, design of two dual-band Class-E PAs is presented with two different transistors; Gallium Arsenide Heterojunction Field Effective Transistor (GaAs HFET) and Gallium Nitride High Electron Mobility Transistor (GaN HEMT). These PAs are designed without switches to minimize the number of components and reduce the losses introduced by switches. High efficiency is observed from these PAs but higher efficiency is obtained in one band and relatively lower in the other band. The effect of the shunt capacitor across the transistor on efficiency is studied and the reason for the difference in efficiency of both bands has been investigated.

To overcome the efficiency difference of the dual-band Class-E PA (in Chapter 5) and to maintain the same performance in terms of output power and efficiency at both bands of operation, a switched-band Class-E PA has been proposed in **Chapter 6**. Switches have been applied in the OMN of the switched-band PA to switch between two optimum termination impedances and switching shunt capacitor value across the transistor at two different frequencies. This PA is called Switchable Matching PA (SMPA). Later, another switched-band Class-E PA has been designed with dual-band OMN and switched shunt capacitor and called Fixed Matching PA (FMPA). The FMPA reduces the number of switches in the OMN compared to the SMPA. This chapter is finished by a discussion on performance of dual-band and switched-band PAs.

The last chapter, **Chapter 7**, is a summary and conclusion of this research. Achievements of this study are also discussed and this thesis is finished by proposing future works.

Chapter 2

Power Amplifier Theory

This chapter will present all of the basic criteria to design a power amplifier. The Power Amplifier (PA) converts DC input power to deliver RF output power at a great magnitude (as high as required to pass through wireless medium). Descriptions of some important definitions such as: Output power, Efficiency, Gain and Linearity, are discussed in the first section. Then, different classes of operation for PAs are explained briefly. Devices and linearization techniques that they are essential to design Radio Frequency Power Amplifier (RFPA) are also covered.

2.1 Specification of Power Amplifier

Some important figures of merit are used to describe the performance of a PA quantitatively. These values are useful when comparing how well different techniques of PA will perform.

2.1.1 Output Power and Gain

The power delivered to the load at the band of interest (fundamental frequency) is defined as Output Power (P_{OUT}). Gain is defined as “the ratio of the output power and the input power” and is normally expressed as dB, (2.1).

$$G = 10 \log \left(\frac{P_{OUT}}{P_{IN}} \right) \quad (2.1)$$

2.1.2 Efficiency

The next and probably the most important one is efficiency and this can be divided into two groups: Drain efficiency (η) and Power Added Efficiency (PAE). The DC power (P_{DC}) and RF input power (P_{IN}) are the inputs of a PA, Fig. 2.1. Some of the inputs will appear in the harmonic frequencies and some will dissipate inside the PA.

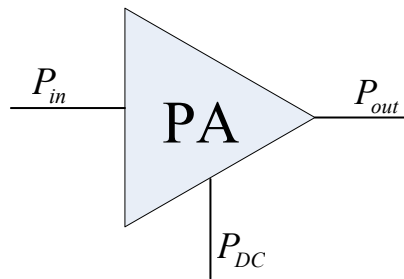


Figure 2.1-Power in PA

Drain efficiency is used to calculate how efficiently the DC power has been converted to the RF output power:

$$\eta = \frac{P_{OUT}}{P_{DC}} \quad (2.2)$$

PAE is very useful to show the PA's performance, as it includes the gain of the PA as well. The PAE is defined as:

$$PAE = \frac{P_{OUT} - P_{IN}}{P_{DC}} \quad (2.3)$$

High efficiency PAs are preferred to increase battery life, reduce the power dissipation, lower the cost and minimize the size [9]. All the possible losses of a PA are recognized as shown in Table 2.1 with the possible solutions to minimize these losses and accordingly maximize the efficiency of the PA [10]:

Table 2.1-Possible losses in PA with the possible solutions

Losses	Solutions
Dissipation power in the transistor	Avoid overlapping between voltage and current (switched mode PA)
Some of the output power appears at harmonic frequencies	Terminate the harmonics reactively
Losses in the components	Utilize distributed MNs

2.1.3 Linearity

Linearity is another important specification for the PAs as it describes how well the output signal can be reproduced in the receiver. This merit is vital for non-constant amplitude modulation. There is no harmonic generation in the linear PA and input and output signal have a linear relation together, Fig.2.2 (a). In the linear PA, the active device can be modelled by S-parameters. In contrast with the linear PA and as it shown in Fig. 2.2 (b), the output is not in a linear relation with the input signal and also some harmonics are generated. Basically, some distortion occurs in the output of the non-linear PA. Gain compression is another effect of the non-linearity. In linear region, increasing the input will increase the output with the constant gain. Gain is decreased in the non-linear region and more input power will cause less gain and more non-linearity performance from the PA. In this type of PA, where the active device is close to the compression point, the S-parameters are no longer valid and the non-linear model of the active device should be used.

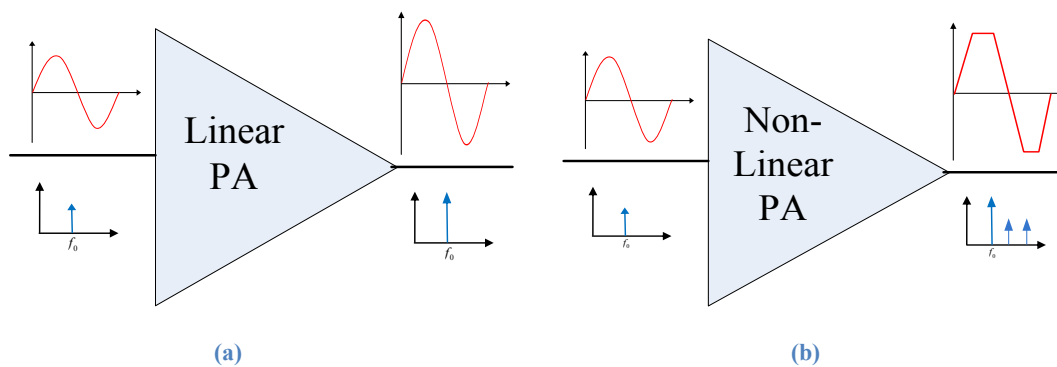


Figure 2.2-Input and output signal of (a) linear PA and (b) Non-linear PA

Different techniques are available to measure the linearity of the PA [11]:

- *C/I* (Carrier to Inter-modulation): is a traditional technique. Two or more carriers with the same amplitudes are used to drive the PA. By comparing the third order and intermodulation distortion (IMD) product to the carriers, the *C/I* can be found which is desired to be about 30dB [11].
- *NPR* (Noise Power Ratio): In this technique, a PA is driven with Gaussian noise with a notch in its spectrum. The notch power (which appears because of the non-linearity of PA) over the total power is NPR. It is mostly used for broadband Pas [11].
- *ACPR* (Adjacent Channel Power Ratio): this measures the effect of non-linearity into an adjacent channel. The ratio of the out-of-band power (the power leaked to the adjacent channel) to the in-band power is ACPR.

$$ACPR_{|dBc|} = 10 \cdot \log \left(\frac{\int_{\omega_{adj}} PSD(\omega) \cdot d\omega}{\int_{\omega_{ch}} PSD(\omega) \cdot d\omega} \right) \quad (2.4)$$

Where, $PSD(\omega)$ is the power spectral density of the signal in bandwidth of adjacent channel (ω_{adj}) and bandwidth of the main channel (ω_{ch}), [11] and [12].

- *EVM* (Error Vector Magnitude): is showing the effect of non-linearity on the detection process and focusing on distortion in the main channel. The deviation of the actual signal vector from the desired signal vector calculates with EVM, Fig. 2.3. EVM can be calculated in the limited number of symbols (K):

$$EVM_{(RMS)} = \sqrt{\frac{\sum_{k \in K} |S_k - R_k|^2}{\sum_{k \in K} |R_k|^2}} \quad (2.5)$$

Where, S_k and R_k are the actual vector and the desired vector, respectively [11] and [12].

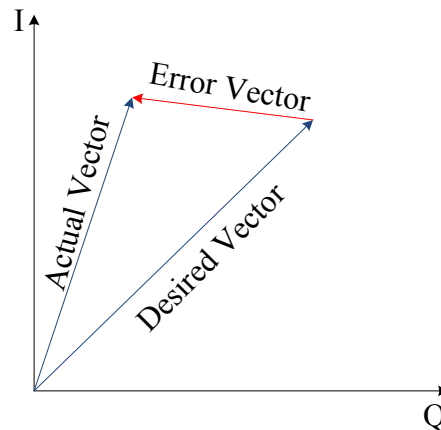


Figure 2.3-Error Vector

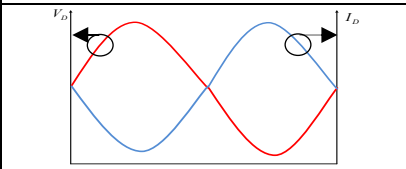
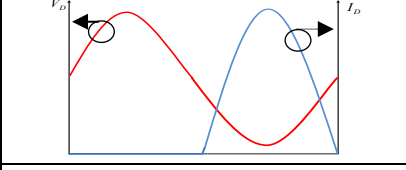
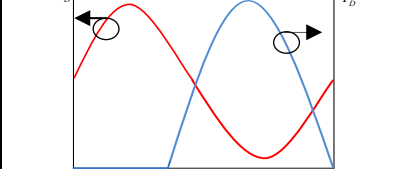
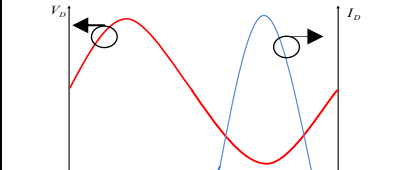
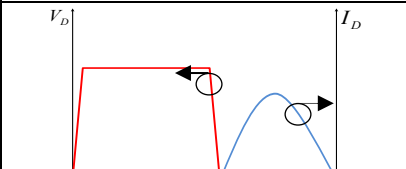
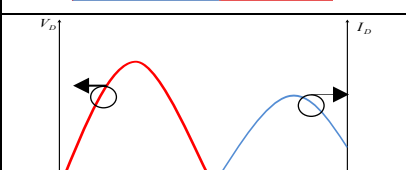
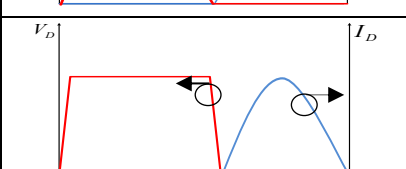
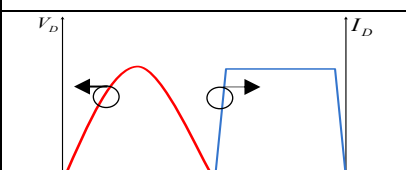
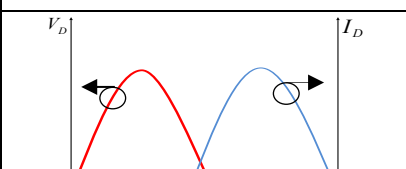
2.2 Classes of Power Amplifiers

There are different classes of PA and they are classified based on their bias point and Matching Network (MN) topology [11]. Different classes of amplifiers and their specification are summarized in Table 2.2 and each of the classes is explained briefly in this section.

Classes of PAs can be categorized in two groups: the transistor is the voltage controlled current source (linear) or acts as a switch (nonlinear). In switch-mode PA, the transistor is considered as two ideal conditions such as, ON state (short circuit) and OFF state (open circuit). Improving efficiency will cause some nonlinearity in the PA and we can say there is a trade of between linearity and efficiency. Depending on specific requirements a highly efficient or a highly linear PA is used. Linear PAs are used in base stations and efficiency of PA is a crucial factor in hand held units [13].

Class A: is the classic PA and the transistor is biased in linear region and always ON with continuous current conduction. This class offers high linearity and gain in broadband application at the cost of low power and efficiency. The output voltage and current waveform has the same shape (for example sinusoidal) as the input signals (sinusoidal) without harmonic content, [13] and [14]. The output power and efficiency for Class-A are:

Table 2.2-Classes of amplifiers

Reference	Classes	Ideal efficiency	Linearity	Conduction angle	Waveform
[14]	A	50%	Yes	360°	
[14]	B	78%	Yes	180°	
[14]	AB	70%	Yes	180° to 360°	
[14]	C	80%	No	<180°	
[13]	D	100%	No	Switched	
[12]	E	100%	No	Switched	
[12]	F	100%	No	Switched	
[7]	F^{-1}	100%	No	Switched	
[15]	J	70%	Partially	180° to 360°	

$$P_{out} = I_{DD}^2 \cdot R_L = \frac{I_{max}^2 \cdot R_L}{4} \quad (2.6)$$

$$\eta = \frac{P_{out}}{P_{in}} = \frac{I_{max}^2 \cdot R_L}{4 \cdot I_{DD} V_{DD}} = \frac{V_{DD} - V_{Knee}}{2V_{DD}} \quad (2.7)$$

As I_{DD} is $\frac{I_{max}}{2}$; in the perfect scenario, V_{Knee} is zero and the efficiency is $\frac{1}{2} = 50\%$. The

low efficiency of Class-A encouraged PA designers to reduce conduction angle below 360° , such as Class-AB, B and C. Conduction angle means the angle that the active device is ON and conducting current [14].

Class-B: is similar to Class-A with slightly difference in biasing (biased close to cut-off). The conduction angle of this class is 180° as the active device is ON for half of the cycle (positive side of the input signal). The amplitude of the output signal is proportional to the input signal and the drain current shape is unchanged, this class is classified as the linear PA [14]. By reducing the conduction angle from 360° to 180° , the overlap between current and voltage waveforms is decreased and efficiency is increased compared to Class-A [11]. This class is mostly applied in push-pull PA [11]. The DC current can be found by Fourier coefficient (2.8), and the efficiency (2.9):

$$i_D = \frac{1}{T} \int_0^{\frac{T}{2}} \frac{2V_{DD}}{R_L} \sin(\omega t) dt = \frac{2V_{DD}}{\pi R_L} \quad (2.8)$$

$$\eta = \frac{P_{out}}{P_{in}} = \frac{\pi R_L V_{DD}^2}{4 R_L V_{DD}^2} = \frac{\pi}{4} = 78.5\% \quad (2.9)$$

Class C: is biased at or below the cut-off and its conduction angle is less than 180° . This class presents sinusoidal voltage waveform and narrow current pulses [10]. By reducing the conduction angle towards zero, the efficiency is increasing towards 100% at the cost of decreasing output power to zero. The best compromise is reported in [11], which provide efficiency of 85% with 150° of conduction angle.

Class D: The transistor acts as a switch and has two extreme values; zero and V_{DD} . Two transistors are applied in a Class-D PA to provide a square waveform for the drain voltage. This class is a non-linear PA as the output and input have no linear relation. The Output Matching Network (OMN) in this class provides open circuit for harmonics. Theoretically, efficiency of 100% is expected from Class-D PA. Practically, this class has lower efficiency due to losses. Switching speed and drain capacitance are the main sources of losses. Due to the finite switching speed, the transistor conducts current while it is in its active region and causes losses in this class of PA. Also, the other main source of losses is charging and discharging the drain capacitance which dissipates power proportional to $\frac{V_{DD}^2}{2}$. This drawback has been covered in Class-E PA [11] and [13].

Class F: Class-F and Class-E are the most popular switched-mode PAs. Square voltage waveform and half sinusoidal current waveform are expected from a Class-F PA. The odd harmonic resonator in the OMN shapes the drain voltage to be a square waveform, as the drain voltage is sum of fundamental and odd harmonic voltages. The half sinusoidal current is achieved by biasing the active device at pinch off [12]. The output filter in Class-F configuration is more complex than other PA circuits [11]. Open circuit termination in odd harmonic and short circuit termination in even harmonic frequencies are required [14].

Class F⁻¹: is basically similar to Class-F PA with different harmonic termination criteria. Odd and even harmonic frequencies are required to be terminated with short and open circuit impedances. The obtained waveform of this class as shown in Table 2.2 is required to have half-wave rectified voltage and square current [7].

Class J: is capable of providing linear performance with high efficiency like Class-B. The starting point to design a Class-J PA is Class-B. Half sinusoidal current and voltage waveforms are observed in this class. Presenting the second harmonic component in voltage provides half-wave rectified sinusoidal voltage. The impedance requirements at the output port of the transistors are, [4] and [15]:

$$Z_{f_0} = R_L + jR_L \quad (2.10)$$

$$Z_{2f_0} = 0 - j\frac{3\pi}{8}R_L \quad (2.11)$$

$$Z_{3f_0} = 0 \quad (2.12)$$

Impedance at the fundamental frequency, second and third harmonic frequencies represent by Z_{f_0} , Z_{2f_0} and Z_{3f_0} ; also, the load substitute with R_L .

The focus of this thesis is on Class-E PA. Class-E is explained more in detail in the next section.

2.2.1 Class-E PA

It is a switched amplifier and the active device works as a switch. It was invented in 1970s by Nathan and Alan Sokal (father and son) [19]. The basic topology of the Class-E PA is shown in Fig. 2.4.

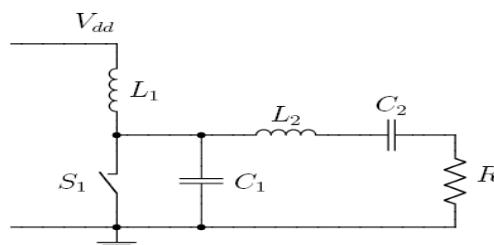


Figure 2.4-Class E Amplifier [20]

L_2 and C_2 are the resonators and R is a load. Supply choke (L_1) has high inductance to provide open circuit for RF signals [21]. The shunt capacitor is shown by C_1 in Fig. 2.4 which contains the internal capacitance of the transistor and the external capacitor. In the OFF state of the transistor, current flows through the shunt capacitor and in the ON duration current flows through the transistor; where the transistor is in saturation mode [20]. This topology aims to avoid conducting current and existing voltage at the same time and reduces overlap between them. Therefore, the power dissipation in ideal switches is zero as it is multiplication of voltage and current and provides a high efficiency nearly to 100% [18] and [22]. In practice, limiting factors of the efficiency are drain to source saturation resistance and loss of parasitic element [23]. Most of the dissipated power is in the transistor because while transistor is ON, it has some low impedance and the voltage is not completely zero. In this duration, internal capacitances store energy and produce some current while transistor is OFF [20] and [22]. Moreover, in practice, even with the proper switch device, the switching time may be a fraction of the ac cycle and lose some power. In designing a Class-E amplifier we should be concerned about minimizing the switching time and it could be done by designing a proper non-resistive load network [20].

As explained earlier, Class-E PA is a transition between pinch-off and saturation region and ideal Class-E load line (red line) is shown in Fig. 2.5. The OFF state of the transistor is represented with the horizontal line (current is zero) and the ON state is the vertical line (voltage is zero) [18].

The OMN plays a crucial role in designing a highly efficient Class-E PA. The OMN includes a set of specific valued components at the design frequency to avoid any overlap between voltage and current waveforms; which in ideal case results in 100% efficiency. In practice some of the delivered power will appear in second and third harmonic frequencies.

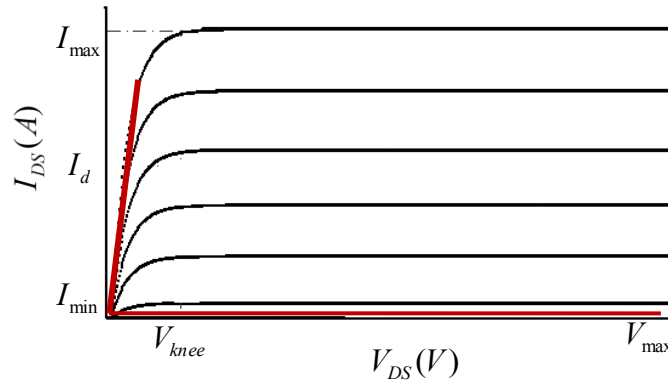


Figure 2.5- Transistor I-V characteristic and Class-E load line

To maximize the efficiency, all harmonics should be open circuit. The transistor should be biased at pinch off and driven into compression, so the transistor will be ON for the forward cycle of sinusoidal input RF waveform and for all of the reverse cycle the transistor is switched OFF.

2.2.1.1 Class-E Design Equations

The first stage of designing a Class-E PA is to calculate optimum parameters of OMN. Equations (2.15) to (2.18), taken from [16], are applied to provide values of components (i.e. load resistance (R), shunt capacitance (C_1), series capacitance and inductance, (C_2) and (L_2) respectively). These equations are derived from a time domain equation, according to the required voltage and current assumption across the transistor, in ON and OFF state, respectively, (2.13) and (2.14).

$$V_D(t)|_{t=T} = 0 \quad (2.13)$$

$$\frac{dV_D(t)}{dt}|_{t=T} = 0 \quad (2.14)$$

V_D is the voltage across the transistor and T is the period of the input signal. These components are calculated based on specific supply voltage V_D and required output power P_{out} . Loaded quality factor (Q_L) is a free choice variable and chosen by designers based on a trade-off between operating bandwidth and rejection of harmonics. With the duty ratio set at

the usual choice, 50%, the minimum value of Q_L is 1.7879. The most desirable range to provide acceptable efficiency and linearity is between 5 and 10.

$$R = 0.5768 \left(\frac{V_D^2}{P_{out}} \right) \left(1 - \frac{0.451759}{Q_L} - \frac{0.402444}{Q_L^2} \right) \quad (2.15)$$

$$C_1 = \frac{1}{5.44668\omega R} \left(1 + \frac{0.91424}{Q_L} - \frac{1.03175}{Q_L^2} \right) + \frac{0.6}{\omega^2 L_D} \quad (2.16)$$

$$C_2 = \frac{1}{\omega R} \left(\frac{1}{Q_L - 0.104823} \right) \left(1 + \frac{1.101468}{Q_L - 1.7879} \right) - \frac{0.2}{\omega^2 L_D} \quad (2.17)$$

$$L_2 = \frac{Q_L R}{\omega} \quad (2.18)$$

2.3 Active Devices

In some applications, switches are required in the circuit. Different types of switches are discussed here. Switching devices are used in circuits for opening and closing a connection or for changing the branches. Ideally, a switch should present zero resistance in the ON state and infinite resistance in the OFF state; whereas a certain amount of resistance on connection state and a finite resistance on disconnection state will be presented by a switch in practical cases. Isolation and insertion loss are the fundamental parameters to describe a switch's performance. Measurement of the power not transferred to the load when the switch is OFF is named isolation (2.19), and insertion loss is a transmission loss through the switch in ON state (I_L) [24]. Low insertion loss and high isolation switches are desired.

$$Isolation = (P_{OUT})_{ON} - (P_{OUT})_{OFF} \quad (2.19)$$

The brief descriptions of some switching devices are provided in the next sections. Some factors are important to select a suitable switch such as switching speed, power handling capacity, and cost. These factors are discussed later on and accompanied with a graph to compare performance of switches in the published multiband PAs.

2.3.1 MEMS

Micro Electro Mechanical Switches (MEMS) provide open or short circuit by mechanical movement. The mechanical movement is forced by electrostatic, magnetostatic, piezoelectric or thermal design. There is almost no power loss in MEMS switches because they hardly consume any current. MEMS switches are very linear devices. These switches are fabricated with air gap and provide high isolation and low insertion loss of about -0.1 dB. On the other hand, MEMS switches have some drawbacks such as low switch speed, limited power handling (20-50mW) and requiring high voltage to drive. These switches are not reliable and their efficient life time is 0.1-10 billion cycles only [25] and [26].

2.3.2 Varactors

Varactor diodes are P-N junction voltage controlled devices [24]. By changing the bias voltage which is applied to the varactor diode the value of capacitance and resistance will vary [27]. The varactor diodes work in reverse bias, so no current is required (i.e. no power loss) [28]. Varactor diodes can be modelled with lumped elements as shown in Fig. 2.6. This model consists of variable junction capacitance ($C_j(V)$) and variable series resistance ($R_s(V)$), and C_p is fixed parasitic capacitance. The package parasitic effect has been modelled by aid of L_p [27].

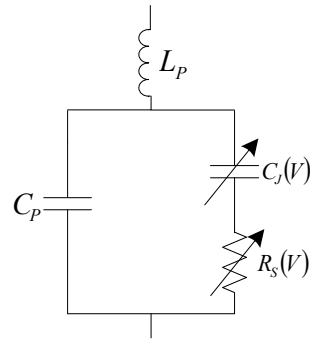


Figure 2.6-Varactor diode equivalent circuit

2.3.3 PIN Diode

A PIN diode is a semiconductor current controlled device [24]. The high resistivity intrinsic I-region which is sandwiched between P- and N-type regions is a general structure of a PIN diode [24] and [29]. Holes and electrons are injected into the I-region in forward bias of PIN diode and the PIN diode appears as a resistor. In the reverse bias, the I-region has no stored energy and PIN diode acts as a parallel plate. The equivalent circuit model of PIN diode in OFF and ON state is illustrated in Fig. 2.7.

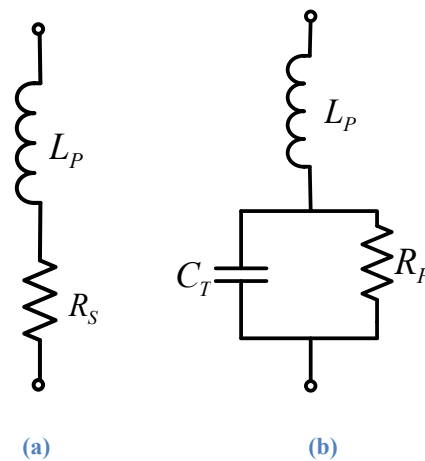


Figure 2.7-lumped element model of PIN diode (a) forward bias and (b) reverse bias

The equivalent circuit of a PIN diode in forward bias (Fig. 2.7 (a)) consists of a series resistor (R_s) and a small inductor (L_p). This inductor represents the package properties of the PIN diode. The resistance of a PIN diode in forward bias can be found by, [24] and [30]:

$$R_S = \frac{W^2}{(\mu_N + \mu_P) \cdot \tau \cdot I_F} \quad (2.20)$$

I-region width is W and forward bias current is I_F . Electron and hole mobility are denoted by μ_N and μ_P , respectively. The electrons and holes in I-region stay alive for an average time that is referred to carrier life time (τ) [30]. The maximum and minimum forward resistance (R_S) can be calculated by (2.20) at maximum forward current of 100mA and minimum forward bias current of 10 μ A. Conduction higher current in a PIN diode will decrease the resistance as it acts as a variable resistor. The equivalent circuit in reverse bias is composed of the diode capacitance (C_T), loss element (R_P) and parasitic inductance (L_P), Fig. 2.7 (b). The value of the capacitance is:

$$C_T = \frac{\epsilon A}{W} \quad (2.21)$$

Where, ϵ is dielectric constant and A is area of junction [29]. A PIN diode can be connected in series or shunt in the circuits. Series connection provides low insertion loss whereas when high isolation is required a shunt connection is applied that is capable of handling more power, and it is easier to cool the device [14] and [30]. The junction temperature of a PIN diode increases while it is controlling the power signal and therefore, dissipates some power [24]. The maximum allowable power dissipation is:

$$P_d = I_{RF}^2 R_S + I_{DC} V_{DC} \quad (2.22)$$

Similar to all diodes, PIN diodes have two terminals; therefore separate DC biasing is required from RF path with an external decoupling element. As mentioned above, a PIN diode is a current control device and therefore consumes high amounts of power. Small physical size, high switching speed, low package parasitic reactance, ability to control large RF-signal-power, low cost and low loss are the advantages of PIN diodes [24] and [31].

Because of wide I-region of PIN diode, it can handle large RF voltages which other diodes are unable to handle.

2.3.4 FET Switches

Field Effect Transistor (FET) switches are a good candidate due to relatively high ratio between their ON and OFF state resistance. To control switching in FET devices, the voltage on their gate needs to be adjusted. Basic switch performances of PIN diode and FET switches are fairly similar as both have ON state resistance and OFF state capacitance. The difference is in the amount of DC power consumption. FET switches require very simple bias network (high resistor). PIN diodes require a bias current in the ON state and consequently have more complicated bias networks. FET switches can provide broadband operation. By increasing the frequency, the isolation of the FET is degraded due to the drain-to-gate capacitance and also has high loss [14] and [31].

2.3.5 Performance Comparison

The published switched-band PAs (which they are discussed in Chapter 3) utilise different switches such as: MEMS, PIN, FET and varactor diode. One way to analyse the performances of these switches in the switched-band PAs application, is to use the published data of the performance of these switches. PAE and output power of the switched-band PAs that use a switch, have been considered and plotted in a graph as shown in Fig. 2.8. As illustrated in the graph, highest PAE with desired output power is provided by PIN diode.

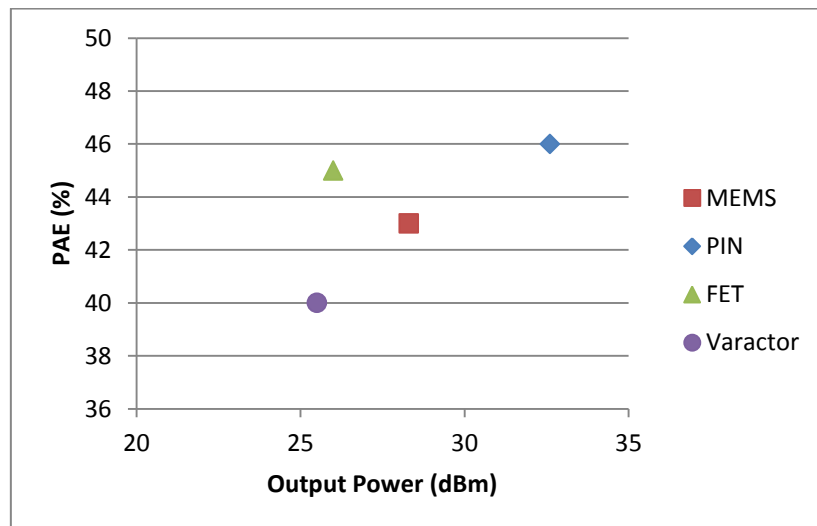


Figure 2.8-Comparison between PAE and output power of switches used in multiband matching network techniques

2.4 Linearization Techniques

Any signals which are non-constant envelope require linear amplification. As mentioned earlier, there is trade-off between efficiency and linearity; by achieving one we can lose the other. Switched-mode PAs are capable to provide high efficiency but nonlinear performance. By considering power series for PAs as:

$$V_{out} = aV_{in} + bV_{in}^2 + cV_{in}^3 + \dots \quad (2.23)$$

With higher input power, output voltage has a more nonlinear relation with the input power. The switched mode PA requires high input power. The nonlinearity causes some problem such as, splatter into next channels and errors in detection and reproduction. By applying one of the linearization techniques and providing linear output signal, both requirements (high efficiency and linearity) can be fulfilled. Linearization techniques are not applied just to improve linearity; they are also used to develop efficiency by decreasing the need of back off [11]. Basically, in linearization techniques, amplitude and phase of the input are used as a template and will be compared to those of the output, allowing the required correction to be determined and applied [13].

Closed and open loop are two linearization methods. Open loop is not as accurate as closed loop technique, but it can handle much wider bandwidth [13]. There are three linearization techniques; feedback, feed-forward and pre-distortion. Feedback is a closed loop linearization technique, whereas feed-forward and pre-distortion are open loop. Fig. 2.9 summarizes the linearization techniques from [11], [13]-[14], [32] and [33] with their specifications and more explanation of these techniques is in the following section.

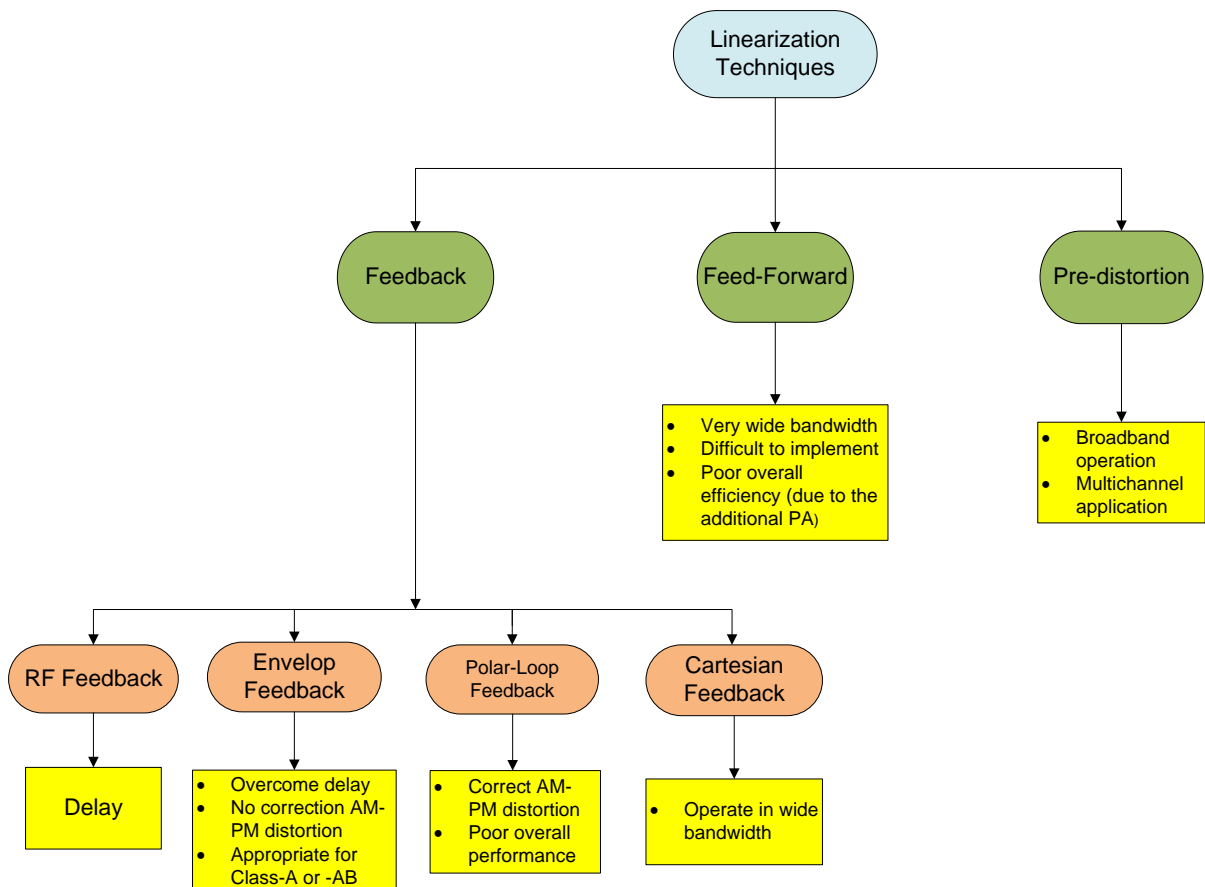


Figure 2.9-Linearization Techniques

2.4.1 Feedback

There are four different techniques for feedback linearization: RF feedback, Envelope feedback, Polar-Loop feedback and Cartesian feedback.

- **RF Feedback**

A small amount of RF output signal is entering back to the input of the PA and finds the difference with its input. This technique suffers from delay (which cause instability) and loss of gain at RF frequencies [11].

- **Envelope Feedback**

By using the signal envelope as a feedback parameter, the problem of delay can be resolve in the envelope feedback. The drawback of this linearization technique is its inability to correct phase distortion (AM-PM distortion). Variation in phase of the output signal by the change in amplitude of the input signal is known as AM-PM distortion [34].

- **Polar-Loop Feedback**

Polar-Loop feedback overcomes the shortage in the envelope feedback technique by adding a phase-locked loop. The amplitude and phase feedback path are separate and require different bandwidths, therefore reduce the overall performance [11].

- **Cartesian Feedback**

The Cartesian feedback applied modulation feedback in Cartesian component (I and Q). Two identical feedback processes is applied to I and Q channels independently. In Cartesian feedback, closed loop baseband feedback in I and Q channel is used to ensure that the vector modulated output from the PA has I and Q components matching those at the input. The drawback of this technique is narrow bandwidth performance [11] and [33].

2.4.2 Feed-Forward

As shown in Fig. 2.10 feed-forward consists of two amplifiers; main and error amplifier. The input signal split into two branches; one goes directly to the main PA. The output of the main PA is combined with the original delayed signal of other branch. The distortion

component of the main PA is obtained and the error amplifier (which is a linear, low power amplifier) amplifies this signal. The outputs of both amplifiers are combined and result in the cancelling the distortion components from the main signal [11]. This technique is mainly applied for high power PAs, such as cellular base station [14].

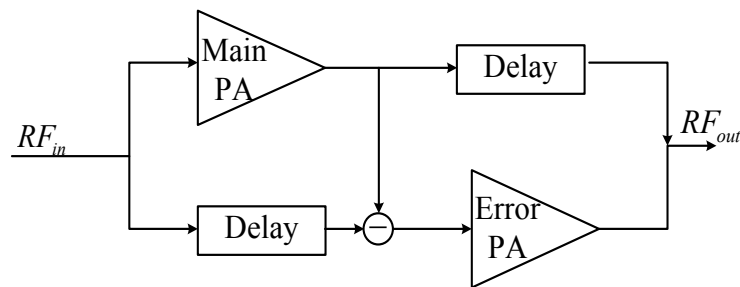


Figure 2.10-Feedforward Linearization Technique

2.4.3 Pre-Distortion

This technique was common in analogue implementation [35] and then, thanks to Digital Signal Processing (DSP) is popular in digital implementation as well [32]. In the pre-distortion technique, the amplitude and phase of the signal are modified (using the inverse characteristics of the PA) before the amplifier in such a way that by combining them a linear output is generated. Concept of pre-distortion is shown in Fig. 2.11. When nonlinearity characteristic of PAs change during their lifetime (with temperature or with changes in environment) the fixed pre-distorter is unable to adopt its characteristic. Adaptive Pre-distortion overcomes this drawback and is providing better performance and wider bandwidth. The other type of pre-distortion is digital pre-distortion which can be used in broadband and narrowband [11].

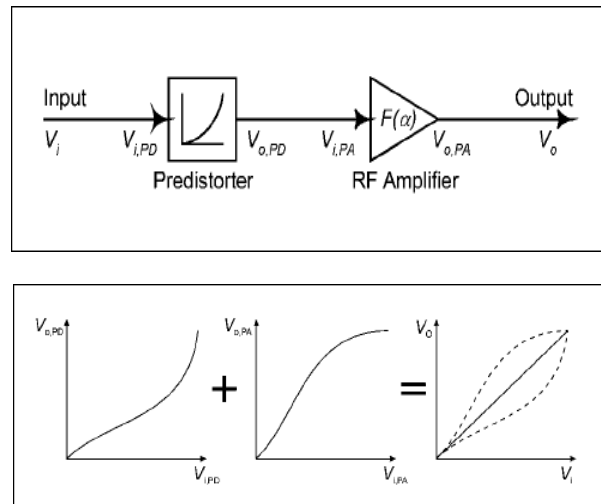


Figure 2.5-Concept of Pre-distortion [36]

2.4.4 Envelope Elimination and Restoration

The basic idea of this technique is to provide a highly efficient linear RFPA by aid of highly efficient and nonlinear RFPA and highly efficient envelope driver [11]. EER has two paths as shown in Fig 2.12. One path just modulates the phase of the signal. The limiter eliminates the amplitude modulation and provides the constant envelope signal for the PA. This PA can operate in Class-C, D, E and F [11]. The other path provides the amplitude modulation. The PA restores the envelope by varying the drain voltage to correct the output amplitude. The amplitude and phase modulated signal add together and make the original signal [37]. The phase information need to be delayed to enable both modulated signal arrive at the same time. The switching speed is hundreds of MHz due to requirement of high oversampling for switched-mode PAs and this is a challenge in wideband applications. The other down side of EER is consumption of high power by the modulator which reduces the efficiency [38].

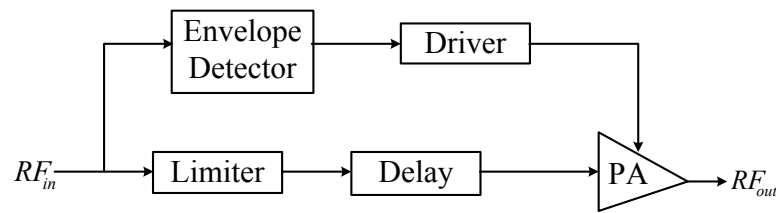


Figure 2.6-Envelope Elimination and Restoration

2.5 Discussion

This chapter presents all the required background knowledge for this research. At the beginning, important metrics to evaluate performance of the PA such as, output power, gain, efficiency and linearity, have been covered. Furthermore, different classes of PAs are explained, starting with the linear Class-A and continuing to the switched-mode PAs. High efficiency PAs (switched-mode PAs) are of interest to meet the requirement of modern communication systems. To provide higher output power Class-F is preferred and Class-E is more capable to achieve higher efficiency [10] and [17]. The advantage of Class-E PA is having a small number of reactive components as well as high efficiency performance. Another feature of the Class-E PA which makes it more preferable is that the internal capacitance of the transistor can be absorbed as a component of OMN [18] and [39].

In the switched-band application, switches play an important role. A brief overview of different switches presented. The switches introduce nonlinearity in the circuit. Also, the switched-mode PAs (which are of interest in this research) are inherently nonlinear. Linearization techniques are important for this research to provide linear output. Finally, the linearization techniques which are vital for wireless communication to enhance the linearity and efficiency of the PA were explained.

Chapter 3

Multiband and Switched-Band Power Amplifiers-A Literature Review

Increasing demand for wireless communication systems requires high efficiency, multiband, adaptable and high linearity transmitters. A cognitive radio system is trying to work in different frequency ranges in such way that it does not cause interference with other communication systems, and does not get affected by interference from the other systems. Designing adaptive front-end components has attracted lots of attention during the past couple of years. The adaptive Power Amplifier (PA) is the most critical component to design. As required for cognitive radio system the PA should be able to adapt its characteristics such as frequency and power according to the environment. Designing highly efficient, adaptive PAs is a critical research area.

One approach to design a PA to suit the requirement of the cognitive radio is the broadband PA. A broadband PA covers the whole required bandwidth with the constant gain. Fig. 3.1 shows the gain performance of an ideal broadband PA over the frequency. Class-A can be a candidate to operate in the broadband applications. Higher efficient classes are problematic to design broadband due to their requirement for harmonic terminations. Some attempts to design broadband switch-mode PA has been done; one of them reported in [23] (a broadband Class-E PA) to operate in multiband applications. Distributed second harmonic termination has been designed with three half wavelength short circuit stubs in three different frequencies in this PA.

One possible way to design broadband PAs is using wideband Input Matching Network (IMN) and Output Matching Network (OMN) which is challenging and complex. Such PAs are low in cost and small in size but at the cost of design complexity, less gain and lower efficiency.

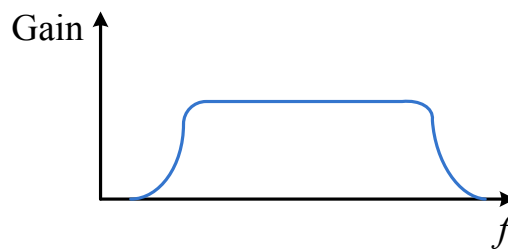


Figure 3.1-Frequency response of an ideal broadband PA

Balanced and distributed PAs are two examples of broadband PA. Balanced amplifier as it is shown in Fig 3.2 consists of two identical amplifiers and two hybrid couplers. The input signal divides into two parts with equal amplitude and 90° phase difference. Each of these signals goes to one of the amplifiers. Outputs of amplifiers are recombined in the second hybrid coupler. The hybrid coupler in input and output provide phase shift for any reflection from amplifiers to compensate them at the terminating terminals; therefore, both amplifiers are well matched in the balanced amplifiers. This amplifier is complex, as it requires two couplers, two amplifiers and two DC supplies [40] and [41].

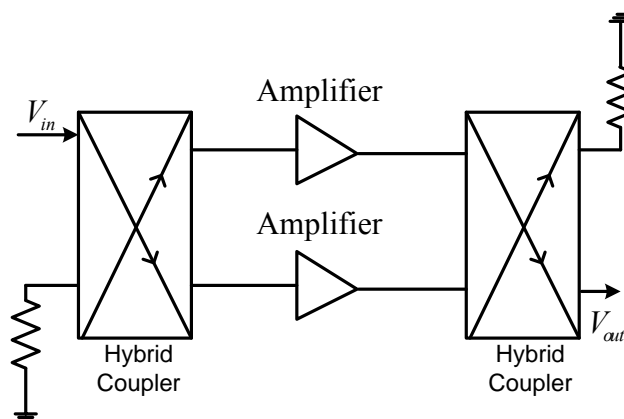


Figure 3.2-Balanced amplifier

A distributed amplifier contains several cascaded transistors, Fig 3.3. The gates of the transistors are connected along a transmission line with the specific characteristic impedance and length; and also the drains of the transistors are connected via another transmission line. The main advantage of this amplifier is its operation in a very broad bandwidth. The circuit of this amplifier is large and unable to perform with high gain and efficiency [40] and [42].

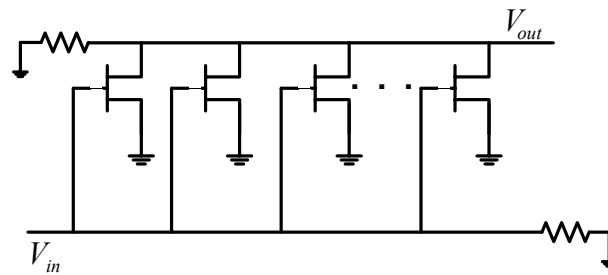


Figure 3.3-Distributed Amplifier

As mentioned in Chapter 1, design of highly efficient frequency adaptive PA is the main aim of this thesis. Therefore, the broadband PA is not a good candidate. Other possible approaches to a design frequency adaptive PA is: multiband PA (MB-PA) and switched-band PA (SB-PA). This chapter explains these two techniques and presents an overview of the researches have been done on designing MB-PA and SB-PA.

3.1 Adaptive Power Amplifiers

In this thesis, adaptive PA refers to the PAs that can adapt their frequency response to the environment requirement. Techniques of designing an adaptive PA can be divided into two main groups; known as: MB-PA and SB-PA. MB-PAs do not use switches in their circuit and can provide concurrent amplification in different frequencies. A switch is a key component in SB-PA and it works in one band at a time. These two kind of adaptive PAs are going to explain in the following section along with some examples.

3.1.1 Multiband Power Amplifiers

The MB-PA is capable of working in different frequencies simultaneously. Gain over frequency of an ideal MB-PA (dual-band in this example) is expected to be the same as it shown in Fig 3.4. Table 3.1 summarises the techniques of reported MB-PA in chronological order as well as their achieved results; below a short description of each method listed in the Table 3.1 is provided.

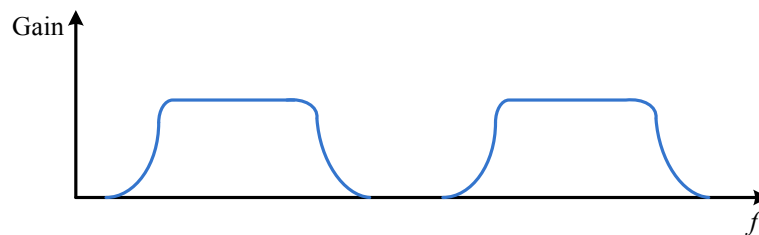


Figure 3.4-Frequency response of an ideal dual-band PA

One technique of designing MB amplification is implementing multiple parallel amplifiers for each operating band; such as a dual-band PA reported in [43] which was designed with two parallel amplifiers. This PA is big in size and requires a large amount of components as it required one PA for each frequency band. There is another technique with multiband input matching network (MB-IMN) and multiband output multiband matching networks (MB-OMN). This technique is smaller and has fewer components. The IMN and OMN are designed without switches or tuneable elements and provide the required impedances and optimise PA performance at individual working bands. MB-MN can be designed with transmission line or lumped element. Distributed MB-MNs are more popular than lumped element MB-MNs as the performance of the distributed element differs in different frequency bands. First, MB-PAs with distributed MB-MN will be reviewed.

The dual-band PA in [44] has been designed with transmission lines and utilises quarter wavelength stub at an adequate distance from the device for the proper impedance

termination. Low-pass Chebyshev-form impedance transformer is one way to design MB-MN and it has been used in a reported MB-PA in [45]. Composite right/left-handed transmission line (CRLH TLs) is another possible way of designing MB-MN which has been used in [46], [47] and [48]. Harmonic terminations were neglected in [46], whereas, this important factor is taken into account in [47]. The dual-band PA in [47] consists of two CRLH diplexers in input and output with two amplifiers between them and as well as matching at the fundamental frequency and terminating the harmonics.

A multi-section transformer has been used in the OMN in [49], [50] and [51]. Each section of the transformer has been designed to match at a specific frequency; tank circuit [51] or branched stub [49] is used in each section to prevent any mismatch at other frequencies. A three section microstrip transmission lines used in the IMN and OMN of dual-band PA [52]. The first section was replaced with an open stub in the OMN with the purpose of terminating harmonics. The result shown in the table for this PA is the simulation result. The OMN in [53] has three sections:

- Real-to-Complex impedance transformer: to transform complex impedances at the two operating frequencies to real impedances
- Transmission line: to tune the harmonics
- Real-to Real Impedance transformer: to transform the obtained real impedances to the system impedance. A distributed dual-band filter was designed for this purpose with dual-band resonator and J-inverter.

T-type and Pi-type transformers are equivalent to quarter-wave transformer and have different impedances for different frequencies. The author in [54] called them dual-band/dual-impedance and they transform 50Ω to the real part of the required impedances at two different frequencies. A dual-band/dual-susceptance stub is applied to provide the

imaginary part of the required impedance. However, this technique is not feasible for all the frequencies and impedances as in some cases the width of the transmission line is not practical.

Different operation modes in each working band are reported in [55] and [56]. The OMN of [55] consists of two blocks; harmonic control and fundamental MN. The harmonic control network designed with transmission line and length of them has been chosen in the way to provide short circuit at $2f_1$ and open circuit at $3f_1$ (Class-F) and open circuit at $2f_2$ and short circuit at $3f_2$ (Class- F^{-1}). A distributed OMN provides Class-AB condition at the lower band and Class-J at the higher band in [56].

Distributed IMN and OMN have been designed based on load-pull/source-pull simulations in [57]; the OMN consists of two sub-networks: harmonic termination and fundamental matching. Two stubs provide short circuit at second harmonic of the fundamental frequencies in its harmonic termination network. This PA has been used in [58] to design Doherty PA later in June 2012. Doherty PA (DPA) contains two PAs: carrier PA and peaking PA which they operate in Class-AB and Class-C mode, respectively. The main advantage of DPA is to maintain high efficiency over wider range of input power [68]. Each component of a conventional Doherty PA is replaced by a dual-band version in [59]. A dual-band branch-line hybrid (using Pi-type transformers) replaces the input splitter. Dual-band carrier PA (Class-AB) and peaking PA (Class-C) have been designed with dual-band MNs and followed by dual-band phase offset lines.

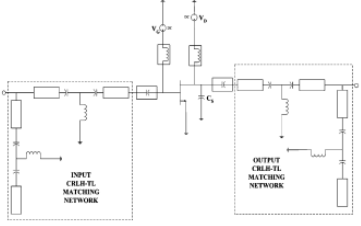
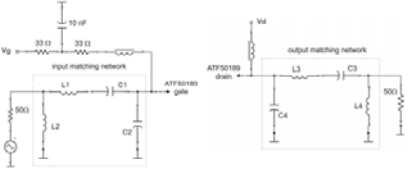
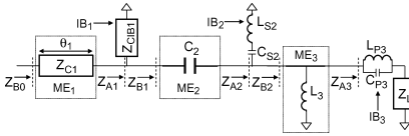
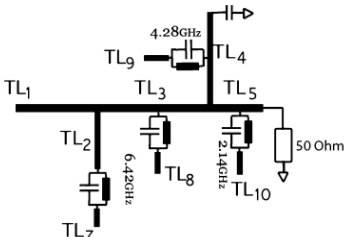
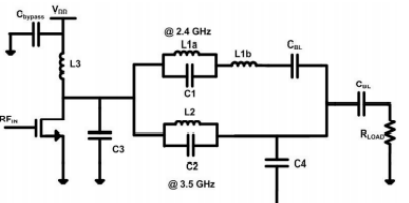
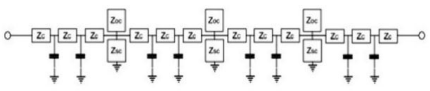
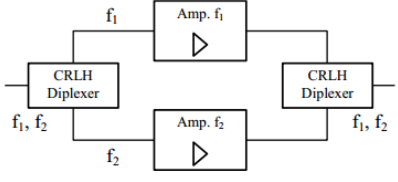
There are some reported MB-PAs with lumped element MB-MNs; one of them is shown in [60]. The lumped element MB-IMN and MB-OMN have been designed based on the load-pull/source-pull simulation to operate in both working bands. A passive MN is applied in the PA of [61] as well, to provide high reactive impedance and terminate the harmonics.

Another common technique is parallel resonators which have been applied in [62], [63], [64] and [65] to provide dual-band performance. At each frequency, one path is blocking the signal (at its resonant frequency) and the other path behaves as an inductor or capacitor. In the paper [63], the lumped element MN is converted to microstrip transmission line; whereas, the parallel LC resonator is constructed by the bias line in [64] and it is applied in IMN and OMN. In [65], transmission line OMN has been design; the length and characteristic impedance of the transmission line have been adjusted to provide proper impedances at the harmonic and fundamental frequencies, respectively. The role of the resonators in this design is to increase the electrical length of the transmission line at the lower band.

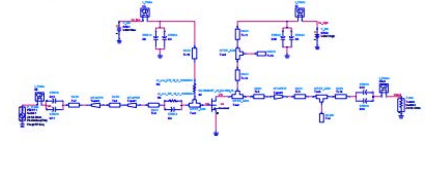
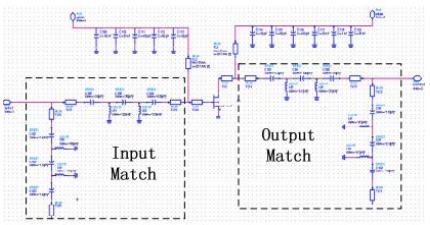
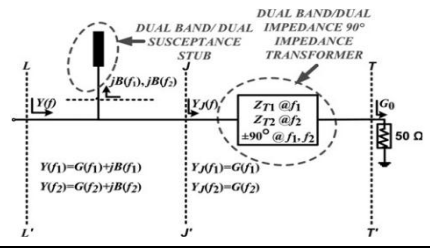
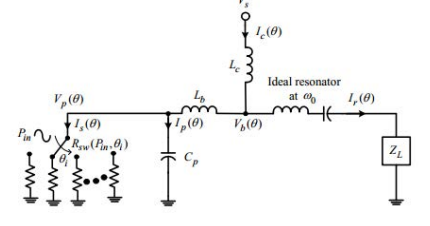
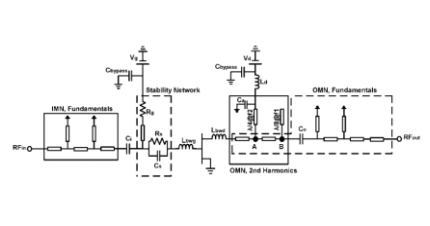
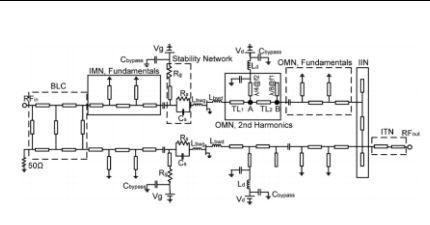
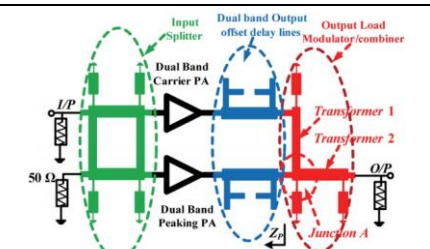
Two Class-E dual-band PAs are reported in [66] and [67]. A multi-level switching resistance model is incorporated in [67] and two cascaded L-shaped OMN are used to provide dual-band operation. Sub-optimum Class-E operation is assumed in [66] with element values evaluated for a compromise between two bands.

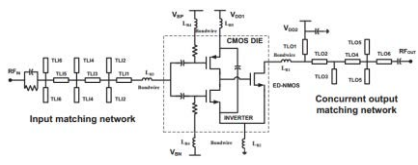
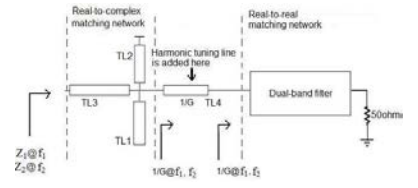
Table 3.1-Multiband Power Amplifiers

References	Class of operation	Band of frequency	Gain	Output power	PAE	Circuit
[43]	AB	824-849 1850-1910 MHz	30 dB	28 dBm	36%	
[45]		800 and 1500 MHz		30.9-28.2 dBm	51%	

[46]	E	800 and 1700 MHz		22.2dBm	42.5%	
[60]	AB	1.9 and 3.5 GHz	11-6 dB	24-17 dBm	20%	
[61]	AB	2.45 and 3.3 GHz		33-32.5 dBm		
[65]	F	1.7 and 2.14 GHz	5 dB	32.8-34.4 dBm	31.1-50%	
[62]	AB	2.4 and 3.5 GHz		18 dBm	42%	
[63]	AB	2.5 and 3.5 GHz	10.8-10.5 dB		68-54.5%	
[47]	CE	0.38 and 0.96 GHz			64.5-61.2%	

[49]	AB	0.9, 1.8 and 2.1 GHz	12 dB	30 dBm	55-56-63%	
[44]	E	1.8 and 2.6 GHz		37.8-36.9 dBm	78.4-61.3%	
[64]	B	1.7 and 2.14 GHz	9.8-10.5 dB	36.7-39.7 dBm	58.4-59.9%	
[55]	F/F^{-1}	0.8 and 1.25 GHz	12 dB	40.6-41.8 dBm	81.7-80%	
[50]	AB	0.8 and 3.3 GHz	13-9 dB	30.1-30.5 dBm	62-53%	
[51]	AB	1.47, 1.94 and 2.65 GHz	9.6-10-12.9 dB	30.5-31.5-30.5 dBm	60-54-57%	
[56]	AB/J	1.5 and 3.8 GHz	18-12 dB	37.3-35.7 dBm	47-52%	

[52]		0.915 and 2.14 GHz	16 dB	46 dBm	60%	
[48]		0.98 and 1.9 GHz	17.6-14 dB	45.6-48 dBm	64.8-61.4%	
[54]	AB	1.96 and 3.5 GHz	13-10 dB	53-50 dBm	57-49.5%	
[67]	E	1.95 and 2.6 GHz	8.3-8.8 dB	29-28 dBm	65.8-63.6%	
[57]	AB	1.8 and 2.4 GHz	12 dB	42.3 dBm	64%	
[58]	Doherty	1.8 and 2.4 GHz	13-11 dB	43 dBm	60-54%	
[59]	Doherty	1.96 and 3.5 GHz	7 dB	31 dBm	15.8-17.7%	

[66]	E	1.2 and 3 GHz	13-8.5 dB	30-28 dBm	50-30%	
[53]	J	0.8 and 1.9 GHz		46 dBm	70%	

3.1.2 Switched-Band Power Amplifiers

The SB-PAs utilize switches or tuneable elements to provide multi-band amplification. The gain performance of an ideal SB-PA is desired to be the same as it shown in Fig 3.5 (in this example, the PA works in two bands). Different SB-PA has been reported during last decade and they are summarized in Table 3.2 according to their year of publications. Their architectural technique is discussed briefly here.

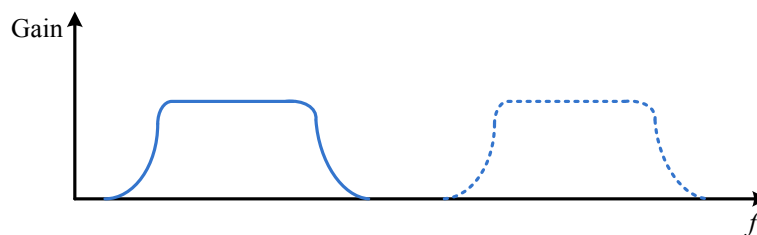


Figure 3.5-Gain performance of an ideal SB-PA over frequency

The SB-PA can be designed in two ways:

- Switching between numbers of narrowband PAs (Fig. 3.6 (a))
- Switched-band matching networks (SB-MN) (Fig. 3.6 (b))

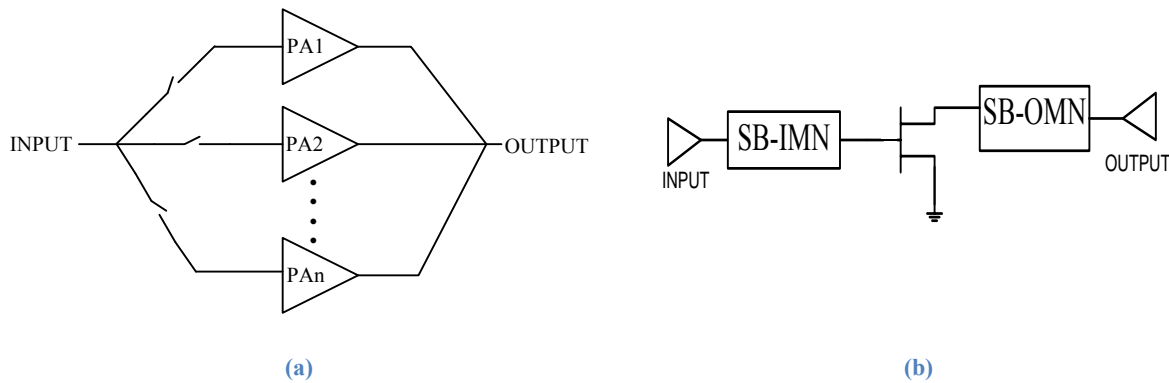


Figure 3.6- SB-PA (a) switching between numbers of narrowband PAs (b) switched-band matching network (SB-MN)

The first technique utilizes a number of narrowband PAs and based on the environment requirement one of them will be selected by using a switch. This technique is easy to implement due to simplicity in the designing of narrowband PAs. Each of these narrowband PAs are capable of providing high gain and good linearity, individually. As the number of required operating bands increases this structure will become bulky and complex. A PA based on this technique is expensive and noisy due to the existence of many internal connections. Examples of this PA are reported in [69] and [70]. Two PAs (optimized for their operating bands) and two bias circuits are designed with a bias switch in [69]. The bias switch is selecting the band of operation by activating one PA and deactivating the other. In [70], the first PA is common and then band switch is applied to choose the desired path for each frequency. The performance of the lower band of operation (where the switch is ON) is relatively smaller than the higher frequency (switch is OFF), as the loss of switch is high in its ON state. Band selection is applied in [71] as well, by aid of conducting two different bias currents. In this PA, a dual-band IMN and two individual OMNs for each band of operation have been designed. Three-stage amplification has been used in [72] and there is band selection control which switches between two bands of operation.

The second approach to have an SB-PA is to integrate the system with a SB-MN which provides optimum matching at each operating frequency. This method, in comparison with

the other method, has a relatively low cost, smaller circuit and higher efficiency. SB-MNs can be designed with distributed elements or lumped elements.

Distributed SB-MNs are designed by connecting or disconnecting the distributed element into the circuit. In 2004, a technique for dual-band PA was introduced using an OMN to provide the first frequency and a shunted switchable stub to produce the second frequency [21]. ON/OFF state of switches provides optimum matching in two different frequencies. The same technique was used in 2005 and 2010 with additional stubs to provide three bands of operation in [73] and [74]. In 2006, the designers tried to make the transmission line shorter and compact the circuits even more in [75] and [22]. This aim was achieved by implementing a reconfigurable stub for the first MN. The reconfigurable stub consisted of two stubs with a transmission line between them in [22]; and a series of transmission lines with switches in [75]. Obviously, the number of switches increases in [75] and they introduce more losses in the circuit. A 3-stage PA is illustrated in [90] in which the first two stages are driver stages and provide required power for the input of the last stage. The last stage is the power stage and uses a reconfigurable MN with the same technique introduced in [21] and [73]. A quad-band PA is presented in [76]. The PA is designed specifically for the higher band of operation and different MNs are connected via switches; by controlling the ON/OFF state of the switches the performance of the PA is shifted to other required frequency bands.

Lumped element SB-MNs are designed in different ways. Here, they are classified in two main groups: (i) utilizing variable performance of the switches and (ii) using switches to control the value of an inductor or a capacitor. Variable performance of the switches is used to provide optimum matching in different frequencies in technique (i). One example of these SB-PAs is presented in [77], where a double stub MN is implemented in the input and output networks. In this design, MEMS switches replace the shunt stubs to provide required

matching for both bands at the source and the load of the transistor. MEMS and varactors are used in [78], where the ON/OFF state of MEMS and varying biasing of varactors provide matching for different frequency bands. Anti-series varactor is another technique which is shown by [28]. This technique used a high value resistor and two diodes that provide high impedance for the centre of the tunable capacitors. Capacitance of varactors is controlled based on the level of input voltage at C1 and C2 points marked in the schematic diagram. Variable inductors are used in the RF choke and OMN of [79]. The PA in [80] uses BST (Barium Strontium Titanate) varactors in the circuit to change impedance for different frequencies. The BST varactors are tuned by two bias voltages and change the impedance of the circuit.

The other technique (ii) uses switches to change the value of inductor or capacitor to obtain a desired impedance based on the required operating frequencies. In [81], reconfigurable capacitors and switches are implemented to produce required impedance at two frequency bands. Changing the value of capacitors by controlling the ON/OFF state of switches used in [82] varies the operating frequency in that model. Also, this technique has multilevel output power with the aid of a switch to activate only two transistors at the same time, to create a push-pull power amplifier. Parallel parasitic capacitance at the drain of the transistor results in lower performance in the higher band. A PA with two switchable OMN has been used in [83]. The first OMN utilizes switchable capacitor to change the load impedance between two values to switch the value of output power. Another switchable capacitor is used in the second OMN to switch between two bands of operation. A broadband PA is followed by a reconfigurable OMN in [84] and [85]. The OMN uses two parallel inductance-capacitance (LC) tanks in OMNs that adjust the inductance value using a PIN diode; when the PIN diode is ON the parallel inductor is introduced into the circuit and

change the inductance value. ON and OFF states of the switch change the value of inductance from large to small, thus changing the resonant frequency from 0.9 to 1.8 GHz.

In [86] and [87], SB-MN contains multiple paths which are connected via switches. Connecting or disconnecting each path is executed by selecting the ON/OFF state of the switches and the operating band of the SB-PA will alter accordingly. One of them is reported in [86] which consists of two output paths and provide different operating frequencies based on the chosen path. The PA in [87] is able to operate in two frequencies by aid of two output paths which each of them provide two different bands. One path is operate at the time and other path is deactivated by switching the shunt SPDT switches. ON state of the switches provide short circuit at the intended frequency and will transform to open circuit at the drain of the transistor.

Class-E SB-PAs are designed and reported in [81], [88] and [89]. A quad-band Class-E PA is proposed in [88] which consist of four transistors and a single IMN and OMN. It works in one of the frequency bands at a time and is switched between bands by controlling the gate bias. A switched-band Class-E PA with finite DC-feed inductance is presented in [89]. A switch is applied to achieve optimum performance in the selected band, while the inductors are constant. The presented results for this PA in Table 3.2 are simulation results.

Table 3.2- Switched-band Power Amplifiers

References	Switch	Class of operation	Band of frequency	Gain	Output power	PAE	Circuit
[72]		B	0.9 and 1.8 GHz	28 dB	35 -32.5 dBm	48-44%	

[69]			0.9 and 1.8 GHz	29.5-27 dB	34.5-32 dBm	52-42%	
[77]	MEMS	AB	6 and 8 GHz	7.2-6.1 dB		26.4-16.7%	
[71]			0.85 and 1.75 GHz	26-21 dB	30-29 dBm	42-37%	
[21]	MEMS		0.9 and 1.9 GHz	16 dB	31 dBm	30%	
[70]	NMOS	AB	2.4 and 5.2 GHz	24-3.7 dB	19.5-9.7 dBm	15.3%	
[73]	MEMS	Class B	0.9, 1.5 and 2 GHz	13 dB	30 dBm	61%	
[78]	MEMS - Varactor	AB	7.5, 8.5, 9.5, 10.5 GHz		20-24-26 dBm		

[84]	PIN diode	AB	0.9 and 1.8 GHz	27 dB	30 dBm	40%	
[28]	Varactor	AB	0.9, 1.8, 1.9 and 2.1 GHz	15 dB	27 dBm		
[22]	MEMS	AB	0.9, 1.5, 2 and 5 GHz	10.7-8.3-8.6-8.1 dB	30.5-31-31-30.8 dBm	64-58-58-45%	
[75]	MEMS	AB	0.9, 1.5, 1.9 and 2.5 GHz	8.3-8.2-8.4-9.6 dB	30.6 dBm	46-53-43-62%	
[79]	NMOS		2.4 and 5.2 GHz	10.4-5.1 dB	13-8.7 dBm	16.2-10.8%	
[76]	MEMS	AB	0.9, 1.5, 1.9 and 2.6 GHz	8.9-8-8.9 and 9.5 dB	30.4-31-30-30.4 dBm	45-50-44-50%	
[81]	MEMS	E	0.9 and 1.8 GHz		20 dBm		
[86]	MEMS		0.9 and 1.6 GHz		33-30 dBm	42-26%	

[90]	FET	B	0.7, 0.8, 0.9, 1.4, 1.7, 1.8, 1.9, 2.3 and 2.5 GHz	30 dB	34 dBm	40%	
[80]	BST Varactor		1.7 and 2.3 GHz	27 dB	24.1 dBm		
[87]	PIN diodes		1.4 and 2.5 GHz	28 dB	28 dBm	38%	
[82]	MOSFET	D	0.45 and 0.73 GHz	22.4 dB	18 dBm	50%	
[74]	PIN diodes		0.9, 1.5 and 1.9 GHz	12-20-15 dB	39.1-39.4-40 dBm	64-65-61%	
[88]		E	1.9, 2.3, 2.6 and 3.5 GHz		24.2-23.8-23.4-20.5 dBm		
[89]		E	1.7 and 2.5 GHz		28-27 dBm	57-61.5%	

[83]		D	0.6 and 0.78 GHz	20 dB	16-19 dBm	36.6-46.6%	
------	--	---	------------------	-------	-----------	------------	--

3.2 Discussion

Table 3.1 and 3.2 summarise different techniques that have been applied to design MB-PA and SB-PA. To conclude, MB-PA and SB-PA can be designed by a number of parallel single-band PAs or with reconfigurable MNs (with or without switch). Fig. 3.7 summarizes all the techniques with their advantages and disadvantages. MB-PA and SB-PA with parallel single-band PAs are easy to design. These adaptive PAs require one PA for each band of operation; lots of components (transistors and MN's component) are required and make these PAs large in size and expensive. Implementing lots of components, connection between PAs and biasing for transistors could increase the amount of loss in these PAs. On top of all these losses, SB-PA with parallel single-band PAs has one more source of loss; the switches used for connecting to the desired PA. Designing adaptive PA with reconfigurable MN (MB-MN or SB-MN) is more efficient, smaller and cheaper. As only one transistor is used in these adaptive PAs, the number of active devices, components and size is dramatically decreased. SB-MN can provide theoretically more exact impedances compared to MB-MN and consequently more output power by applying switches at the cost of introducing more losses in the circuit.

The lack of study on the efficient approach to design adaptive highly efficient PAs (switched-mode PAs) motivates the author to do the research on the approaches and evaluate their performances. Also, developing a methodology with a recursive analytical solution for improving efficiency of SB-PAs is found to be essential to consider as today's wireless communication systems designers are continuously seeking better performances.

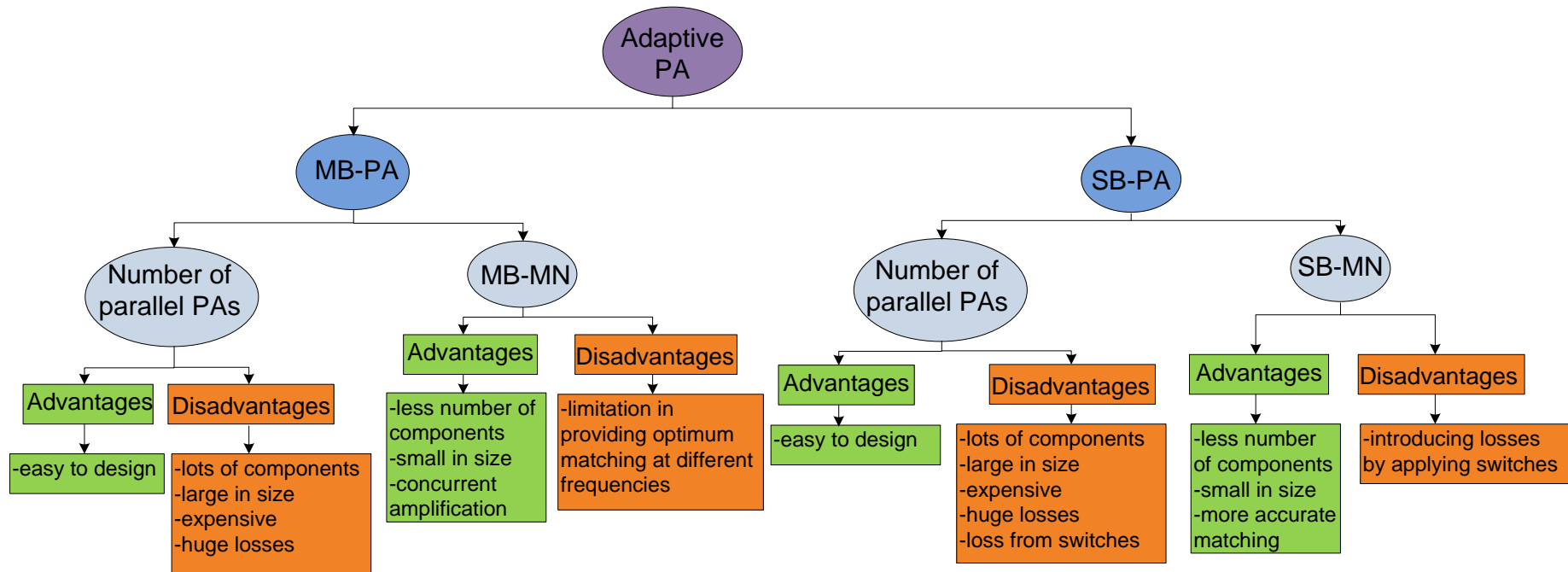


Figure 3.7-Summary of adaptive PAs

Chapter 4

Analysis and Design of Switched-Band Matching Networks for Power Amplifiers

A Matching Network (MN) is mainly to transfer load impedances to the desired source impedances at the specific frequency. At RF and microwave component level, one of the challenges is the design of multiband MN (MB-MN). Different circuit topologies are defined for MNs; such as L-match, quarter-wave transformer, single stub and etc [40]. Some MB-MN problems are more conveniently solved using networks that include switches to increase the number of degrees of freedom available. Some of the switched-band MNs (SB-MN) use switches to change the value of inductance or capacitance to obtain the desired impedance based on the required operating frequency [28], [81]-[82], [84] and [91]. There are some reported distributed SB-MNs, such as MNs in [21], [73], [86]-[87] and [92]. In [86] and [87], two output paths were provided and based on the chosen path the circuit operates at different frequencies. Another technique for SB-MN was introduced by [21] and [73], which use switchable stubs to provide optimum matching at different operating frequencies. The SB-MN in [92] used parallel quarter-wavelength transmission line and PIN diode switches at both ends of transmission line. This MN is switched to different impedances by providing different characteristic impedances which are achieved by controlling the switches and connecting or disconnecting the transmission lines [92]. Switches are the main source of losses in the SB-MNs and the main concern in designing a SB-MN is to decrease these losses. In some of these topologies, switches are applied in the main signal path and increase the overall effect of their losses. The other important concerns in designing SB-MNs are power handling and size issues that need to be taken into account.

The SB-MNs proposed in this chapter address these issues by focusing on stub length switching, such that all switches are grounded. By designing a MN in such way that the switches are placed between a point on a stub and the ground, the thermal resistance is reduced, resulting in lower junction temperatures in semiconductor switches. Lower average temperatures lead to more reliable operation, and lower temperature excursions reduce the tendency for memory effects in the non-linear behaviour. This would in turn make artificial linearization (for example, using pre-distortion) less problematic.

All the presented MNs have been built and tested. The description of all the proposed MNs is followed in this chapter by an analytical solution and comparison in terms of their accuracy and size. Multiband MNs for PAs is an important research area and needs very precise design due to the difficulty in managing optimum impedance matching and harmonics termination at the same time in each band. In the last section, the presented SB-MN is composed of two blocks, one for optimum matching at fundamental frequency and one for providing open or short circuit at harmonic frequencies.

4.1 Detach Stub Matching Network

The employed MN is based on the concept which is used in [21]. This MN composed of two transmission line and two stubs, as shown in Fig. 4.1. The first stub is fixed and the second one is connected by a switch, and called *Detach Stub MN*. With the switch OFF, the MN provides a required impedance at the first required frequency (f_1) and in ON state of the switch (second stub introduced into the circuit), the desired impedance at the second frequency (f_2) is met.

4.1.1 Analytical solution

The derived analytical solution of the detach stub MN provides values for the length of the transmission lines and stubs to give more precise results and shorten the design stage.

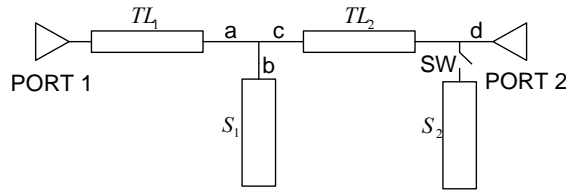


Figure 4.1- Detached stub matching network

Furthermore, such a solution will help circuit designers to arrive at optimum SB-MNs in a shorter time. Mainly, the analytical solution is helpful to find any forbidden region for this MN. The area on the Smith Chart which is unable to be matched with the particular MN circuit is called 'Forbidden region'. The equations are derived for ideal and physical transmission lines with effective dielectric constant (ϵ_r).

The ideal transmission line is utilised to prove the possibility of using an analytical solution. The whole idea of this method is to match by aid of a designated transmission line and a stub for each frequency. The transmission line TL_1 of length l provides admittance $Y_0 + jB$ at point 'a' and jB is eliminated by introducing the susceptance of an open stub (S_1). The required impedance looking into TL_1 at port 1 at the first frequency is Z_{L1} and defined as $R_{L1} + jX_{L1}$. At point 'a', admittance (Y_1) can be written as:

$$Y_1 = Y_0 \frac{Z_0 - X_{L1} \tan \theta_{L1} + jR_{L1} \tan \theta_{L1}}{R_{L1} + j(X_{L1} + Z_0 \tan \theta_{L1})} \quad (4.1)$$

where Z_0 and θ_{L1} are the characteristic impedance and the electrical length of TL_1 , respectively. Splitting Y_1 into real part and imaginary part yields (4.2) and (4.3) respectively.

$$\operatorname{Re}(Y_1) = \frac{R_{L1}(1 + \tan^2 \theta_{L1})}{R_{L1}^2 + (X_{L1} + Z_0 \tan \theta_{L1})^2} \quad (4.2)$$

$$\operatorname{Im}(Y_1) = \frac{R_{L1}^2 \tan \theta_{L1} - (Z_0 - X_{L1} \tan \theta_{L1})(X_{L1} + Z_0 \tan \theta_{L1})}{Z_0 [R_{L1}^2 + (X_{L1} + Z_0 \tan \theta_{L1})^2]} \quad (4.3)$$

Given that the real part of Y_1 is equal to the characteristic admittance of the system, Y_0 , the electrical length of the transmission line can be obtained by the following equation.

$$\theta_{L1} = \tan^{-1} \left(\frac{X_{L1} - \sqrt{R_{L1} [(Z_0 - R_{L1})^2 + X_{L1}^2] / Z_0}}{R_{L1} - Z_0} \right) \quad (4.4)$$

By substituting θ_{L1} value back into (4.3), the susceptance part of Y_1 , B , can be obtained. The admittance at 'b' in Fig. 4.1 is $jY_0 \tan \theta_{S1}$ and electrical length of the stub (S_1) should be found to eliminate the susceptance of Y_1 . So the electrical length of the stub can be calculated by:

$$\theta_{S1} = \tan^{-1} \left(\frac{B}{Y_0} \right) \quad (4.5)$$

To provide the desired impedance $Z_{L2} = R_{L2} + jX_{L2}$ at f_2 , the second stub is introduced into the circuit by turning the switch ON. To calculate the length of the second transmission line and stub (TL_2 and S_2 respectively), the admittance at 'c' (Y_3) is calculated by (4.6).

$$Y_3 = Y_0 \frac{Z_0 - X_{L2} \tan(\theta'_{L1}) + jR_{L2} \tan(\theta'_{L1})}{R_{L2} + j(Z_0 \tan(\theta'_{L1}) + X_{L2})} + jY_0 \tan(\theta'_{S1}) \quad (4.6)$$

The physical length of TL_1 and S_1 are fixed but their electrical lengths vary as the frequency changes; therefore, θ'_{L1} and θ'_{S1} are introduced which are the electrical length of the

first transmission line and stub at f_2 , respectively. Following the same procedure by applying $1/Y_3$ instead of Z_{L1}^* , we can calculate the electrical lengths of TL_2 and S_2 . The derived analytical solution is also applicable for SB-MNs covering more than two bands. This can be done by adding additional switched stubs, positioned relative to S_1 , by repeated application of (4.6) and back to (4.3)-(4.5).

For practical applications, the above introduced algorithm needs to be implemented in a physical transmission line medium such as microstrip. To find the lengths of transmission lines and stubs in microstrip, the physical lengths need to be divided by $\sqrt{\epsilon_e}$ yielding (4.7) where ϵ_e denotes effective dielectric constant.

$$l = \frac{\theta \cdot c}{\sqrt{\epsilon_e} 2\pi f} \quad (4.7)$$

4.1.2 Numerical Example

To verify the presented approach, the equations have been applied to several different numerical values in different ranges of frequencies and one of them is presented in this section. A Gallium Nitride High Electron Mobility Transistor (GaN HEMT) from Nitronex is chosen as an example. Two different frequencies are selected and appropriate impedances are obtained from load pull information in the device datasheet. Load pull analysis is a graphical technique, generating a set of contours on the Smith chart of required impedances for DUT to achieve specific performances. These contours represent the impedance loci for given performance parameters for the PA and they are obtained by varying the impedances and measuring the performance of the PA (output power, gain and efficiency) [94]. The required normalized impedances are $0.49 + j0.366$ and $1.052 + j0.456$ at 1800 and 900 MHz, respectively, with the bandwidth of 400 MHz. The required impedance for the higher frequency is provided by the OFF state of the switch, since the amount of loss in switch in its

ON state increases at higher frequency. Appropriate lengths for the transmission lines and stubs are calculated in two different versions, ideal and physical transmission lines.

4.1.2.1 Ideal Transmission Line

Using (4.3-4.5) the value of B , θ_{L1} and θ_{S1} are calculated respectively. In the next step Y_3 is obtained using (4.6). Using the same procedure θ_{L2} and θ_{S2} are calculated. These results are used in the simulation and the results are shown in Fig. 4.2. Good agreement between the simulation results and the required impedances taken from the device datasheet has been confirmed.

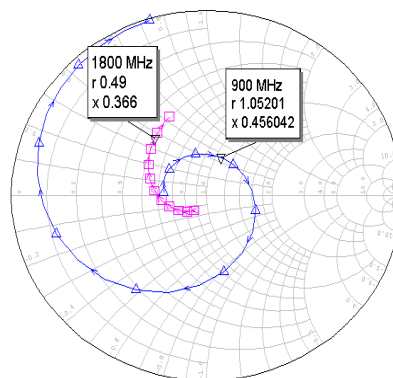


Figure 4.2-Simulation result of detach stub MN with ideal transmission line

In the first frequency, one transmission line and one stub is used to match to the required impedance. The second desired impedance is converted to Y_3 at point 'c' in Fig. 4.1. The second transmission line and stub parameters are calculated to transform Y_3 at the second frequency to Y_0 at points 'c' and 'd', respectively. No further iteration of the first line and stub are required to achieve this. The presented method proves that there is no forbidden region to match any dual frequencies by this MN, because whatever the value of Y_3 , it can, in principle, be matched using a single line and stub.

4.1.2.2 Physical Transmission Line

The electrical lengths of the transmission lines and stubs in this case are evaluated as before and their physical lengths are found by use of (4.7). Fig. 4.3 shows the simulation results based on the calculated lengths with physical transmission line and stubs.

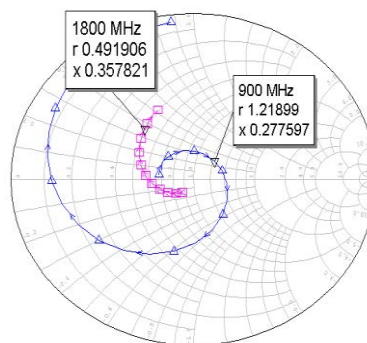


Figure 4.3-Simulation result of detach stub MN with physical transmission line

The results show a perfect match at 1800MHz and a reasonably close match at 900MHz. The reason for the difference observed in the second frequency is the discontinuity of the T-junction. Discontinuities are abrupt changes in geometry of microstrip lines which alter the electromagnetic wave propagation down the line. Some of the common microstrip discontinuity are open-ends, steps, T-junction and cross junctions. As the reference plane is shifted by the junction, so by adjusting the length of the transmission line and the stub, the discontinuity effect of the T-junction can be compensated as shown in [93] and [95]. Taking into account the discontinuity and fine tuning the simulation will give the result presented in Fig. 4.4 that shows good agreement at 900 MHz.

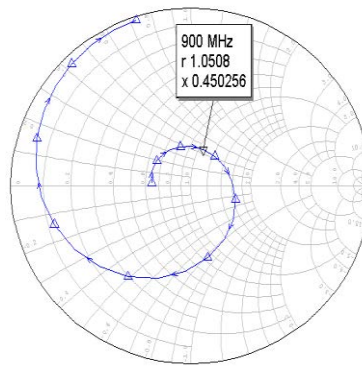


Figure 4.4-Simulation result after adjustments at the first band

A PIN diode is applied as the switch in all the presented MNs in this work because of its advantages such as low insertion loss, high isolation, high switching speed and excellent power handling at microwave frequencies [24]. Two PIN diodes from two different companies have been selected:

- Silicon PIN diode from Infineon (BAR50)
- Silicon PIN diode from Skyworks (SMP1302-085LF)

The detach stub MN has been tested with both of these PIN diodes and their result have been analyzed. The simulation results obtained from both models are satisfactory in terms of providing appropriate impedance at the output port of the transistor. Dissipation of power in the PIN diode will consequently introduce loss in the MN. Hence, to choose the best design, loss in the circuit should be minimized. The loss of these MNs are analysed by aid of the definition of total loss factor which is based on the concept of energy conservation. A loss factor can be derived by studying the total power emerging from the network in response to an input at one port. On this basis, the loss factor has been derived as:

$$Loss = |S_{11}|^2 + |S_{21}|^2 \quad (4.8)$$

Where a value of one indicates a lossless circuit and a value less than one shows that there is loss. The simulated values of this equation for both MN with two PIN diodes are plotted in

the following two graphs, Fig. 4.5. The result desired to be close to one and minimise the losses introduced by PIN diode into the circuits.

Comparing both results presented in Fig. 4.5, Infineon PIN diode gives better results for both frequencies with total loss factor very close to one while Skyworks gives a lower total loss factor. Obviously, the first model has less loss and dissipates less power in the MN.

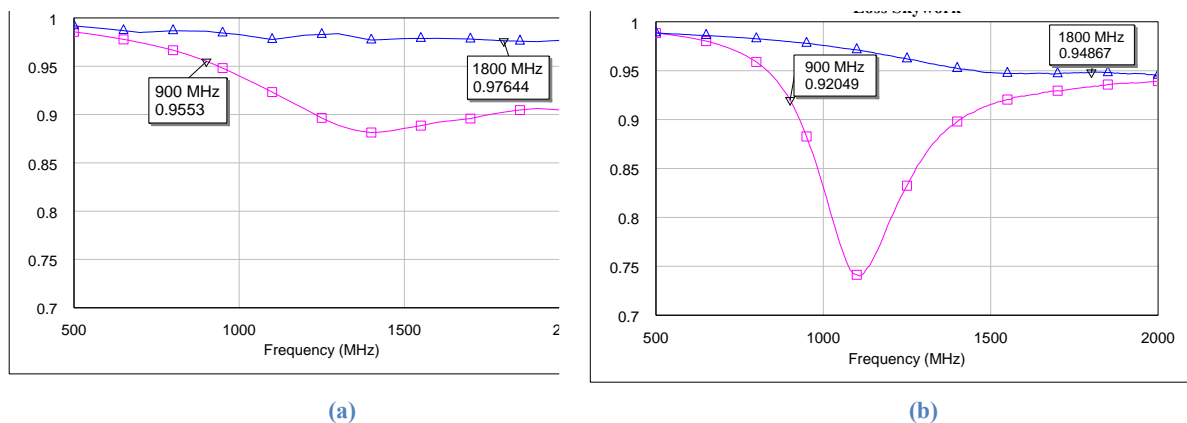


Figure 4.5-Total loss factor of the detach stub MN in OFF (blue) and ON (pink) state with PIN diode (a) Infineon and (b) Skyworks

4.1.3 Experimental Result

The MN based on the calculation in the previous section has been built, to prove the validation of the algorithm. It was fabricated on Microstrip substrate of thickness of 0.76 mm and relative dielectric constant of 3.5. The PIN diode, as mentioned earlier, is type BAR50 from Infineon.

The simulation and measurement results are compared and plotted by their magnitude (Fig. 4.6) and on the Smith Chart (Fig. 4.7). The markers on Fig. 4.7 ((a) and (b)) indicate the reflection coefficient at the intended frequencies for the ON and OFF state (1800 and 900 MHz, respectively). Both graphs show good agreement between simulation and measurement. The small differences are due to real components and their tolerances.

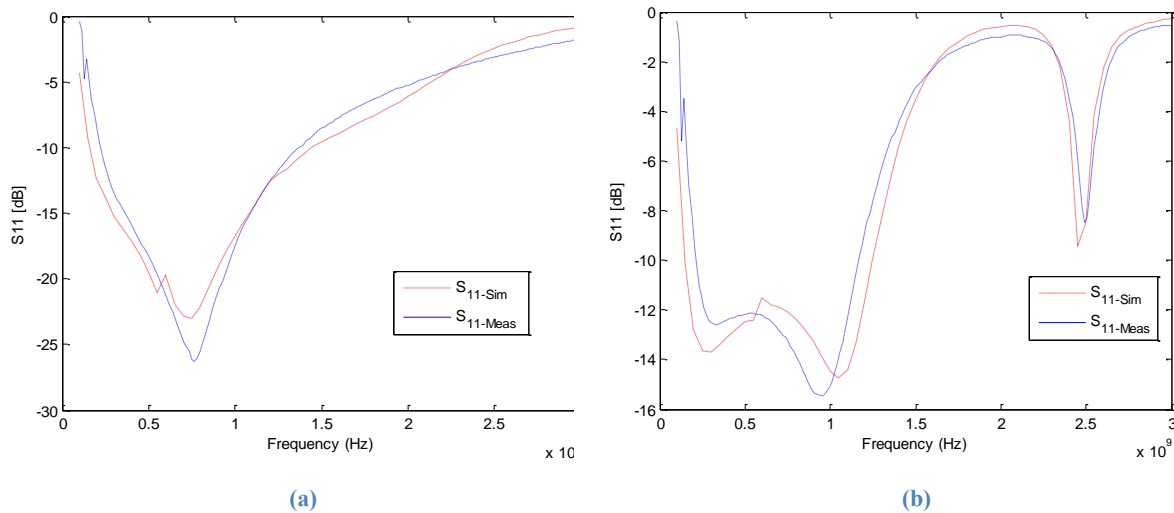


Figure 4.6-Simulated and measured S_{11} in (a) OFF (1800 MHz) and (b) ON (900 MHz) state

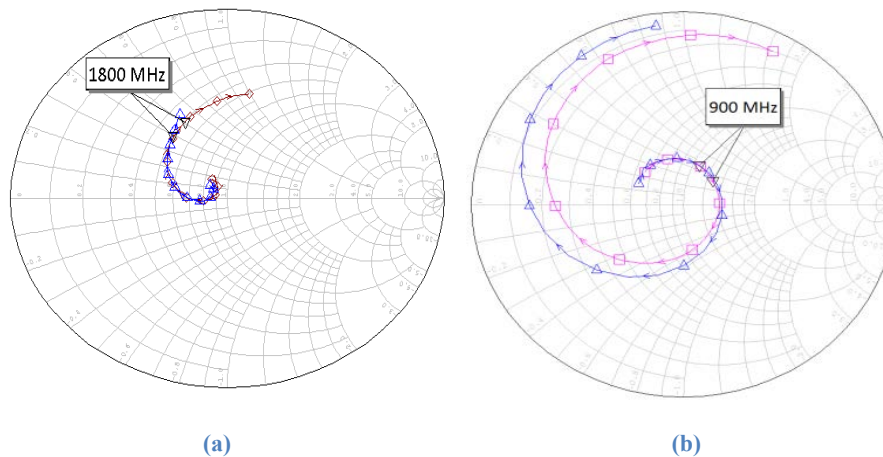


Figure 4.7-Simulated and measured input impedance of detach stub MN in (a) OFF state and (b) ON state

4.2 Open to Short Stub (OTS) Matching Network

Any Switched-Band Output Matching Network (SB-OMN) which contains switches will degrade the output power and efficiency. The MN proposed here are composed of one transmission line and one stub and utilise a switch to connect the stub to ground. Placing the switch between stub and ground to open or short stubs can provide different impedances in different operating frequencies and helps to minimize losses which are introduced by the switch. Since, the switches are not in the main path of the signal their resistive elements can dissipate less power, helping to reduce losses.

4.2.1 Design

The whole idea of this MN is to provide required impedances by a single stub and varies in two different frequencies by aid of a switch at the end of the stub to obtain open- or short-circuit stub. This is referred to as Open to Short MN (OTS) (Fig 4.8). The ON state of the switch provides a short stub at the lower frequency and the stub is open when the switch is OFF, for the higher frequencies use. The length and the characteristic impedance of the transmission line and the stub are optimized to provide required impedances at the specific frequencies.

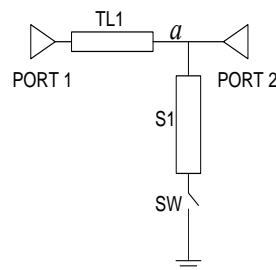


Figure 4.8-Open to Short MN

4.2.2 Analytical solution

In OTS, only one transmission line and stub are available to adjust their length and characteristic impedance to achieve desired impedance at both operating frequencies. Generally, the method of the OTS MN is to suppose the required impedances are presented at 'port 1' and aim to provide the system impedance at 'port 2' by aid of a transmission line and a stub. The steps that have been followed to derive an analytical solution for this MN are:

- Suppose required impedances at both bands are provided at 'port 1'
- Adjust length and characteristic impedance of the transmission line to present $Y_0 + jB_1$ at f_1 and $Y_0 + jB_2$ at f_2
- Eliminate jB_1 by appropriate length and width of short-circuited stub

- Eliminate jB_2 by appropriate length and width of open-circuited stub

The aim of deriving the analytical solution is to be able to calculate length and characteristic impedance of the transmission line (TL_1) and stub (S_1) accurately. The physical lengths of the transmission line for both frequencies have been derived the same way as explained in section 4.1.1. Practically, both physical lengths should be the same as they refer to the same transmission line, (4.9).

$$\frac{1}{f_1} \tan^{-1} \left(\frac{-X_{L1} - \sqrt{\frac{R_{L1}}{Z_1} [(Z_1 - R_{L1})^2 + (X_{L1})^2]}}{R_{L1} - Z_1} \right) = \frac{1}{f_2} \tan^{-1} \left(\frac{-X_{L2} - \sqrt{\frac{R_{L2}}{Z_1} [(Z_1 - R_{L2})^2 + (X_{L2})^2]}}{R_{L2} - Z_1} \right) \quad (4.9)$$

where the required impedances are $Z_{L1} = R_{L1} + jX_{L1}$ and $Z_{L2} = R_{L2} + jX_{L2}$ for the first (f_1) and second (f_2) band which are known values. Z_1 is the characteristic impedance of TL_1 and is unknown. Both sides of equation (4.9) include \tan^{-1} with different coefficients ($\frac{1}{f_1}$ and $\frac{1}{f_2}$) and they cannot be equal for a particular Z_1 and any Z_{L1} and Z_{L2} . Therefore, this MN has forbidden region. In order to find an analytical solution and define the coverage region of the OTS MN, different special cases need to be considered.

To begin with, the assumption has been made that the transmission line is quarter wavelength at f_1 . So, the length of the transmission line in air space is $L_1 = \frac{c}{\sqrt{\epsilon_c} 2\pi f_1} * \frac{\pi}{2}$. The admittance at point 'a' is $\frac{R_{L1} + jX_{L1}}{Z_1^2}$. The conductance should be equal to the normalized

system admittance and therefore, $Z_1 = \sqrt{R_{L1}}$. The switch is ON when the circuit is operating at the first frequency and the length of the short-circuited stub can be found by:

$$L_2 = \frac{-c}{\sqrt{\epsilon_e} 2\pi f_1} \tan^{-1} \left(\frac{R_{L1}}{X_{L1} \cdot Z_2} \right) \quad (4.10)$$

There are two unknowns in (4.10), length (L_2) and characteristic impedance (Z_2) of the stub. To be able to find unique values for L_2 and Z_2 , another equation for L_2 is needed at the second frequency. The physical length of the transmission line is obtained and the electrical length of the transmission line in the second band (θ_{L2}) can be found by $\frac{f_2}{f_1} * \frac{\pi}{2}$. Three

different cases are going to analyze:

- *Case 1:* $\frac{f_2}{f_1}$ = even integer number $\rightarrow \theta_{L2} = n\pi$
- *Case 2:* $\frac{f_2}{f_1}$ = odd integer number $\rightarrow \theta_{L2} = n \frac{\pi}{2}$
- *Case 3:* $\frac{f_2}{f_1}$ = any value $\rightarrow \theta_{L2} =$ any value

In *case 1*, $\tan(\theta_{L2})$ is zero and the admittance at point 'a' for the second band is $\frac{R_{L2} - jX_{L2}}{R_{L2}^2 + X_{L2}^2}$. The normalized conductance should be unity to meet the system impedance at 'port 2'. To satisfy this, the length and width of transmission line would need to be adjusted. However, they had been calculated earlier to meet the first band requirement and they are fixed. Therefore, the only way to meet this condition (the normalized conductance to be unity) is X_{L2} should be $\sqrt{R_{L2} - R_{L2}^2}$. At the second band, the switch is OFF and the stub is open. Length of the stub can be found by:

$$L_2 = \frac{-c}{\sqrt{\varepsilon_e} 2\pi f_2} \tan^{-1} \left(\frac{X_{L2} Z_2}{R_{L2}^2 + X_{L2}^2} \right) \quad (4.11)$$

Z_2 and L_2 are unknown in (4.11) like (4.10). Now there are two equations and two unknowns and this can be easily solved. This has been done in this work by finding L_2 with substituting different value of Z_2 in an acceptable range. Different values for L_2 have been obtained from (4.10) and (4.11) and they are plotted in the same graph with respect to Z_2 in order to find the crossing point, which identifies the appropriate values.

According to the equations, this MN with frequency condition of $\frac{f_2}{f_1} = \text{even integer number}$ can be applied for the certain output impedances for which they met the conditions. These conditions are:

- $X_{L2} = \sqrt{R_{L2} - R_{L2}^2}$
- $R_{L2} \leq 1$

MATLAB has been used to find the coverage region of the OTS MN in the first case. All the conditions have been applied in MATLAB to locate the impedances on the Smith chart. The impedances for which OTS MN can be designed are shown in Fig. 4.9(a), the blue dots show Z_{L1} and red dots show Z_{L2} . The reason that they are only capacitive loads for Z_{L1} is that (4.10) results in a negative length when inductive loads applied and need to add quarter wavelength to the stub and in that case the stubs cannot have the same physical length for both bands of operation. To be able to match inductive loads as well we need to shift switching condition in the frequencies: the ON state of the switch at the higher band and the OFF state at the lower band of operation. The equation for calculating length of the stub will be:

$$L_{21} = \frac{c}{\sqrt{\epsilon_e} 2\pi f_1} \tan^{-1} \left(\frac{X_{L1} \cdot Z_2}{R_{L1}} \right) \quad (4.12)$$

$$L_{22} = \frac{c}{\sqrt{\epsilon_e} 2\pi f_2} \tan^{-1} \left(\frac{R_{L2}^2 + X_{L2}^2}{X_{L2} \cdot Z_2} \right) \quad (4.13)$$

L_{21} and L_{22} are the length of stub at first and second frequency, respectively. The coverage region in this case has been analyzed in MATLAB and plotted the impedances on the Smith chart in Fig. 4.9(b).

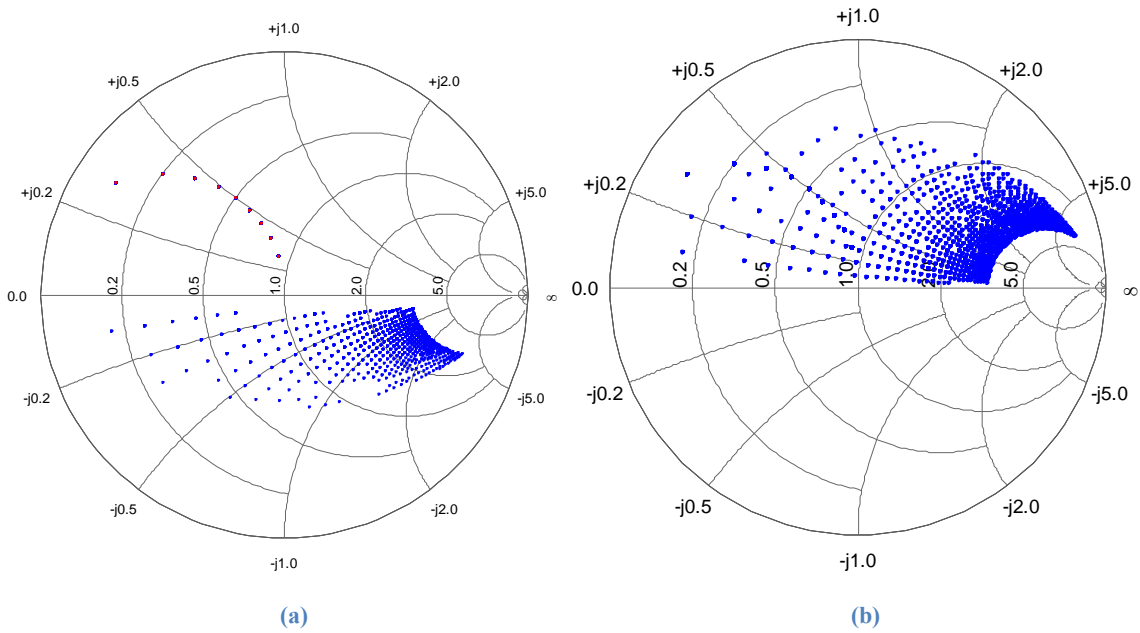


Figure 4.9-Coverage region of OTS in case 1(a) capacitive load and (b) inductive load

The second case is when the ratio of the frequencies is an odd integer number. The admittance at point 'a' in Fig. 4.8 for the second bands is $Y_2^* = \frac{R_{L2} + jX_{L2}}{Z_1^2}$. To provide the system impedance at 'port 2' Z_1 should be equal to $\sqrt{R_{L2}}$. The characteristic impedance of the transmission line (Z_1) at the first band has been calculated to be $\sqrt{R_{L1}}$; therefore, R_{L1} has to be equal to R_{L2} . At the second frequency, the switch is OFF and the stub is open, so the length of the stub can be calculated by:

$$L_2 = \frac{c}{\sqrt{\epsilon_e} 2\pi f_2} \tan^{-1} \left(\frac{X_{L_2} \cdot Z_2}{R_{L_2}} \right) \quad (4.14)$$

The same technique is applied here to plot both L_2 from (4.10) and (4.14) in the same graph and find Z_2 and L_2 . The only condition applied in this case is the same resistance for both required impedances. Fig. 4.10 is shown the coverage region of OTS in case 2 that obtained in MATLAB.

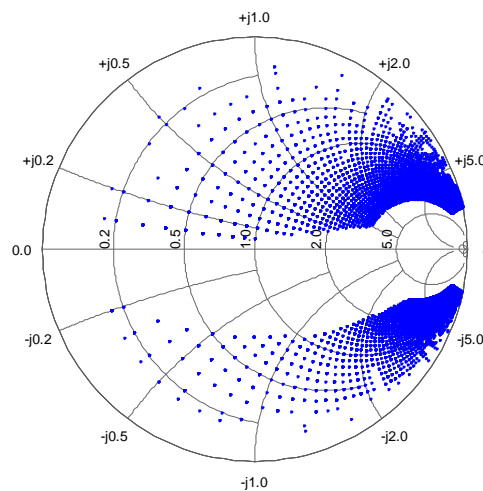


Figure4.10-Coverage region for OTS in case 2

The next step is analyzing the third case. By assuming the required impedance at 'port 1' in the second band of operation, the input impedance at point 'a' can be written as:

$$Z_2^* = Z_1 \frac{R_{L_2} + j(X_{L_2} + Z_1 \tan \theta_{L_2})}{(Z_1 - X_{L_1} \tan \theta_{L_2}) + jR_{L_2} \tan \theta_{L_2}} \quad (4.15)$$

Then the conductance is found:

$$\text{Re}(Y_2^*) = \frac{R_{L_2} (1 + \tan^2(\theta_{L_2}))}{R_{L_2}^2 + (X_{L_2} + Z_1 \tan(\theta_{L_2}))^2} \quad (4.16)$$

Equation (4.16) needs to have specific values for R_{L_2} and X_{L_2} to be equal to one. The length of the stub in ON state of the switch (short-circuited stub) and OFF state (open-circuit stub) can be found by (4.10) and (4.17):

$$L_2 = \frac{c}{2\pi f_2} \tan^{-1}(-BZ_2) \quad (4.17)$$

B is the susceptance of Y_2^* . Z_2 and L_2 can be found by plotting both equations ((4.10) and (4.17)) in one graph with respect to different value of Z_2 . The coverage region of the OTS in third case is shown in Fig.4.11. According to Fig.4.9, 4.10 and 4.11, this MN results in a poor coverage region of the Smith chart. Therefore, this MN is not able to work over a wide range of frequencies and achieve any required impedances due to having too few adjustable elements.

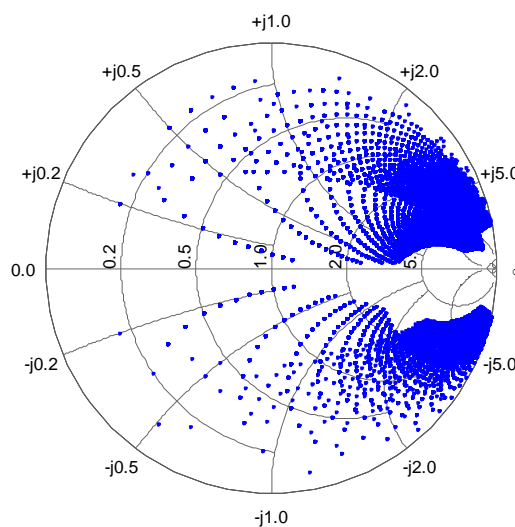


Figure 4.11-Coverage region for OTS in third case

4.2.3 Numerical Example

To verify the technique explained in the previous section, three numerical examples for each case are presented here. Two frequencies and their required impedances have been chosen. The first example is for case 1 where the second frequency is twice of the first

frequency, 900MHz and 1800MHz. The aim is to provide $1.052 + j0.456$ and $0.49 + j0.366$ at 'port 1' in the first and second band, respectively. Electrical length of $\frac{\pi}{2}$ and π at the first and second band results in physical length of 50mm. The normalized characteristic impedance of the transmission line is $\sqrt{1.052}$, so the width of the transmission line will be 1.61mm. Equations (4.12) and (4.13) have been used to find the length of the stub for both frequencies by substituting different values of Z_2 . The logical values for normalized Z_2 is between 0.4 and 1.8, according to the substrate and the feasible width. The two stub lengths are plotted in the same graph, Fig. 4.12. In this figure, red line shows L_2 for the first band and blue is for the second band.

In Fig. 4.12, the point that stub has the same length in both frequencies has been marked. Therefore, width of 1.73mm and length of 11.4mm have been chosen for the stub. These values are applied in the simulation and the simulation results are shown in Fig. 4.13.

The second example (case 2) is for 0.9GHz and 2.7GHz and their required impedances are $Z_{L1} = 0.4 - j1.1$ and $Z_{L2} = 0.4 + j0.8$, respectively. The characteristics impedance of the transmission line is $Z_1 = \sqrt{0.4}$. The electrical length of the transmission line (TL_1) at the first band is $\theta_{L1} = \frac{\pi}{2}$ which is $\theta_{L2} = \frac{3\pi}{2}$ at the second band and its physical length is 48.73mm. To find the length and characteristics impedance of the stub, equation (4.10) and (4.14) are plotted in Fig. 4.14. At normalized Z_2 equal to 0.96 both stub length have the same value which is 10.3mm. The simulation results with these values are shown in Fig. 4.15. These results show a good match with the required impedances at both bands.

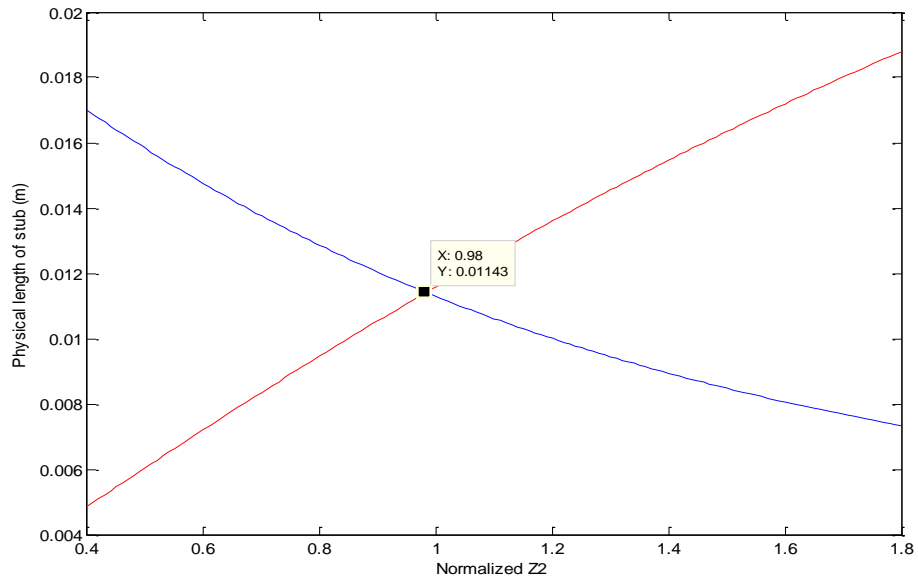


Figure 4.12-Physical length of the stub with different characteristics impedance

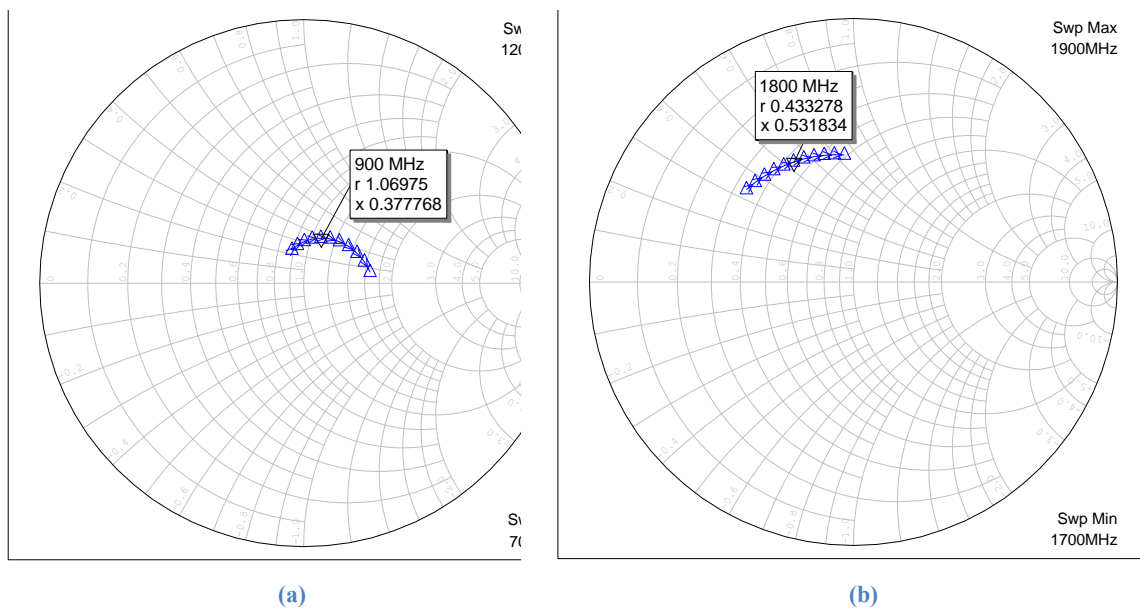


Figure 4.13-Simulation result of OTS in case 1 (a) OFF and (b) ON state of the switch

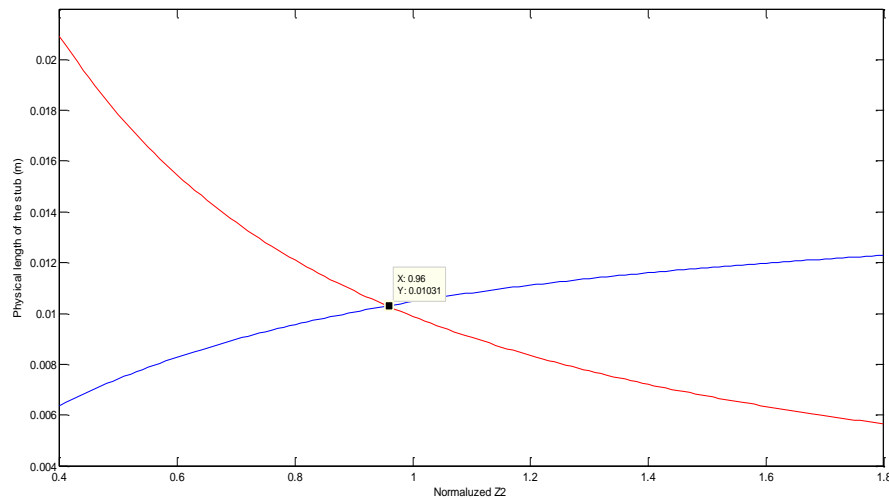


Figure 4.14- Physical length of the stub for different characteristics impedance of the stub

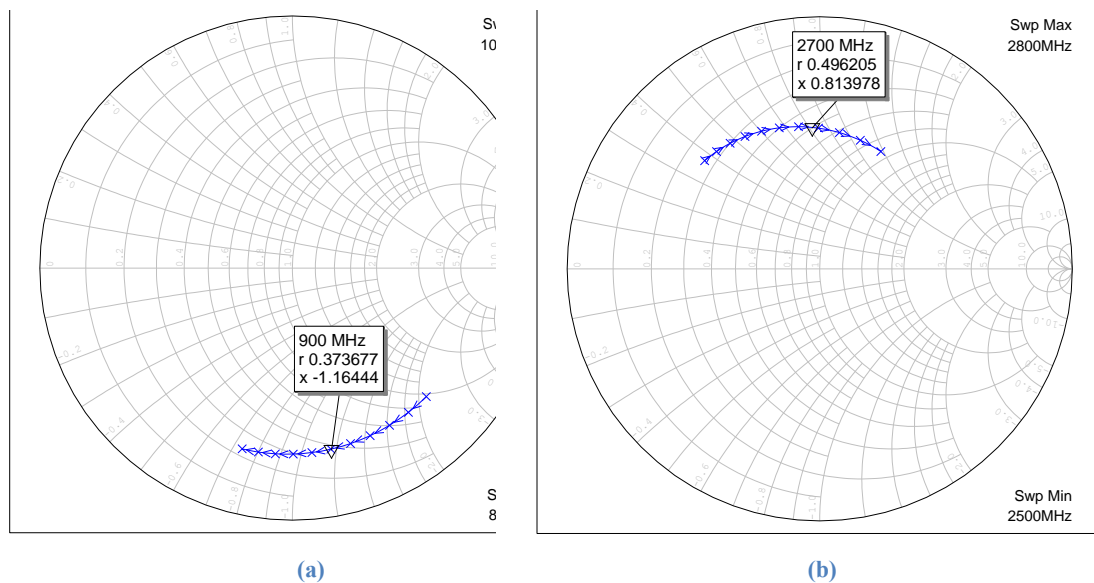


Figure 4.15- Simulation result of OTS MN in case 2 (a) ON state and (b) OFF state

The two required impedances chosen for the example of the case 3 are $Z_{L1} = 0.5 - j0.6$ at 900MHz and $Z_{L2} = 0.3 + j0.75$ at 2000MHz. The normalized characteristics impedance of the first transmission line is found as 0.7 which result in 2.84mm width. The length of the transmission line is 50.7mm. The same process as two previous examples are followed here

and equation (4.10) and (4.17) are plotted in Fig. 4.16. The normalized optimum characteristic impedance of 0.47 and the length of 29.8mm are found.

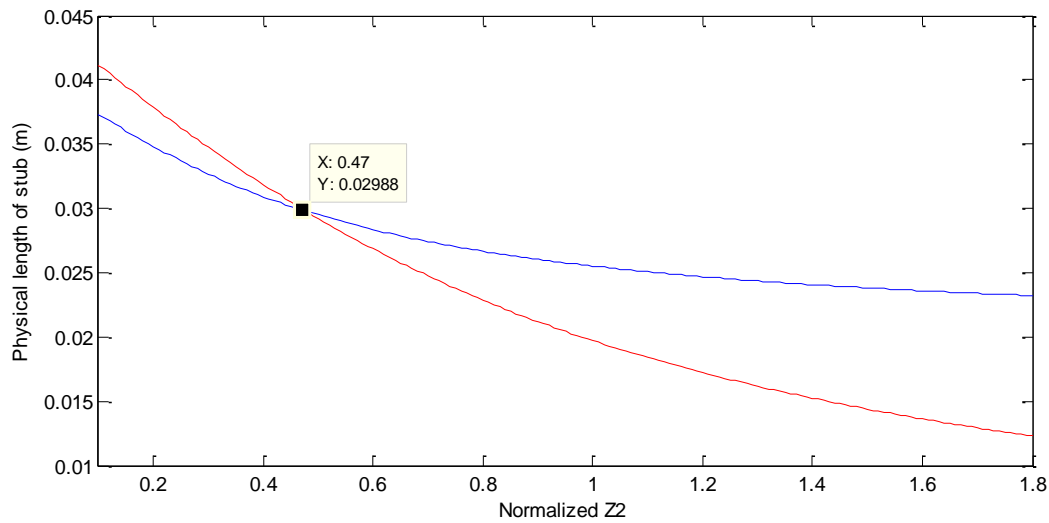


Figure 4.16-Physical length of the stub for different characteristics impedance of the stub

These calculated values are applied in simulation to prove the validity of this algorithm. The simulation results (Fig. 4.17) are shown reasonably close match to the required impedances.

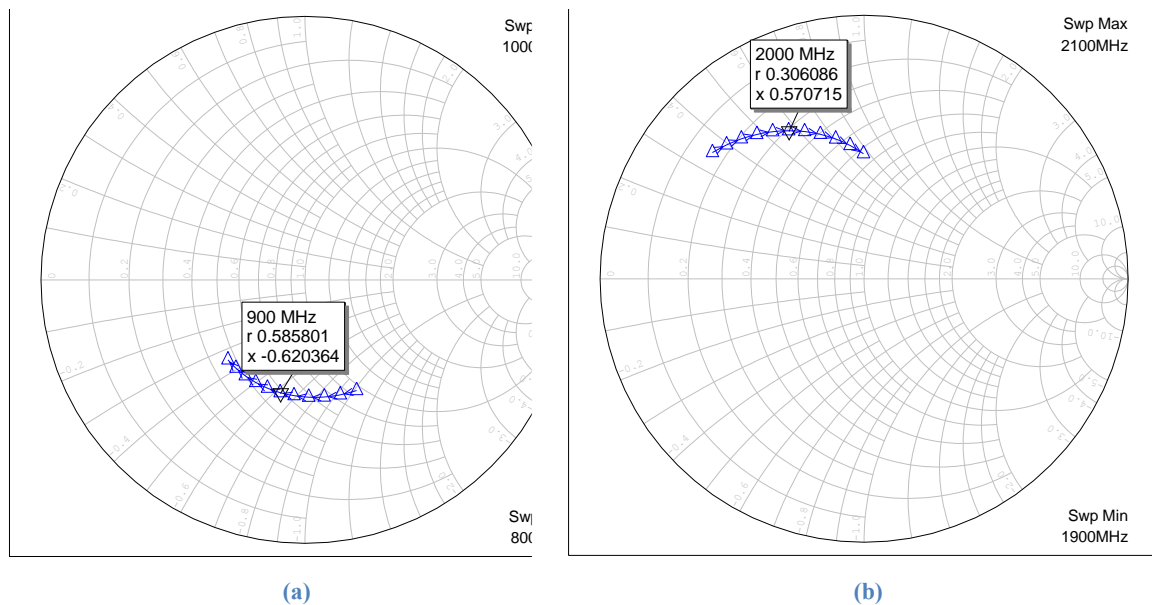


Figure 4.17-Simulation result of OTS MN in case 3 (a) ON state and (b) OFF state

The loss of the OTS MN has been analyzed to prove the improvement in minimizing the loss of OTS MN compare to the detach stub MN. Fig. 4.18 illustrates the loss introduced by

the switch to this MN. As shown in the graph, the losses at both states (ON and OFF) of the switch are very close to one. In ON state of the switch, 3% improvement has been achieved.

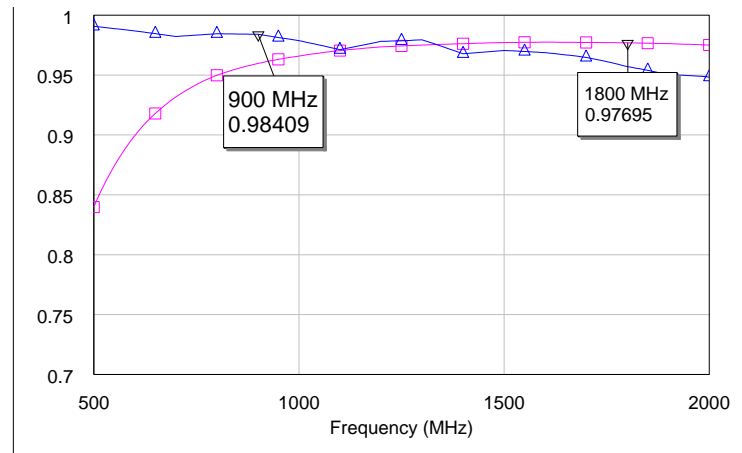


Figure 4.18-Total loss factor of the switch in the OTS MN in OFF state (blue) and ON state (pink)

4.2.4 Experimental

The OTS MN (the case 1) has been fabricated to verify the methods, Fig. 4.19. The PIN diode has been biased with a capacitor and a resistor. The applied voltage is 8 V and the voltage after the PIN diode will be 7.3 V due to the PIN diode forward voltage drop. Therefore, the value of the resistor can be calculated to conduct forward current of 10 mA. A capacitor is used to provide RF ground and low reactance at the intended frequency (same value as DC blocking capacitor, i.e. 47 pF). The simulation and measurement results are compared and plotted on the Smith Chart (Fig 4.20). The experimental results are reasonably close to the simulations and validate the analytical solution and that by switching the stub to the ground is capable of providing the required impedance in the other frequency band.

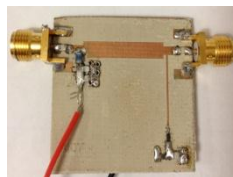


Figure 4.3-Photograph of OTS MN (switch end of the stub)

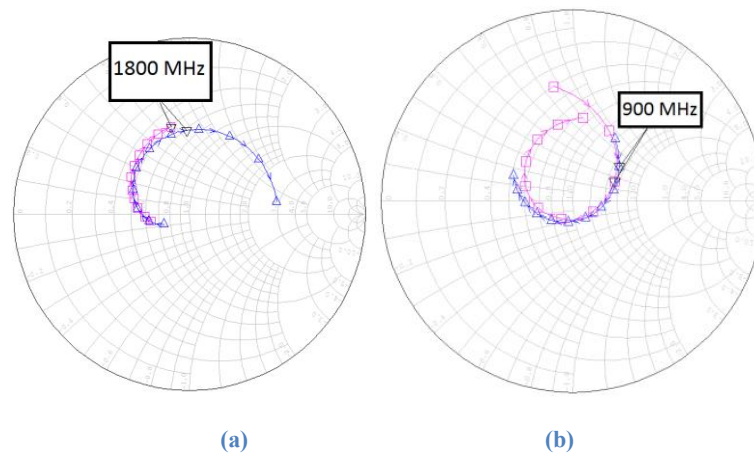


Figure 4.20-Simulated and measured input impedance of OTS MN at (a) ON state and (b) OFF state

4.3 Short to Stub (STS) Matching Networks

The presented MN in this section is a single stub MN and a different matching condition is provided by using a stub which can be adjusted in length and width and made either open- or short-circuit. To make this possible, the position and mode of the switch is altered and it provides different performances.

4.3.1 Design

In the method called Stub to Short switching (STS), the switch is situated somewhere in middle of the stub (Fig 4.21). When the switch is ON, the stub is shorter and is grounded. The longer and open stub is provided in the OFF state of the switch. Typically, the higher frequency needs shorter stub rather than the lower frequency; therefore, ON state of the switch is applied at higher frequency. By optimizing the length and characteristic impedance of the transmission line and stub, optimum matching can be provided at different frequencies.

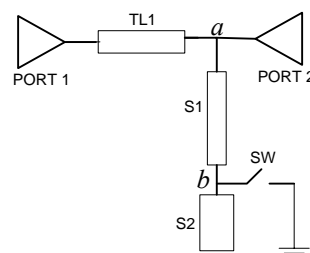


Figure 4.4-Stub to Short MN

By using the switch in the middle of the stub, in STS, one longer stub is used in one of the frequencies and an extra degree of freedom is provided to design; therefore, more frequencies can be covered by this method.

4.3.2 Analytical solution

As for the other two MNs (detach stub and OTS MN), an analytical solution is derived for this MN. The reason to derive equation is not only making the designing MN in the shorter time and more accurate result, but also to discover any forbidden region for this MN. For the start, the electrical length of the transmission line is assumed to be quarter wavelength at first band. The input admittance at point 'a' in Fig. 4.21 is $\frac{R_{L1} + jX_{L1}}{Z_1^2}$, where R_{L1} and X_{L1} are the resistance and reactance of the required impedance at the first band and Z_1 is the characteristic impedance of the transmission line. The characteristic impedance of the transmission line is calculated to be $\sqrt{R_{L1}}$ to provide $Y_0 + j\frac{X_{L1}}{R_{L1}}$ at 'port 2'. At the first band the switch is OFF and both stubs are connected. To find the susceptance of the stub at point 'a', first need to find the impedance at point 'b':

$$Z_1'' = -j \frac{Z_3}{\tan \theta_{S21}} \quad (4.18)$$

Z_1'' and Z_3 are impedance at point 'b' and characteristic impedance of the second stub, respectively and θ_{S21} is electrical length of the second stub at the first band. Then the susceptance at point 'a' can be found by:

$$B_1 = j \frac{Z_2 \tan \theta_{S21} + Z_3 \tan \theta_{S11}}{Z_3 - Z_2 \tan \theta_{S11} \tan \theta_{S21}} \quad (4.19)$$

θ_{s11} is the electrical length of the first stub at the first band and Z_2 is the characteristic impedance of the first stub. Then, the length of the second stub is:

$$L_3 = \frac{c}{\sqrt{\epsilon_e} 2\pi f_1} \tan^{-1} \left(\frac{Z_3}{Z_2} \cdot \frac{X_{L1} - R_{L1} \tan \theta_{s21}}{R_{L1} + X_{L1} \tan \theta_{s21}} \right) \quad (4.20)$$

This equation has four unknowns and makes it impossible to solve. When the switch is ON, the first stub is connected to the ground and the second stub is out of the circuit. In the ON state of the switch, the length and width of the first stub can be found to decrease the number of unknowns in (4.20). The electrical length of the transmission line at the second band is $\frac{f_2}{f_1} \cdot \frac{\pi}{2}$. Three cases are going to analyze, same as the OTS MN.

In the first case ($\frac{f_2}{f_1}$ is an even integer number), $\tan \theta_{L2}$ is zero and admittance at point 'a' is $\frac{R_{L2} - jX_{L2}}{R_{L2}^2 + X_{L2}^2}$. The conductance is fixed and the only way to provide $Y_0 - j \frac{X_{L2}}{R_{L2}^2 + X_{L2}^2}$ at 'port 2' is, X_{L2} to be equal to $\sqrt{R_{L2}^2 - R_{L2}^2}$. The switch is ON and the length of the first stub can be found by:

$$L_2 = \frac{c}{\sqrt{\epsilon_e} 2\pi f_2} \tan^{-1} \left(\frac{R_{L2}^2 + X_{L2}^2}{X_{L2} \cdot Z_2} \right) \quad (4.21)$$

Any value of Z_2 can be chosen and the length of the stub can be found accordingly. By replacing these values back to the equation (4.20), a value of Z_3 can be chosen and find the length of the second stub. The only condition applied for this case is the value for reactance of the second impedance ($X_{L2} = \sqrt{R_{L2}^2 - R_{L2}^2}$). Fig. 4.22 illustrates the acceptable values for Z_{L2} . There is no condition for the impedance at the first band and it can have any values.

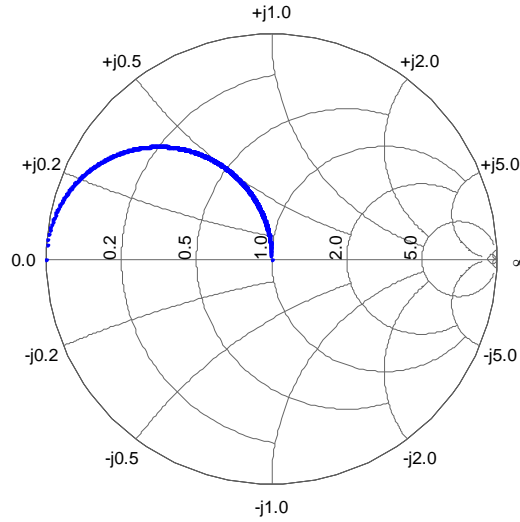


Figure 4.5-Coverage region for STS MN in case 1

The second case is when the ratio of the frequencies is an odd integer number. By considering that $\tan\theta_{L2}$ (is the electrical length of the transmission line at the second frequency) is going to infinity, then the admittance at point 'a' is $\frac{R_{L2} + jX_{L2}}{Z_1^2}$. The characteristic impedance of the transmission line can be found by $Z_1 = \sqrt{R_{L2}}$. For the first band of operation, Z_1 has been found as $\sqrt{R_{L1}}$. The only condition allow this case to be valid is $R_{L1} = R_{L2}$. The switch in ON for the second band and the first stub is just connected to the circuit; therefore, the length of the first stub is:

$$L_2 = \frac{-c}{\sqrt{\epsilon_e} 2\pi f_2} \cdot \tan^{-1}\left(\frac{R_{L2}}{X_{L2} \cdot Z_2}\right) \quad (4.22)$$

The same process applied here, the width and the length of the first stub can be calculated by aid of (4.22). The next step is going back to (4.20) which have two unknowns now; the length of the second stub can be calculated by selecting an acceptable value for Z_3 . As mentioned earlier, the resistance of both required impedances need to be equal and both of

them are equal to Z_1^2 . The STS MN in case 2 can match any impedance on any of the circles shown in Fig. 4.23.

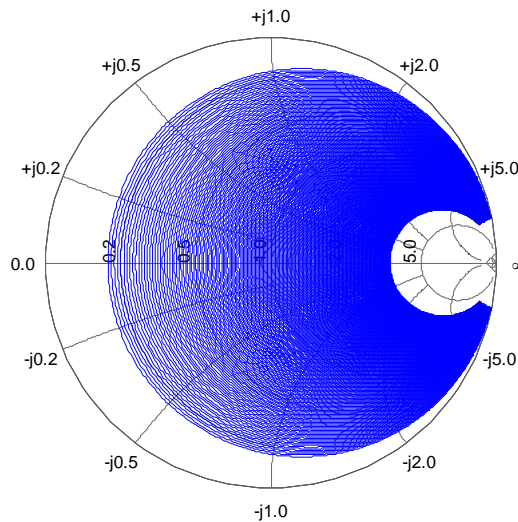


Figure 4.6-Coverage region for STS MN in case 2

The input impedance at point 'a' in the third case is (4.15) and the same condition is applied as well, which is $\text{Re}(Y_2^*)=1$ (equation for $\text{Re}(Y_2^*)$ is (4.16)). The required impedance at the second frequency needs to have suitable value for its resistance and reactance to make this argument true. The length of the first stub, when the switch is ON at the second frequency, is:

$$L_2 = \frac{-c}{\sqrt{\epsilon_e} 2\pi f_2} \tan^{-1} \left(\frac{1}{B \cdot Z_2} \right) \quad (4.23)$$

B is the susceptance of Y_2^* . The length and width of both stubs can be calculated by (4.20) and (4.23). The STS MN has no forbidden region for the required impedance at the first band, whereas, it is able to operate only in the impedances shown on the Smith chart at the second band in Fig. 4.24.

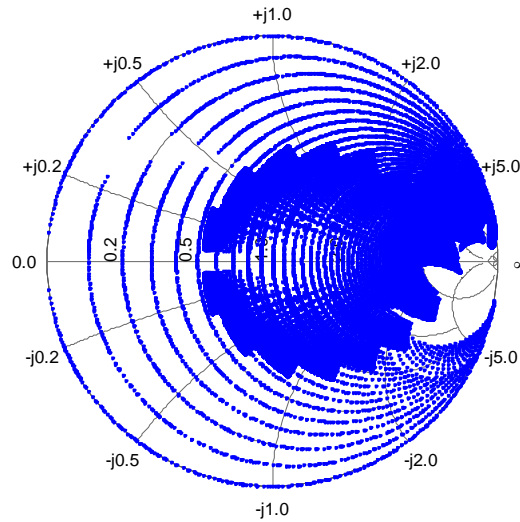


Figure 4.7-Coverage region of the STS MN in case 3

The STS MN compare to the OTS MN has excellent coverage region based on their acceptable points on the Smith chart. Finding the characteristic impedance of the stubs are independent from each other due to providing an additional stub for one band of operation.

4.3.3 Numerical Example

All the presented cases for the STS MN are represented with numerical example in this section. Table 4.1 illustrates the selected frequencies and their required impedances in each case.

Table 4.1-Selected frequencies and their required impedances for all the cases

	f_1	Z_{L1}	f_2	Z_{L2}
Case 1	900MHz	$1.052 + j0.45$	1800MHz	$0.49 + j0.49$
Case 2	900MHz	$0.5 + j0.35$	2700MHz	$0.5 + j0.65$
Case 3	782MHz	$0.8 + j1.8$	1748MHz	$0.9 + j0.13$

The length and width of the transmission line and stubs have been calculated by algorithm presented in the previous section. These values are tabulated in Table 4.2; all the values are in mm.

Table 4.2-Calculated length and width of the transmission line and stubs for STS MN in all the cases

	L_1	W_1	L_2	W_2	L_3	W_3
Case 1	52.7	1.61	8.5	0.5	5.2	0.5
Case 2	52.7	2.83	7.3	1.67	13.1	1.67
Case 3	58.4	2	23.3	0.5	26.1	0.5

The STS MN has been simulated with these values. The simulation result for case1, case 2 and case 3 are shown in Fig. 4.26, 4.27 and 4.28, respectively. The simulation result for all the cases are shown very well matched to the required impedances.

The loss of the PIN diode in the STS MN has been analyzed and is shown in Fig 4.25. There is an improvement compare to the detach stub MN and again it is proof that by this technique the losses of the switch are minimized.

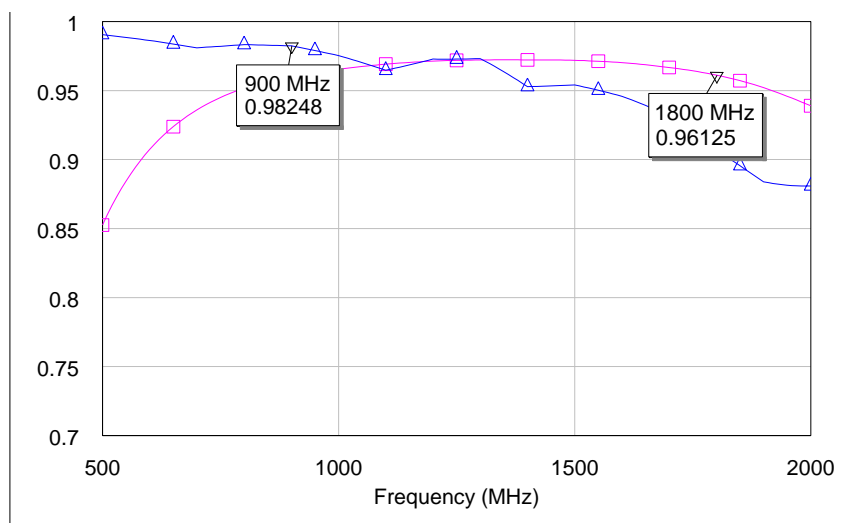


Figure 4.25-Total loss factor analysis of the switch in STS MN in OFF state (blue) and ON state (pink)

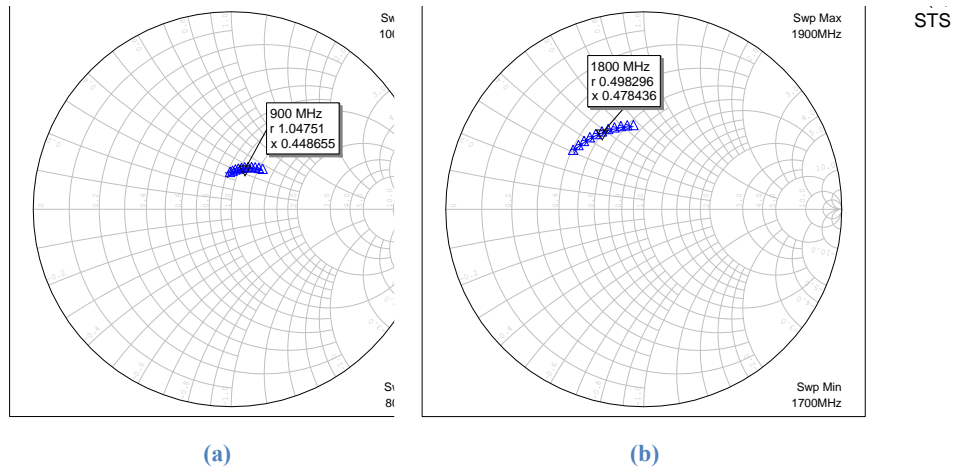


Figure 4.8-Simulation result of the STS MN in case 1 (a) OFF and (b) ON state of the switch

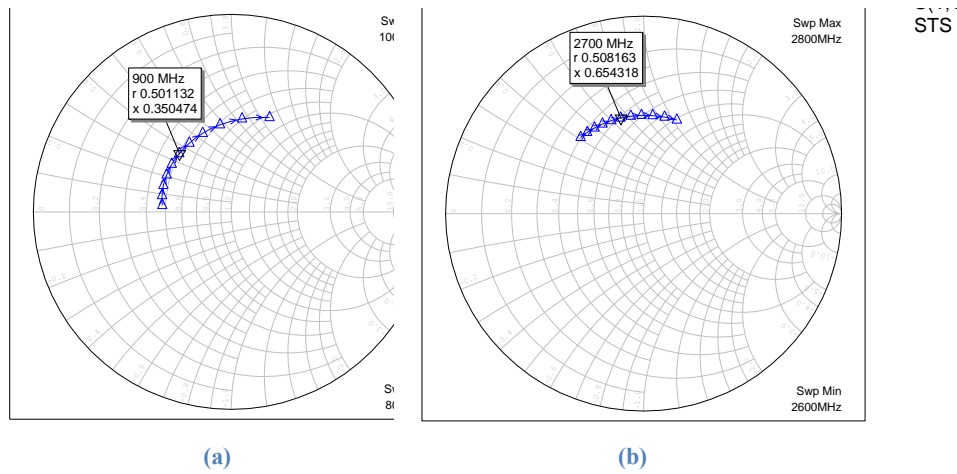


Figure 4.9-Simulation result of the STS MN in case 2 (a) OFF and (b) ON state of the switch

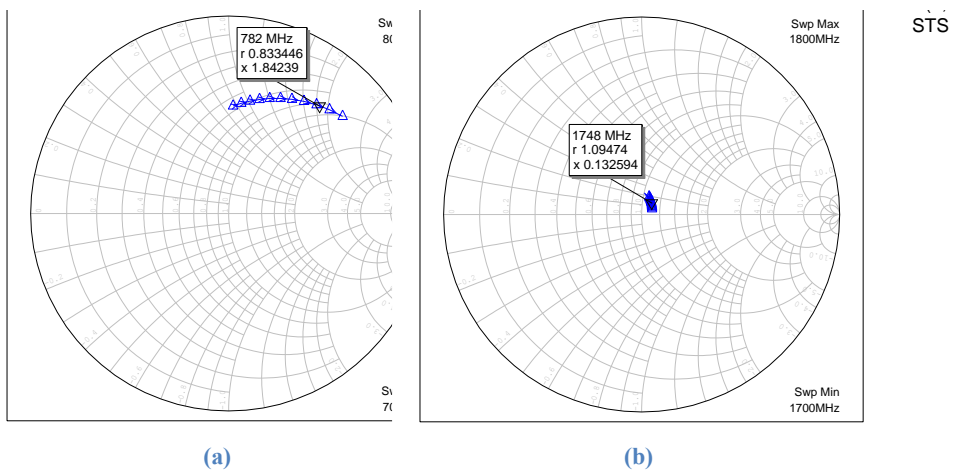


Figure 4.10-Simulation result of the STS MN in case 3 (a) OFF and (b) ON state of the switch

4.3.4 Experimental

The case 1 has been fabricated as an example of the STS MN and it is shown in Fig 4.29. The experiment results are shown in Fig. 4.30 and they are plotted on the Smith chart with the simulation result. The measured impedances and the simulation results agree very well over wide range of frequency. The slight difference between them is due to the variations in parameters in real components.



Figure 4.11-Photographs of the fabricated STS MN in case 1 (switch in the middle of the stub)

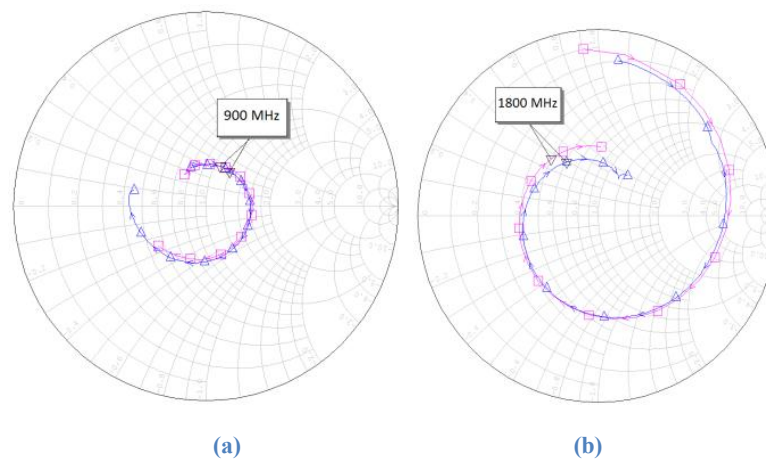


Figure 4.30-Simulated and measured input impedance of STS MN in case 1 (a) OFF state and (b) ON state

4.4 Comparison of Matching Networks

Three SB-MNs have been presented in the previous sections. The switch is not placed in the main path of the signal and this is an advantage for all the presented MNs. The last two MNs (OTS and STS MN) are more preferable than the detach stub MN as they reduced the losses introduced into the circuit by the switches. These two MNs are compared in terms of their performances in this section. One of the advantages of the OTS MN over the STS MN is using ON state of the switch at the lower frequency. But in STS, since the higher frequency

requires a shorter stub, the ON state of the switch is used at the higher frequency. Table 4.3 compares these two methods. To compare the accuracy of MNs in achieving desired impedances, the error in percentages is provided, showing the effect of the limited numbers of degrees of freedom, in ON and OFF state of the switch. These percentage errors shows the accuracy of the MNs and are calculated by $\left| \frac{\text{desired impedance} - \text{obtained impedance}}{\text{obtained impedance}} \right| * 100$. The values in Table 4.3 show that the STS method is more suitable for generating the required impedances than OTS method. Also, their coverage region on the Smith chart is another proof that STS MN can operate over wider range of the impedances.

Table 4.3-OTS and STS MN comparison

	OTS	STS
Size	3.5×3 cm	5×1.8 cm
Limitation degree in ON state	4.1%	2.8%
Limitation degree in OFF state	16.9%	0.3%
ON state of the switch	Lower frequency	Higher frequency

4.5 Harmonic Termination Network

The MNs which are applied in PAs need proper suppression of harmonics. If a MB-PA design is required to support several operation bands, harmonics which need to be terminated will increase and it makes MB-MN even more challenging to design. Impedance Buffer (IB) elements are used to provide either open or short circuit, as required, by aid of an open or short circuited shunt stub at harmonic frequencies in [96]. A shunt transmission line with a capacitor shorted to ground is another technique used by [19] and [23].

High efficiency switching classes of amplifier (Class-E, Class-F, etc) typically require combinations of open and/or short circuit termination at harmonic frequencies. For example, the ideal situation for Class-E PA is to have open circuit terminations at the second and

higher harmonic frequencies [97]. The second harmonics has been shown to be sufficient for reasonable approximation to Class-E waveforms. The problem of achieving such harmonic terminations for two different fundamental frequencies is addressed here.

4.5.1 Theory of Harmonic Termination Network

The basic idea of the proposed Harmonic Termination (HT) network is using a transmission line and an open stub both with electrical length of $\lambda/4$, (Fig 4.31). Thus this block is composed of a transmission line (TL1) and a stub (S1) which is $\lambda/4$ at the second harmonic of the higher frequency. To terminate second harmonic of the lower frequency, a second $\lambda/4$ stub (S2) is required. Then another $\lambda/4$ transmission line is required to convert the short circuit to open circuit at the 'port 1'. This requirement is satisfied by aid of the first transmission line, stub and an added transmission line (TL2). By adjusting the length of added transmission line, the cascaded line-stub-line combination can be made equivalent to a $\lambda/4$ transmission line at that specific frequency. This HT circuit concept could be extended for terminating n harmonics with n transmission lines and stubs.

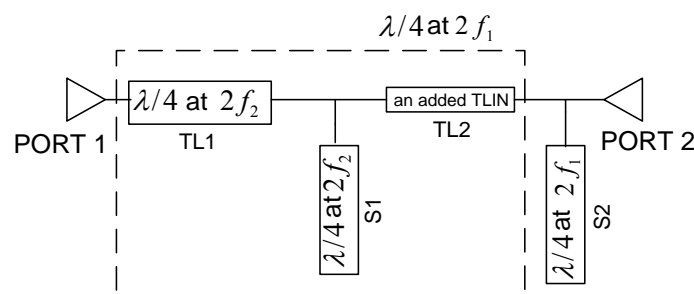


Figure 4.31-Harmonic termination circuit

4.5.2 Simulation

In order to design a multiband MN practically for a PA, termination of the second harmonic frequencies are considered. Thus, the introduced HT circuit aims to provide open circuit at the second harmonic frequencies of operating frequencies, 900 and 1800 MHz.

These two frequencies are harmonically related and the harmonic of the lower frequency will be the higher fundamental frequency; this means the HT circuit will be open for higher frequency which is not desired. To overcome this problem, at the end of the stub which provides open circuit at the higher fundamental frequency, a switch is implemented to connect it to ground. Therefore, in order to have optimum matching at operating frequencies and open circuit at second harmonics, use of a switch in HT circuit is unavoidable. An unswitched stub is applicable if frequencies are not harmonically related; otherwise the switch is implemented in the circuit. The result for simulation show open circuit at the required harmonics (Fig 4.32).

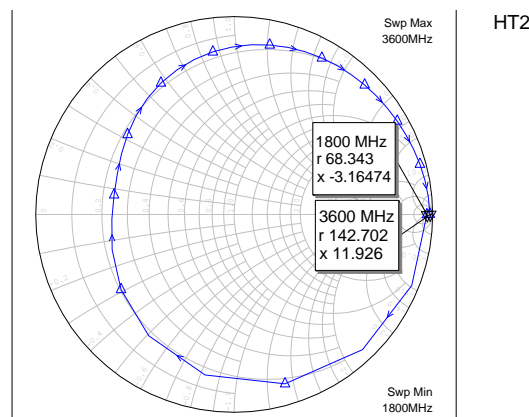


Figure 4.32-HT simulation result

4.5.3 Implementation of Harmonic Termination and Matching Network

The STS MN which uses the switch in the middle of the stub is chosen due to its accurate result. To use this MN as an output MN of PA, implementation of a HT circuit with the MN, to provide optimum matching and suppress harmonic at fundamental and harmonic frequencies respectively, is required. At 1800 MHz, both switches (in HT and MN block) are ON and all the switches are OFF at 900 MHz. Fig 4.33 shows the simulation result of implemented HT and STS MN. The exact obtained impedances at the fundamental frequencies and open circuit at their harmonic frequencies prove the validity of the technique.

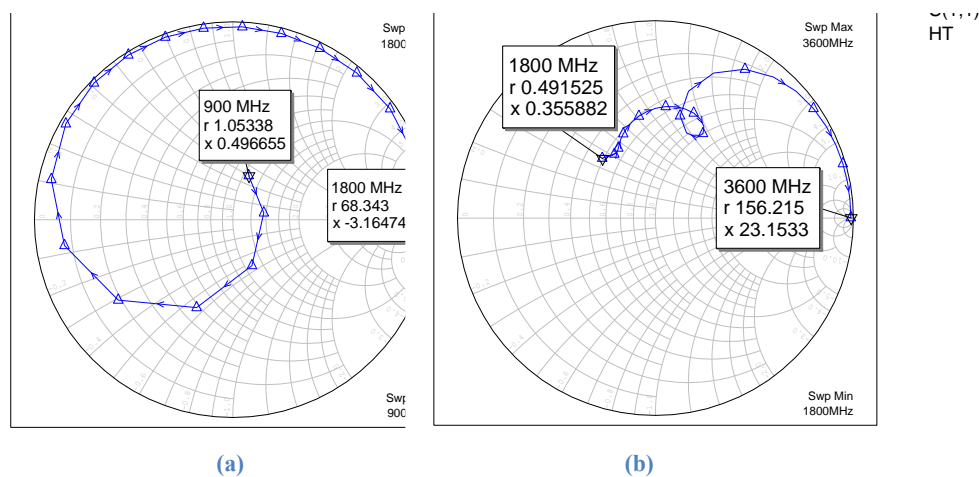


Figure 4.33-Implementation of HT and MN (a) OFF state (b) ON state

4.6 Discussion

Three methods of designing SB-MNs were studied. In this contribution, for the first time, the feasibility of different SB-MNs designed for different frequencies and impedances, by aid of the derived equations, have been shown. The proposed theoretical approaches provide a closed-form and recursive solution to design SB-MNs precisely. Numerical and experimental results have been presented by this work and the results were compared to prove the validity of the algorithm. The demonstrated OTS and STS MNs offer potential for reduced loss and improved thermal resistance control for the switching device, as well as smaller design size. The presented MNs and derived algorithm could be applied to a wide range of multiband components, such as antennas, LNAs and PAs.

Harmonic termination requirements which are important in PA applications have been taken into account for designing SB-MNs. The proposed method consists of two blocks, HT and MN. Furthermore the method of designing MN and HT can be applied not only for two but for several bands. These promising results encouraged further research on applying these MNs to design SB-PAs and they will be covered in the following chapters.

Chapter 5

Design and Simulation of Dual-Band Class-E Power Amplifiers

Improving a PA's efficiency is a big concern for PA designers. Switched-mode PAs theoretically can provide high efficiency as explained in Chapter 2. The conventional switched-mode PAs (such as Class-E) are performing with high efficiency in narrow and single bands. Future wireless communication systems, LTE and LTE advanced, will require PAs to cover more bands of operation with high output power and efficiency. Designing dual-band PAs with high output power and efficiency is a challenge for PA designers.

The proposed technique in this chapter describes the design of high efficiency Class-E PAs for single-band and dual-band purposes. The PAs in this work are designed for LTE communication system. Two bands of LTE standard will cover, 777-787 MHz and 1710-1785 MHz. In the first section, the method of designing high efficiency Class-E PA is presented and two single-band PAs are designed to prove the validity of the proposed technique. In the second and third sections, the same method has been applied to design dual-band Class-E PAs with two different devices. These PAs are showing high output performances in terms of both output power and efficiency.

5.1 Single-band Class-E Power Amplifier

The proposed technique is applied to design single-band Class-E PAs in two working bands. These two PAs are proving the validity of the technique and also, to provide a reference design to be able to compare performances in single-band and multiband applications. This method is focusing on providing the required reflection coefficient at the

drain of the transistor. This discovery is a key point of this work as it simplifies the Output Matching Network (OMN) for multiband purposes.

5.1.1 Theory

In this topology, the transistor is assumed to behave as an ideal switch and a nonlinear capacitor (C_{ds}) as shown in Fig. 5.1. Also, the OMN is considered as two parts, the shunt capacitor (C_s) and distributed output matching network (DOMN). The DOMN is intended to provide the required reflection coefficient at the drain of the transistor.

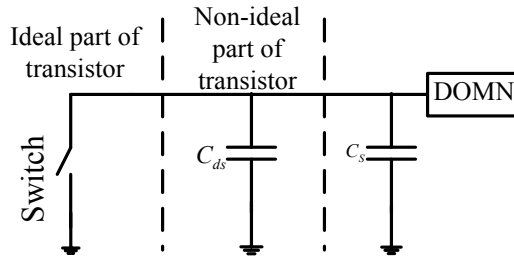


Figure 5.1-Topology of the design

To find out the desired reflection coefficient, the components of the conventional Class-E PA's OMN need to be calculated. The optimum parameters of the lumped element OMN can be calculated from equations (5.1) to (5.4) which are taken from [16], (load resistance R_L , shunt capacitance C_s , series capacitance and inductance, C_0 and L_0 respectively).

$$R_L = 0.5768 \left(\frac{V_D^2}{P_{out}} \right) \left(1 - \frac{0.451759}{Q_L} - \frac{0.402444}{Q_L^2} \right) \quad (5.1)$$

$$C_s = \frac{1}{5.44668 \omega R_L} \left(1 + \frac{0.91424}{Q_L} - \frac{1.03175}{Q_L^2} \right) \quad (5.2)$$

$$C_0 = \frac{1}{\omega R_L} \left(\frac{1}{Q_L - 0.104823} \right) \left(1 + \frac{1.101468}{Q_L - 1.7879} \right) \quad (5.3)$$

$$L_0 = \frac{Q_L R_L}{\omega} \quad (5.4)$$

These component values are calculated based on specific supply voltage V_D , required output power P_{out} and loaded quality factor (Q_L). These equations were explained earlier in more details in Chapter 2.

The DOMN is required to provide the same reflection coefficient as Fig. 5.2 (a); therefore, R_L , C_0 and L_0 are considered to find its reflection coefficient. Then, the required impedance at the drain will be found:

$$Z = R_L + j\left(\frac{-1}{\omega C_0} + \omega L_0\right) \quad (5.5)$$

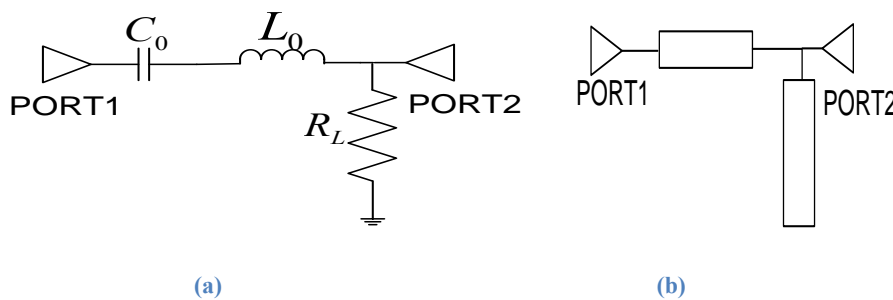


Figure 5.2-OMN (a) basic OMN for Class-E (b) distributed OMN

Transmission lines are preferred to design OMN at microwave frequency as their practical implementation is more convenient and they give a lower insertion loss, [24] and [18]. In this method, a single transmission line and a single stub have been used to provide the same impedance as the conventional lumped OMN, Fig 5.2. Conventional distributed OMN for Class-E is designed by replacing each lumped component with equivalent transmission line or stub.

The required shunt capacitor (C_s) will be added later to the designed OMN. It has been shown that second harmonic termination (HT) is sufficient to have Class-E performance to a

reasonable approximation [97]. Second HT is designed to behave as open circuit at the drain of the transistor at both frequencies. The design principle of HT is explained in Chapter 4.5. The second HT circuit and OMN are implemented together to satisfy Class-E requirement.

5.1.2 Simulation of Single-Band Power Amplifiers

Investigation of the validity of the proposed technique is to be proven by designing two single-band Class-E PAs at two frequency bands, 777-787 MHz and 1710-1785 MHz, which is suitable for LTE standard. Before starting to simulate PAs, some initial considerations needed to be thought about. The first one is to choose the right device based on the required power, operating frequency and etc. The NPTB00004 GaN (Gallium Nitride) HEMT (high electron mobility transistor) from Nitronex has been chosen. The next step is determining bias voltage according to the device datasheet and class of operation.

In PA design, there are two MNs, input matching network (IMN) and output matching network (OMN). The IMN is applied to match the source impedance and the device input impedance and minimize required input power level to obtain desired output power. The IMN has been designed by aid of transmission lines and stubs to achieve a reasonably good match. In this work, the concentration is on OMN to provide high efficiency. The OMN needs to be designed based on the design equation for Class-E operation. As mentioned earlier, one transmission line and one stub are replacing the lumped element OMN and provide the same reflection coefficient. The reflection coefficient of OMN at the drain is sufficient to avoid overlapping between voltage and current, resulting in a highly efficient PA. The lumped element components have been calculated based on equation (5.1) to (5.4). These values are shown in Table 5.1.

Table 5.1-Calculated lumped component values

Frequency band	R_L	C_s	C_0	L_0
777-787 MHz	70.2 Ω	0.6 pF	0.3 pF	142 nH
1710-1785 MHz	70.2 Ω	0.25 pF	0.14 pF	64 nH

The distributed OMN, with one transmission line and one stub, Fig 5.2 (b), has been designed to provide the same impedance as found in equation 5.5. In order to design this OMN practically for Class-E PA, termination of second harmonic has been considered. The HT circuit is designed to provide open circuit at second harmonic frequency at the drain of the transistor. The designed OMN and HT circuit are implemented together and the results are shown in Fig 5.3.

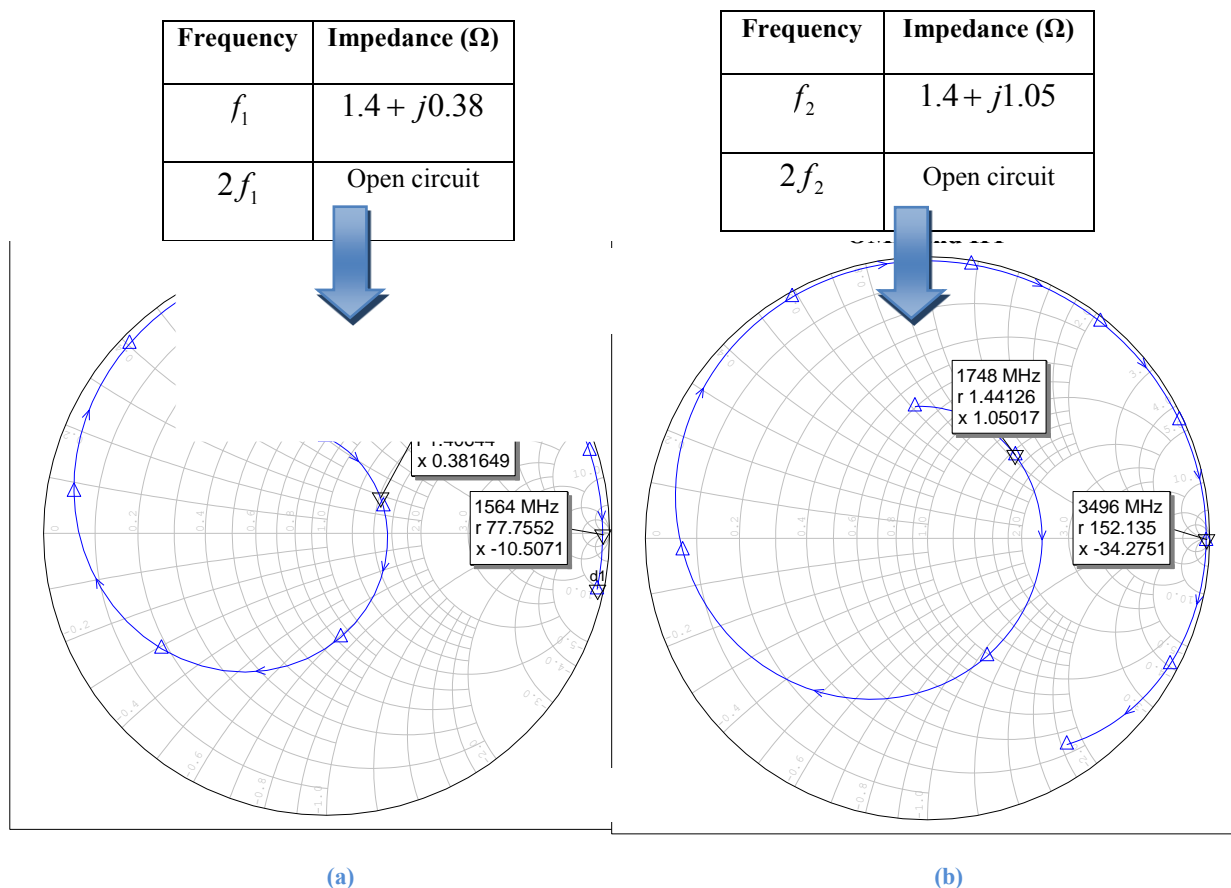
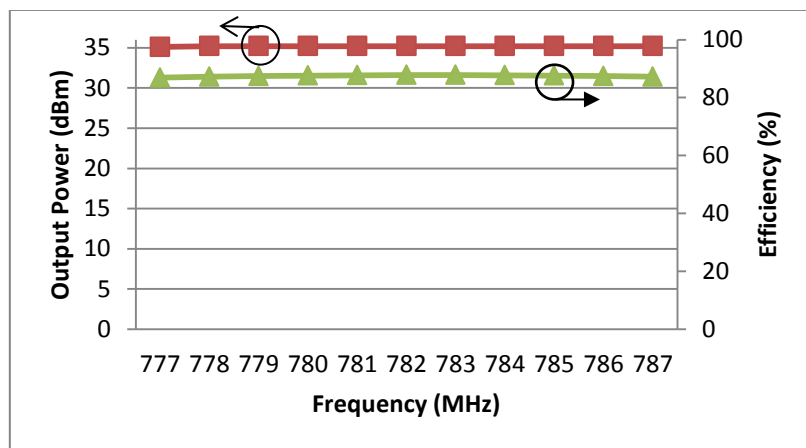


Figure 5.3-Simulation result of implemented OMN and HT circuit (a) first band and (b) second band

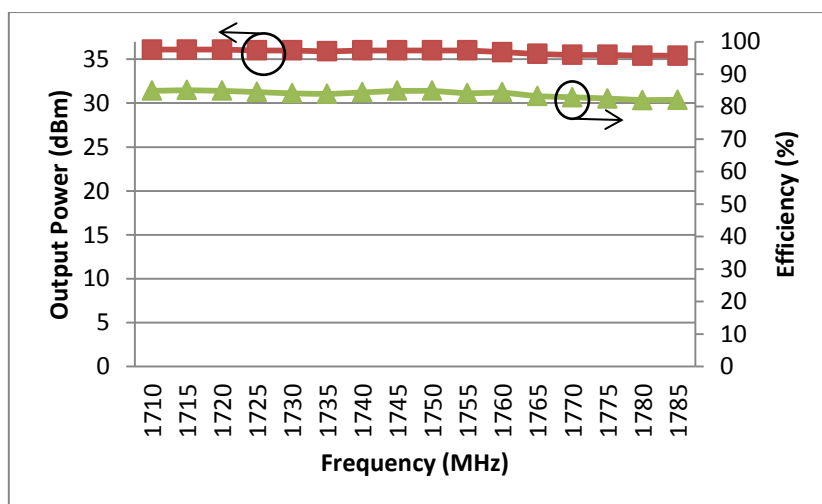
In Fig 5.3, the required impedances at the fundamental frequencies and the harmonic frequencies are revealed and the simulated results in the Smith chart shows the perfect match. This PA has been designed with $V_{DS} = 8V$ and $V_{GS} = -2.5V$. Table 5.2 and Fig 5.4 are illustrating the overall performances of these two single-band PAs at two different bands.

Table 5.2- Output performances of the single-band Class-E PAs

Frequency Band	Output Power	Drain Efficiency	PAE
777-787 MHz	35.2 dBm	87.8 %	82.7 %
1710-1785 MHz	36 dBm	85.1%	80.4 %



(a)



(b)

Figure 5.4-Output power and efficiency of the single-band PAs over the whole band of operation (a) first PA and (b) second PA

In designing Class-E PAs, avoiding overlap between the voltage and current waveform on the device plane is important to minimize the power dissipation in the device and consequently provide high efficiency and optimum performance. The transistors contain both intrinsic model and extrinsic model. The intrinsic model is an equivalent circuit model of the transistor which is dependent on the device, and they are surrounded by a package which can be shown by the extrinsic model and they are dependent on the environment embedding the device [98]. Package parasitic have a significant effect on the transistor behaviour at microwave frequency. Therefore, these effects need to be taken into account to make sure the PA is operating in the intended class of operation. To observe the waveform at the device plane, a model for the package is required, so that it can be de-embedded [99]. A linear packaged model for NPTB00004 GaN is introduced in this work. The model of the package is composed of two inductors and one capacitor. Each physical component is modelled by an electrical lumped element. The lead-frame and bond wire are the physical components which are taken into account in this model. The lead-frame of the package is modelled by capacitor (C_L) and inductor (L_L), as shown in Fig. 5.5. The bond wire is modelled by an inductor and its value can be calculated by [115]:

$$L(nH) = 5.08 \times 10^{-3} \times l(mil) \times \left[L_n \left(4 \times \frac{l(mil)}{d(mil)} \right) - 1 \right] \quad (5.6)$$

where l is the length and d is the diameter of the bond wire. The inductance of bond wire has been calculated 0.4nH as $l=1.69mm$ and $d=0.0254mm$, four of them in parallel. The capacitance of 0.45 pF and inductance of 1.12nH are taken from the package datasheet for C_L and L_L , respectively. C_{DS} is an intrinsic and nonlinear capacitance of the device, as shown in Fig 5.5 [20]. This capacitance has not been taken into account in design of the package model as its effect needs to be considered to satisfy the required shunt capacitpr.

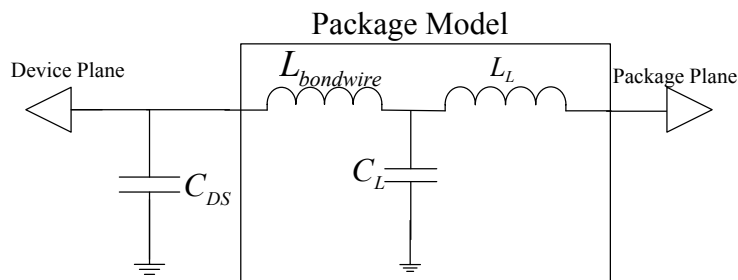


Figure 5.5-The Package model

To access the waveform at the device plane, the effect of the package element needs to be cancelled. Another network needs to be introduced which is mirrored version of the package model with negative values and here this network is called NEGATE. By presenting the NEGATE network at the drain of the extrinsic transistor, the elements of the package will be cancelled. Therefore, the waveform at port 2 of the NEGATE network is the waveform at the device plane, Fig. 5.6. The package model needs to be added after the NEGATE network in cascade. The cascaded NEGATE and package model provide transparent structure. Therefore, the obtained waveforms at port 3 are the waveforms at the package plane.

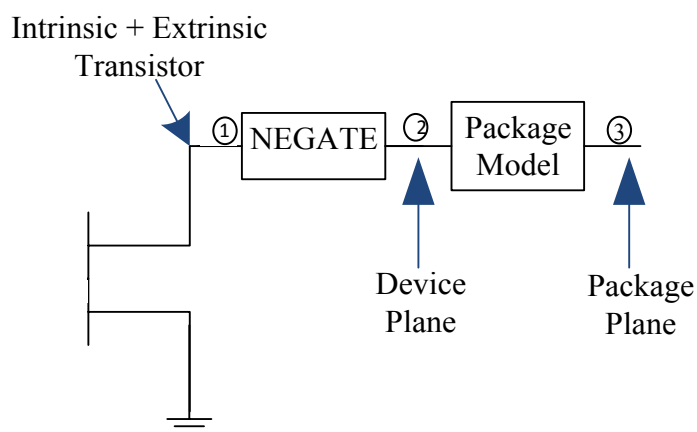


Figure 5.6-De-embedding package of the transistor with mirrored negative the package model

The voltage and current waveforms for both PAs are shown in Fig. 5.7 and 5.8. For both PAs, the waveforms are illustrated at the device plane and the package plane. The desired voltage and current waveforms for Class-E mode are observed at the device plane.

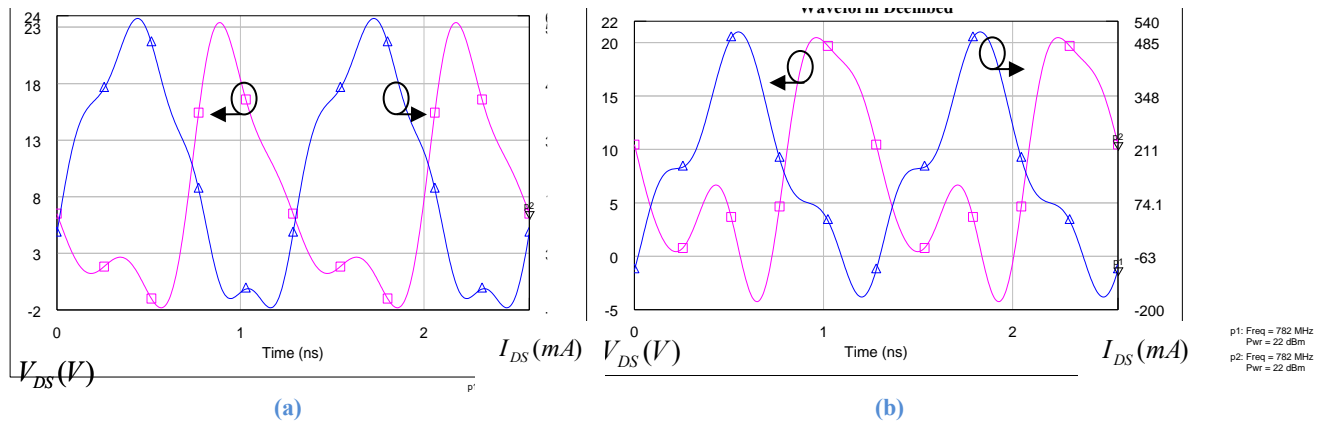


Figure 5.7-Simulated voltage and current waveform for the first PA at (a) the device plane and (b) package plane

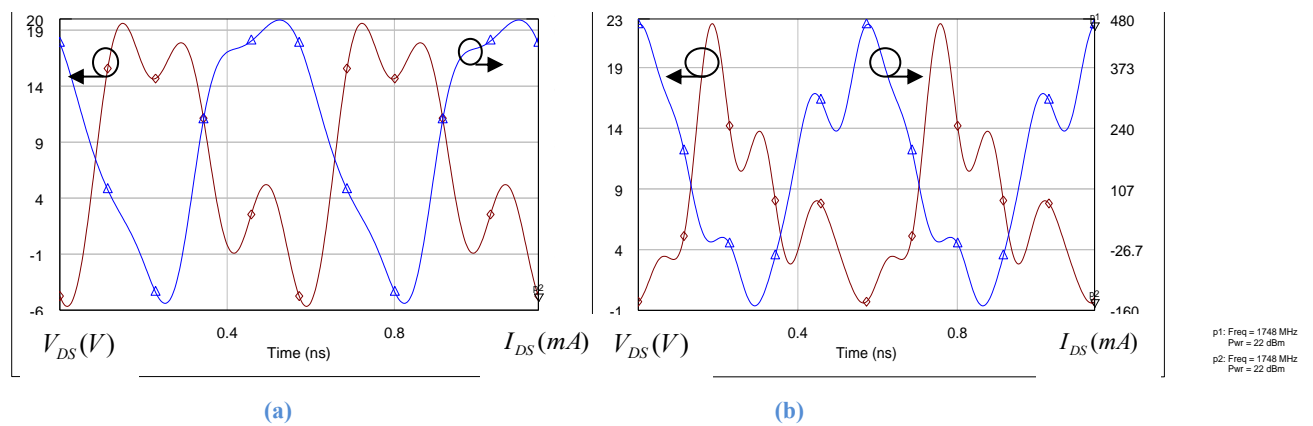


Figure 5.8-Simulated voltage and current waveform for the second PA at (a) the device plane and (b) package plane

When the single-band Class-E PAs have been completed as reference designs and achieved good performances, it is time to move forward and design dual-band Class-E PA.

5.2 Dual-band Class-E Power Amplifier with GaAs HFET

The actual realisation of dual-band Class-E PA is presented here. Class-E PA has highly frequency dependent characteristics. Therefore, designing a dual-band Class-E PA is challenging because optimum output matching and harmonic elimination have to be achieved

in both bands at the same time with a single OMN to satisfy the required efficiency and output power in both operating bands. In Chapter 3, some of the MB-PAs and SB-PAs in the literature, designed with multiband and switched-band MNs, respectively, are discussed. Here, a quick review of the reported dual-band MNs is presented. Impedance transformers are a popular technique to design MB-MNs. Two one-sixth-wave transmission line sections have been proposed with an approximate analytical solution in [100] to provide matching at f_0 and its doubled frequency ($2f_0$). Monzon [102] derived an exact analytical solution for this MN in 2002. Monzon [103] and Orfanidis [104] extended this MN to operate in any two frequencies (not harmonically related frequencies) in 2003. Designed dual-band MNs in [100] and [102]-[104] are just able to match resistive loads. Impedance transformers for complex loads at two frequencies are introduced in [101], [105]-[108]. The obtained characteristic impedance of transmission lines in [101] and [107] are high and resulting in very thin transmission lines (which is not practical). Two-section shunt stub transformers are designed in [108] and provide dual-band matching. The other technique of designing dual-band MN is presented in [109]. This dual-band MN used a LC multi-resonant circuit to provide open or short circuit at different frequencies. These MNs suffer from complexity in design and limitation in the coverage region.

The proposed dual-band MN in this chapter addresses the complexity of the reported dual-band MNs and is able to provide matching for any frequencies and impedances. As mentioned in the introduction of this chapter, it is possible to obtain high output performance in dual-band operation by providing the required reflection coefficient at the drain of the device. The dual-band PA is designed without switches to minimize the number of components and reduce the losses introduced by switches. This proposed technique obtained high efficiency in both bands by simplifying and increasing flexibility of OMN. The

possibility of designing a multiband Class-E PA with acceptable performances is increased by introducing this technique.

5.2.1 Theory

The dual-band Class-E PA presented in this work is designed with a distributed OMN based on two lumped element networks. Starting from calculating optimum lumped element; as it is understandable from the equations (5.1) to (5.4), the OMN's components of Class-E PA are varied with frequency. There are two ways to design OMN (i) lumped element and (ii) distributed OMN. OMN for multiband Class-E PA with lumped element would require switches to satisfy optimum impedance termination for different working bands. Replacing each component with the equivalent transmission line or stub could be the distributed OMN method which still requires switches for required working bands. The Class-E PA design topology in the previous section proved that the reflection coefficient presented at the drain of the transistor shaped the current and voltage waveforms, and avoid overlapping between these two waveforms. A single transmission line and a single stub, tuned by width and length, have been used in the OMN to provide the same reflection coefficient as the lumped element networks at desired frequencies, Fig 5.2. Having only a single transmission line and a single stub will enable working simultaneously in two frequencies and make the design more compact than substituting each component with their equivalent transmission line. This technique of OMN design makes the circuit more compact and gives a more reliable performance at both bands of operation. The key point of this PA lies with the ability to simplify the circuit to enable the achieving of the required Class-E waveform and constant high efficiency in all bands covered.

The IMN can be designed to be broadband, tunable or dual-band. A broadband IMN degrades the performance of the PA over the large bandwidth and tunable IMN will introduce

losses by using a switch in the network. Therefore, the dual-band IMN is designed to have promising return loss in both of the desired bands.

5.2.2 Simulation

This dual-band PA is designed for the LTE system to cover two bands, 777-787 MHz and 1710-1785 MHz and output power of 23dBm in both bands. Gallium Arsenide Hetero junction Field-Effect Transistor (GaAs HFET) is chosen for this dual-band Class-E PA. Components are calculated for both bands, based on the desired output power and supply voltage; and Q_L set as 10.

The impedance of this lumped element network has been found by aid of equation (5.5). The OMN with one transmission line and one stub, Fig. 5.2(b), has been designed to provide the same impedances as found from equation (5.5) at both bands. This dual-band PA designed without shunt capacitor and assumed internal capacitance of the transistor can fulfil the required capacitance. In order to design this OMN practically, termination of the second harmonic frequencies is considered.

5.2.3 Measurement

After completing the CAD design, the PA is ready for physical implementation. The manufactured PA is shown in Fig. 5.9. This PA has been fabricated with microstrip using a substrate from Taconic, RF_35_0300 and its properties are shown in Table 5.3. GaAs HFET from Tri-Quint is used as the power device. In class-E operation, the transistor should be biased close to pinch off and driven into compression. A few measurements are required to find the desired gate voltages and RF input power. The pinch off value was obtained from the device datasheet which is -2.1 V. Then, the PA was driven with different input RF power levels to find the required input power to make the performance of the PA independent of the

gate voltage. The results in Fig. 5.10 show that input powers of more than 12 dBm are appropriate for both bands.

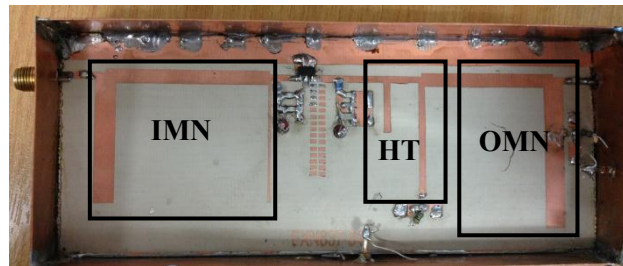
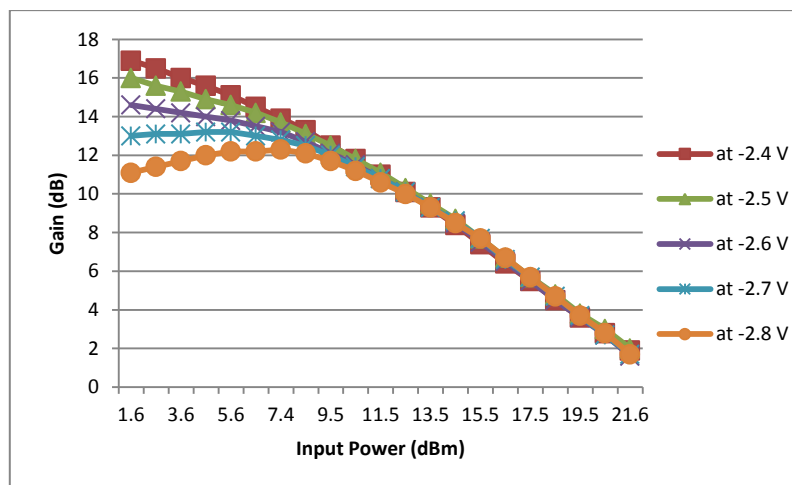
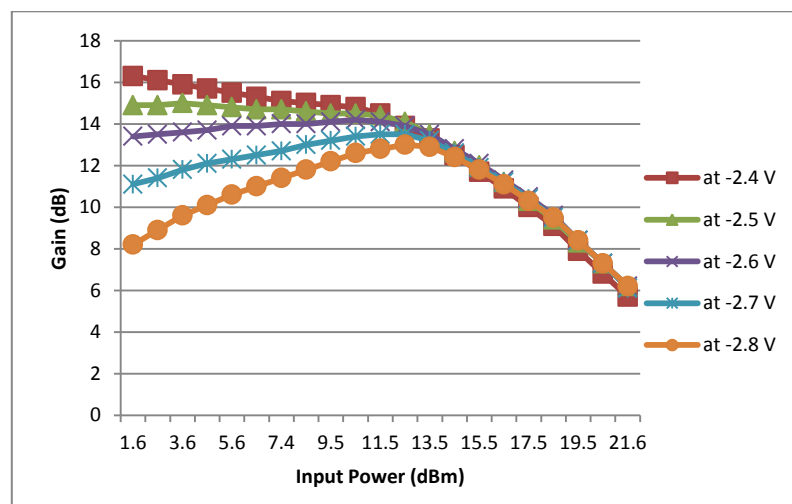


Figure 5.9-Fabricated prototype of dual-band Class-E PA



(a)



(b)

Figure 5.10- Gain versus input power with different gate voltages (a) lower band and (b) higher band

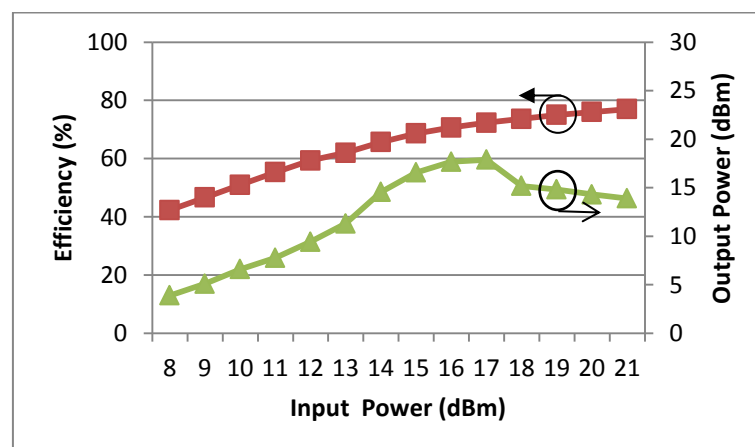
Table 5.3-Substrate properties

Properties	Values
Relative dielectric constant (ϵ_r)	3.5
Substrate thickness (H)	0.76 mm
Conductor Thickness (T)	0.035 mm
Dielectric loss tangent (Tand)	0.0025

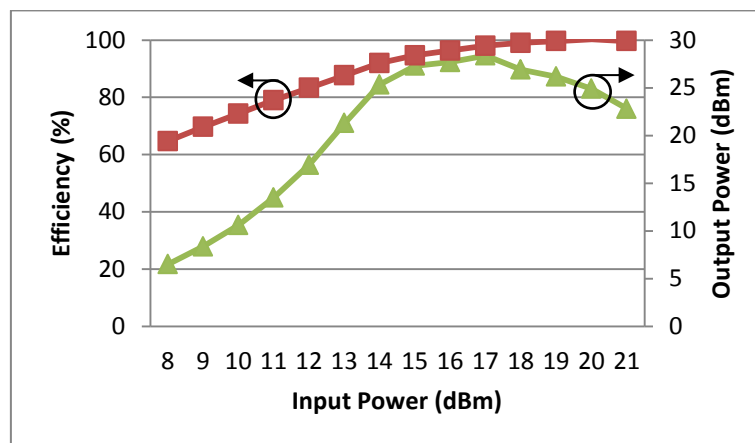
The PA performance using the obtained parameters from the above measurement is presented in Table 5.4 in terms of output power and efficiency. Fig. 5.11 shows the efficiency and output power of the PA with varying input power in both bands. In Table 5.4, the power and efficiency figures given are for 16dBm input power. To the author's knowledge, the obtained efficiency is the highest reported to date for a dual-band Class-E with such a big difference of frequency bands.

Table 5.4-Dual-band PA with GaAs transistor Performance

	Output Power	Drain efficiency	PAE
First band	22dBm	60%	55%
Second band	27dBm	84.5%	72.6%



(a)

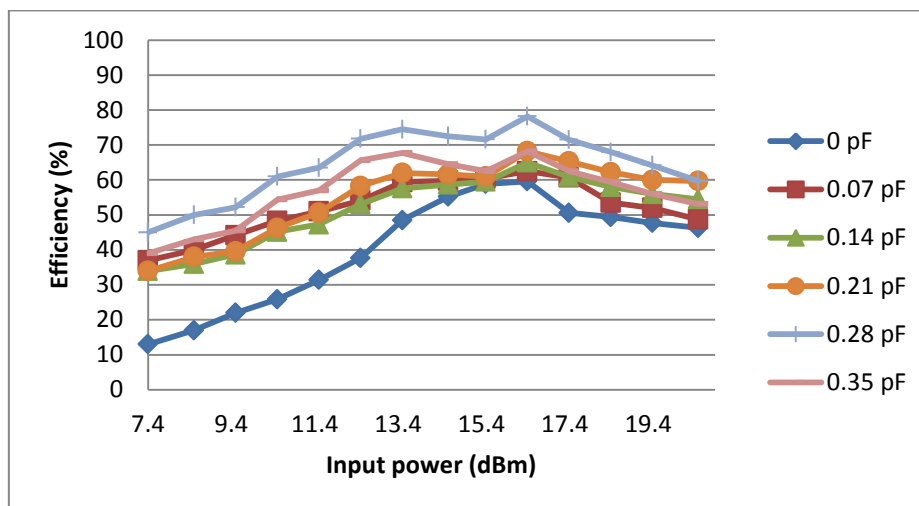


(b)

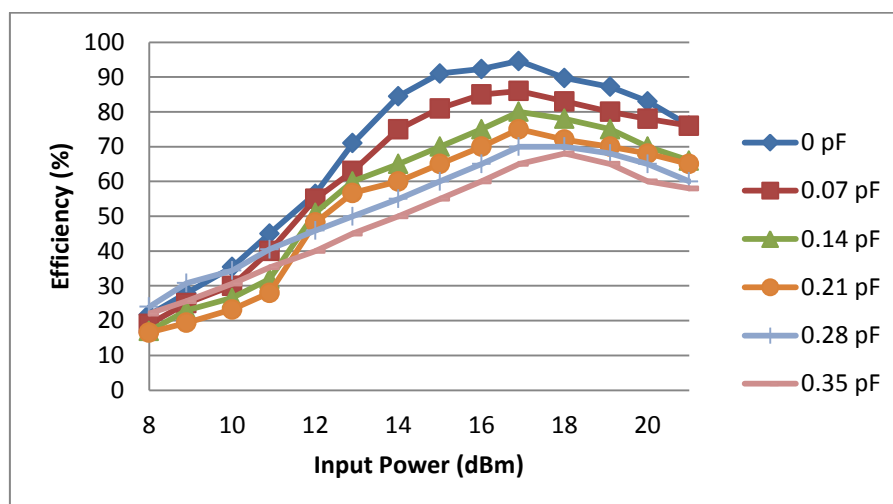
Figure 5.9-Measured efficiency and output power of the dual-bend PA with GaAs transistor versus input power (a) first frequency band (b) second frequency band

5.2.4 Measurement with Different Shunt Capacitor Values

The measurements of the dual-band Class-E PA show higher efficiency in the higher frequency band and more output power. Although the efficiency in the lower band is good among reported efficiencies, the big gap introduced between efficiencies of two working frequency bands is investigated in this section. This dual-band Class-E PA has been designed based on the assumption that the internal capacitance of the transistor is sufficient for both bands. In this section, a different value of capacitor is applied and its effect on the PA's output performance is investigated. The value of the shunt capacitor across the transistor is an important component to produce the desired efficiency and output power and it takes different values for different frequencies. The PA has been tested with different values of shunt capacitor and changes in efficiency are shown in Fig. 5.12 and its effect on output power of PA is shown in Fig. 5.13. Different values of capacitor are provided by tuning the length of the stub. In the lower band, Fig. 5.12 (a), the efficiency reaches a maximum (80%) when the shunt capacitance is 0.28pF. Fig. 5.12 (b) shows that efficiency degrades by adding any capacitance in the higher band. For the higher band, the calculated shunt capacitor is 0.25 pF, and this is provided by the internal drain capacitance in this package transistor.



(a)

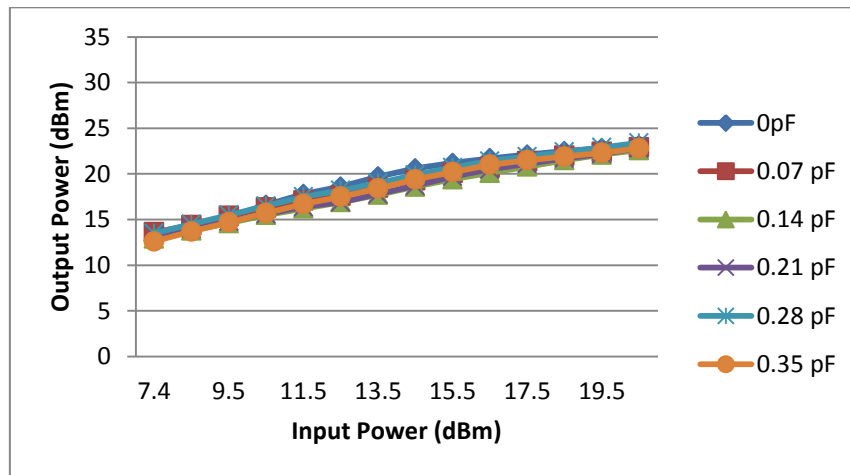


(b)

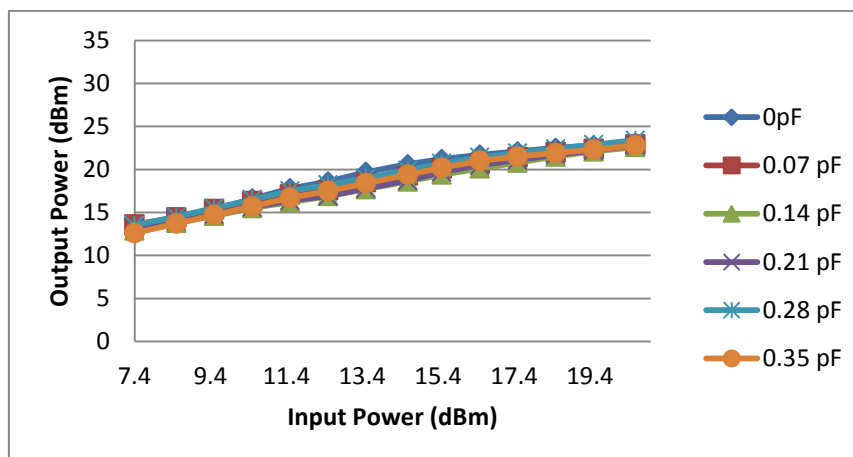
Figure 5.10-Efficiency with different shunt capacitor in (a) lower frequency band and (b) higher frequency band. Legend shows the shunt capacitor values

Setting the value of the capacitance close to the ideal value for one of the operating frequencies using a shunt capacitor will yield a higher performance in that particular band and relatively lower performance in the other band. One option could be using a capacitance in between which would degrade the performance of both bands from their ideal result. For example, 0.14pF could be a suitable compromise capacitance value in between of the required capacitance of both bands. The resulting efficiencies in the lower and the higher bands are 65% and 75%, respectively. The efficiency of the lower band increases by 5%, whereas efficiency of the higher band degrades about 10%. Therefore, to have high efficiency

in both bands, it is required to have different shunt capacitance which could be selected by using a switch.



(a)



(b)

Figure 5.11-Output Power with different shunt capacitor in (a) lower band and (b) higher band. Legend shows the shunt capacitor values

5.3 Dual-band Class-E Power Amplifier with GaN HEMT

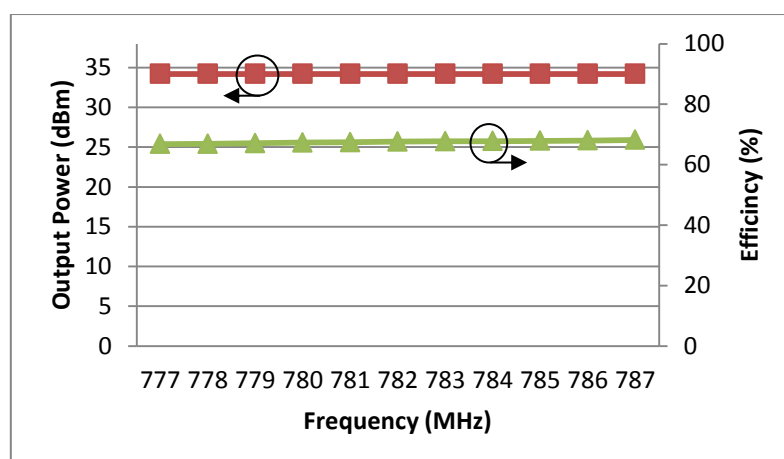
The dual-band Class-E PA with high power transistor, GaN HEMT from Nitronex, has been designed based on the developed theory to prove the validation of the method. The similar performances are expected, but with higher output power, as a high power transistor has been used for this design.

5.3.1 Simulation

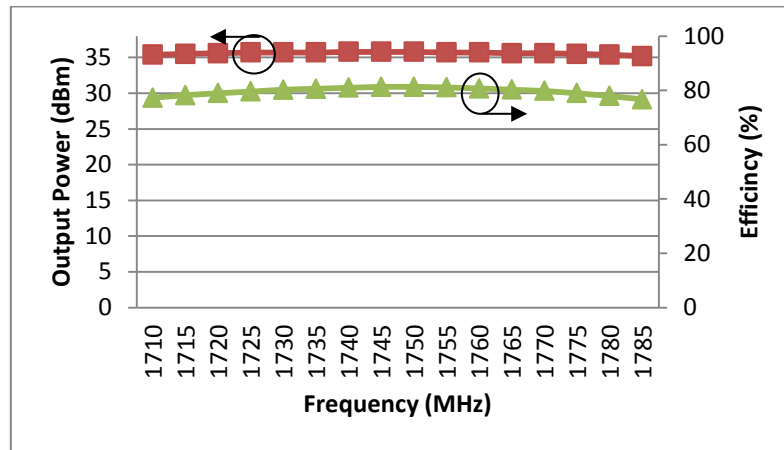
The calculated values for optimum OMN are represented in Table 5.1. The OMN has been designed as explained earlier based on the calculated impedances (equation (5.5)). At the first stage of the design, the required external shunt capacitor has been ignored and it has been assumed that the internal capacitance of the device can satisfy the required capacitance. The simulation result of this PA in both bands is shown in Table 5.5. Output power and efficiency over the whole band of operation are shown in Fig 5.13. The efficiency and output power are staying constant over the whole band. Fig. 5.14 shows the voltage (red) and current (blue) waveform at the device plane in both bands. It is good to note that the waveform of the second band, Fig. 5.14 (b), provides better coverage and resulting higher output performances.

Table 5.5-Dual-band Class-E PA with GaN performances

	Output Power	Drain Efficiency	PAE
First band	34.2 dBm	67.6%	61.4%
Second band	35.8 dBm	81.3%	76.8%

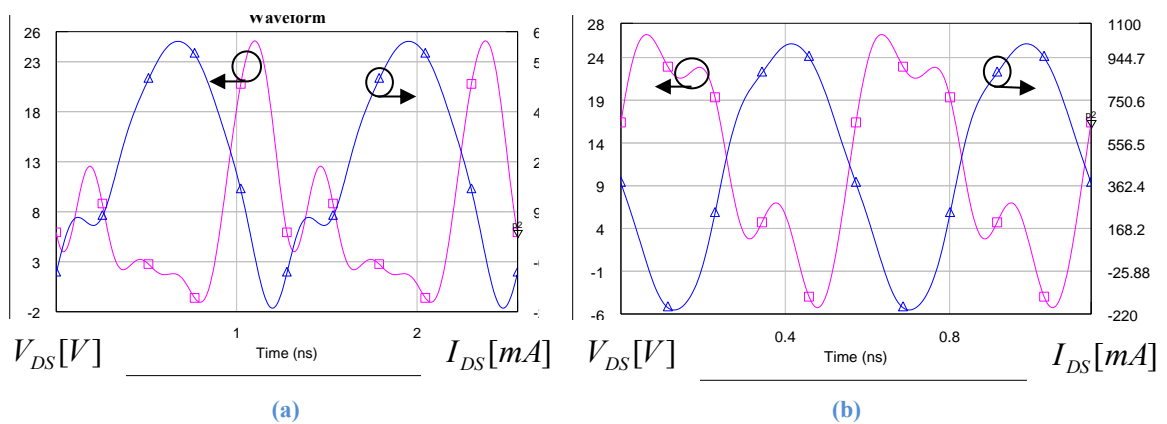


(a)



(b)

Figure 5.12-Simulated output power and efficiency of the dual-band PA with GaN transistor over frequency in (a) lower and (b) higher band



(a)

(b)

Figure 5.13-Voltage and current waveforms in (a) lower and (b) higher band

The two different efficiencies in two bands result from the simulated dual-band PA as explained in the previous section. The higher band provides higher output power and efficiency, 35.8 dBm and 81.3%. Therefore, it can be concluded that the internal capacitance of the transistor is satisfying the calculated shunt capacitance (0.25 pF). Lower efficiency and output power have been obtained in the lower band of operation. The calculated shunt capacitor for the first band is 0.6 pF and to satisfy this required capacitance, an external shunt capacitor is needed.

5.3.2 Measurement with Different Shunt Capacitor Values

The dual-band Class-E PA has been tested with different shunt capacitor values varying from 0.2 pF to 1pF. The efficiencies in both bands with different shunt capacitors are shown in Fig 5.15. As shown in Fig 5.16 (a), efficiency in the lower band is improving from 67% to 76% as capacitance is increasing from 0 pF to 0.6 pF. For capacitance values higher than 0.8 pF, the efficiency is decreasing. The 0.6 pF is the calculated shunt capacitance which fulfils the value for an external shunt capacitance. In the higher band the story is different; efficiency is degraded by adding an external shunt capacitance. The higher efficiency of 81.3% is achieved with 0pF external capacitance. In the higher band, 0.25 pF is covered by the internal capacitance of the transistor.

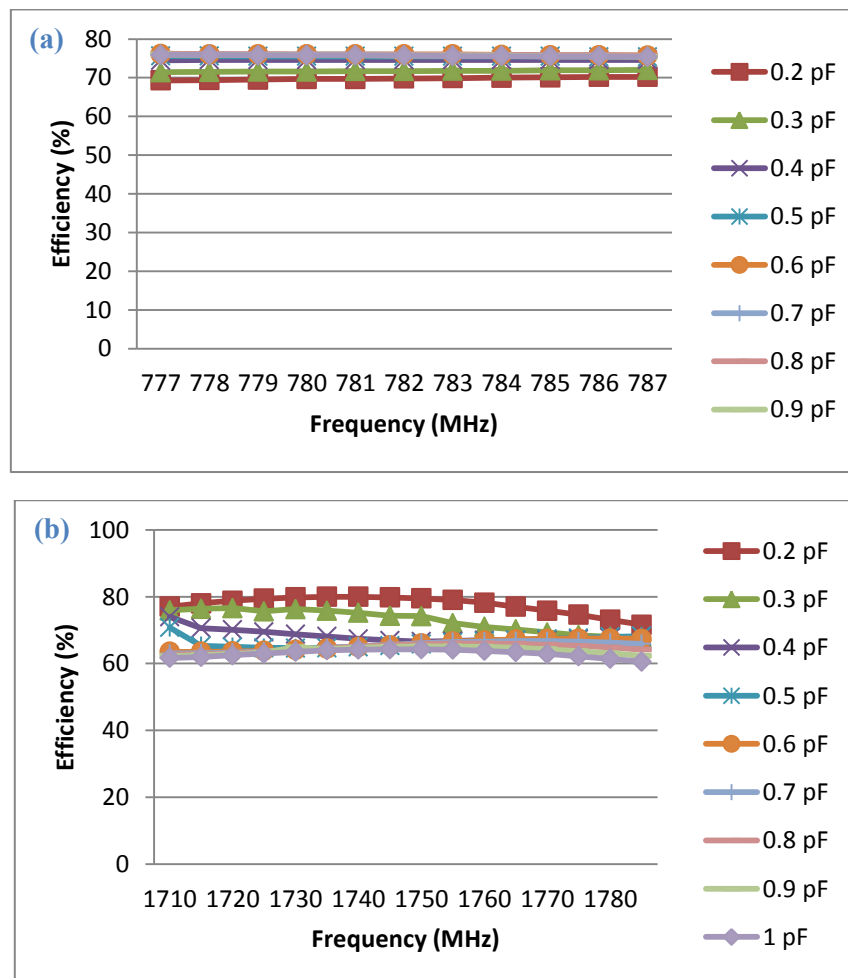


Figure 5.14-Efficiency with different shunt capacitor in (a) lower band and (b) higher band. Legend shows the shunt capacitor values

5.4 Discussion

This chapter was focused on designing dual-band Class-E PA, starting with two reference PA design in both desired bands. Two dual-band PAs have been designed with the same technique but different transistors. Drain efficiency of 60% and 84.5% and output power of 22dBm and 27dBm have been measured for lower band and higher band of operation, respectively. The second dual-band Class-E PA has been designed with a GaN HEMT. 67% efficiency and 34.2dBm is the output performance for the lower band of operation, while the higher band shows 81.3% efficiency and 35.8dBm output power. This design exercise has demonstrated that having a dual-band Class-E PA in two different and widely separated bands is feasible at the cost of having a lower efficiency in one of the bands. The different output performances in the two bands of operation are due to different required shunt capacitance value across the transistor. Simulations and measurements in the previous section prove that applying the required external capacitance will improve the PA's performance at that specific band. Therefore, a new methodology is proposed in the next chapter to provide similar and high performances at both bands of operation.

Chapter 6

Design and Simulation of Switched-Band Class-E Power Amplifiers

The dual-band Class-E PAs, introduced in the previous chapter, proved the feasibility of achieving high efficiency in two bands with the proposed technique. There was one drawback, where higher efficiency was obtained in one band and relatively lower in the other band. These differences in efficiency have been investigated and are due to the different required shunt capacitance for two individual frequency bands. In Chapter 5, one solution has been proposed to achieve the same performance in terms of output power and efficiency in all working bands by switching the shunt capacitance between the values, depending upon which band is required.

This chapter will describe the design procedure for switched-band Class-E PAs. The key point of designing the switched-band Class-E PA in this chapter lies in providing optimum OMN condition and shunt capacitance by aid of switches to achieve high and constant output performances in all working bands. Initially, a switched-band Class-E PA with a switch in OMN and a switched shunt capacitor across the transistor was designed and measured over two bands of operation. However, the measured result of this PA was not satisfactory in terms of efficiency in both working bands, compared to the dual-band PA. Therefore, another switched-band Class-E PA was designed using a switched shunt capacitor and a fixed dual-band OMN. A fixed dual-band OMN used in conjunction with a switched shunt capacitance provides similar performances in both bands but with some compromise arising from the switch losses. A dual-band Class-E PA without a switched shunt capacitance gives better

performances in one band and worse in the other. The tradeoffs between these design approaches are examined at the end of the chapter.

6.1 Switchable Matching Power Amplifier

The challenge in this work is to provide high and similar efficiency and output power in both working bands. A dual-band OMN has been used in the dual-band PA, as explained in Chapter 5, and obviously, the dual-band OMN is not able to provide the exact required optimum reflection coefficient for both bands simultaneously. This will reduce the delivered output power to the load. The proposed switched-band PA in this section has a switch in the OMN to deliver higher output power to the load and another switch to the shunt capacitor across the transistor to provide higher efficiency. This PA is called Switchable Matching PA (SMPA).

6.1.1 Theory

As discussed in Chapter 5, the shunt capacitor is considered as a separate part of OMN in this Class-E PA design methodology. From now on in this work, the OMN refers to the matching network, excluding the shunt capacitor. In the SMPA, both OMN and shunt capacitor are switching to their optimum requirement for each band. The Stub to Short (STS) OMN is implemented in the SMPA. In Chapter 4, the STS OMN has been explained in more detail. The STS OMN consists of a transmission line, stub and a switch in the middle of the stub to switch to ground. The ON state of the switch provides a shorter and grounded stub, where a longer and open stub is provided by OFF state of the switch. The technique of the switching in the STS OMN helps to minimize losses which are introduced by the switches, as explained in Chapter 4. Switching between two optimum OMNs in two different bands results in delivering more output power to the load because of presenting a better match with switched-band OMN, rather than the dual-band OMN.

The presented dual-band PAs in Chapter 5 show that to achieve high efficiency in both bands of operation, the shunt capacitor across the transistor has to be variable. Therefore, the shunt capacitor across the transistor needs to switch between two different required capacitance values. Three methods of switched shunt capacitor are presented here. In the first method, two stubs are used with a switch in the middle, Fig. 6.1(a). When the switch is OFF, the stub provides the required capacitance for the higher band of operation (as a shorter stub is required at higher bands). The length of the ideal stub can be found by:

$$l_1 = \frac{c}{\omega_1} \tan^{-1}(Z_0 \cdot \omega_1 \cdot C_1) \quad (6.1)$$

where C_1 is the required capacitance at the higher band. At the ON state of the switch, the other stub is introduced into the circuit and provides shunt capacitance at the lower band. The length of the second stub can be found by (6.1). The other two techniques are using lumped elements. The first one uses two series capacitors and a switch, Fig. 6.1(b). The OFF state of the switch provides two series capacitors and the ON state just connects the first capacitor. C_1 is the required capacitor at the lower band (switch is ON). The other capacitor should be optimizing to provide required capacitance by the aid of two series capacitors at the higher band, and the switch is OFF. The value of the second capacitor can be calculated by $C_2 = \frac{C_1 \cdot C_t}{C_1 - C_t}$, C_1 and C_t are the required capacitance for the lower and higher bands, respectively, and C_2 is the series capacitor.

The next technique uses two parallel capacitors with one of the capacitors connected by a switch to ground, Fig. 6.1(c). When the switch is OFF, the second capacitor is not connected and required capacitance for the higher band is satisfied by the first capacitor. In the ON state of the switch, the second capacitor is connected to ground; therefore, the parallel combination of the capacitors provides the required capacitance for the lower bands. The ON state of the

switch is applied in the lower band for all of these three methods; on the other hand, the advantage of method 2 and 3 is switching to ground as this minimises the thermal resistance which result in providing more reliable operation and reduce the tendency for memory effects in the non-linear behaviour. Relative performances of these topologies in terms of the amount of loss are related to the actual loss of component (transmission line and capacitors). RF current entering to the switches is another factor need to be monitored to analyse the losses of these topologies.

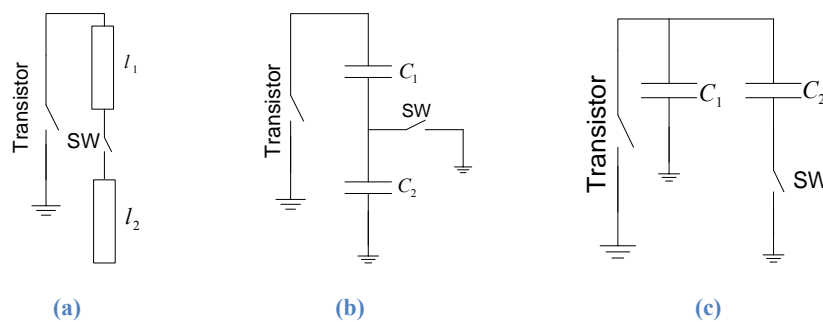


Figure 6.1-Different method of switching capacitors (a) switching between stubs (b) series capacitors (b) parallel capacitors

All of the methods introduced above are feasible if switching between two different capacitances is required. In some cases (for example this work), only switching to one capacitor is required as the required capacitance in one of the states is zero. To make this possible, two switching capacitance methods are presented here. Fig. 6.2(a) illustrates the Method 1. When the switch is ON, a stub is introduced to the circuit and provides the required shunt capacitance. The appropriate length for the stub can be calculated by (6.1). In the OFF state of the switch there is a small residual capacitance which is about 0.007pF. Method 2 utilizes a capacitor with a switch to the ground, Fig. 6.2(b). The latter method is preferable as it switches to ground and reduces the losses of the switch.

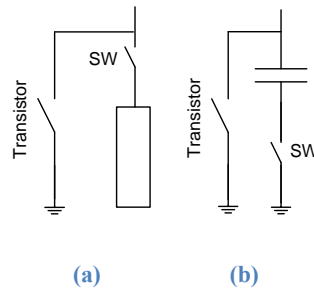


Figure 6.2- Proposed method for shunt capacitance (a) with a stub (b) with a capacitor

The schematic of the SMPA is shown in Fig. 6.3. In the lower band, SW_1 is ON and the shunt capacitor is connected; whereas, SW_2 is OFF and both stubs (S_1 and S_2) are introduced into the OMN to present the required reflection coefficient at the drain of the transistor. There is no need for a shunt capacitor in the higher band as the internal capacitance is sufficient enough (SW_1 is OFF) but SW_2 is ON to present the short stub (S_1).

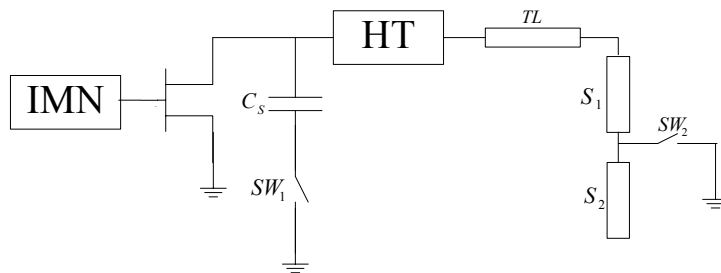


Figure 6.3- SMPA schematic

6.1.2 Simulation

The SMPA has been simulated with STS OMN and method 2 of switching the shunt capacitor. The GaN transistor from Nitronex has been used in the SMPA. The shunt capacitance of 0.6 pF has been calculated for the lower band of operation and 0.4 pF capacitance for the higher band, which is satisfied by the internal capacitance of the transistor. So by turning ON the switch (SW_1) at the lower band and OFF at the higher band, this requirement is met. As mentioned in the previous section, SW_2 (a switch in the OMN) is OFF in the lower band and ON in the higher band.

The dual-band IMN (explained in Chapter 5) and HT (explained in Chapter 4) circuit to terminate the second harmonics have been designed to implement the SMPA. After completing design of SMPA, the next step is to find required gate voltage bias and appropriate input power for Class-E operation by sweeping the gate voltage and input power. The gate voltage of -2.5 V and input power of 22 dBm are desired for this PA. In the lower band, 34.1 dBm output power and 60% efficiency is achieved. Output power of 33.6 dBm and efficiency of 71% is reported in the higher band. The NEGATE network is applied to compensate the effect of the transistor package and observe the waveform at the device plane. All of the waveforms in this chapter are shown observed at the device plane. The voltage (pink) and current (blue) waveforms are shown in Fig. 6.4 for the lower and higher band of operation. As shown in the figure below, there is very small overlap between two waveforms. This demonstrates that the dissipation power in the transistor is small, which is essential for high efficiency PA's performance.

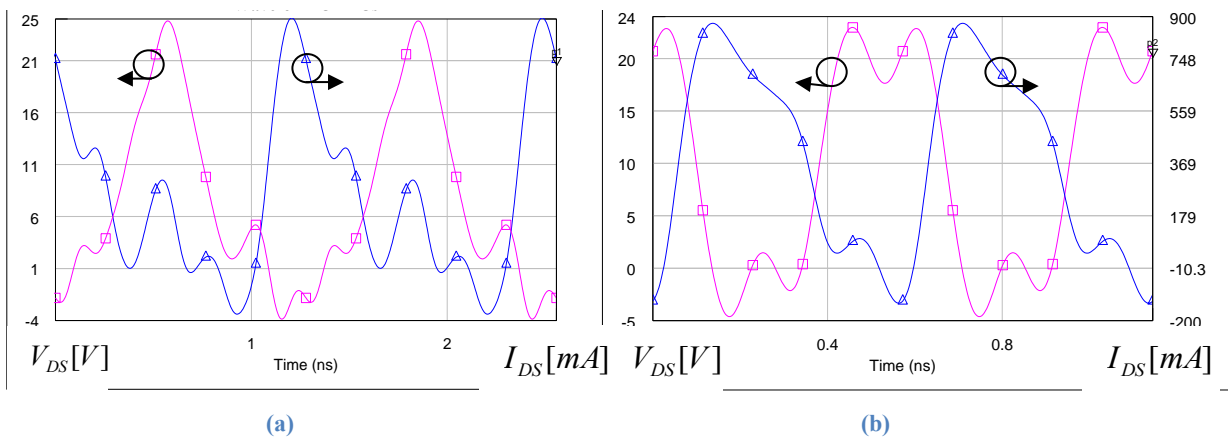


Figure 6.4-Voltage and current waveform of SMPA in (a) the lower and (b) the higher frequency band

6.1.3 Measurement

Fig. 6.5 shows the photo of the fabricated SMPA. A PIN diode is used as the switch. The output performance of the SMPA in terms of output power and efficiency is shown in Table 6.1. The simulated and measured output power and efficiency over both lower and higher

frequency bands are shown in Fig. 6.6. Output power of 30.7 dBm and 31.5 dBm for the lower and the higher band have been measured and show degradation in output power which is due to practical implementation. It is worth highlighting that the efficiency and output power maintain almost constant values over the whole bandwidth of both bands.

Table 6.1-SMPA output performances

	Output Power	Drain Efficiency	PAE
Lower band	30.7 dBm	60%	46%
Higher band	31.5 dBm	61%	44%

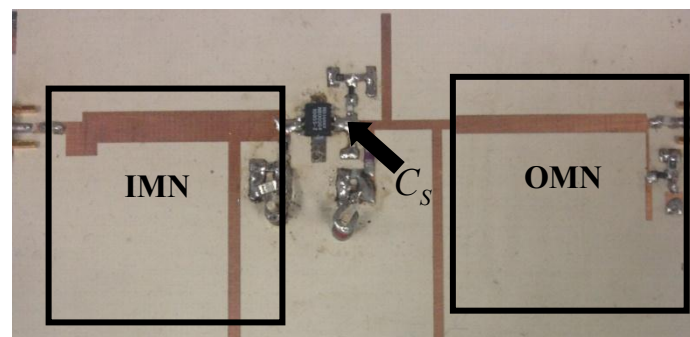


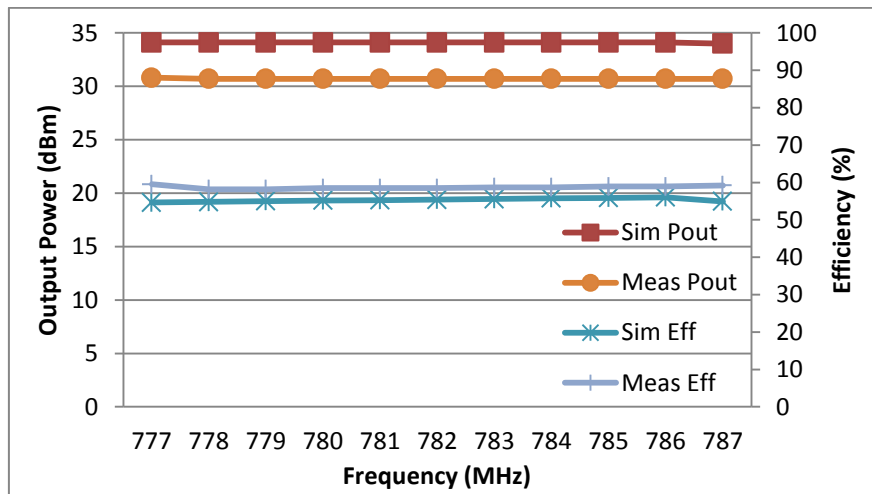
Figure 6.5-Fabricated prototype of switched-band Class-E PA

As the measurement results reveal efficiency and output power are lower compare to the reported efficiency of dual-band Class-E PA in Chapter 5. Two switches have been applied in the OMN of the SMPA and accordingly, two bias networks for PIN diodes. Each of the lumped components and switches will introduce loss in the network. These losses (especially switches' losses) produce heat and dissipate power and have impact on the efficiency. To overcome this problem, a switched-band Class-E PA needs to design with fewer switches.

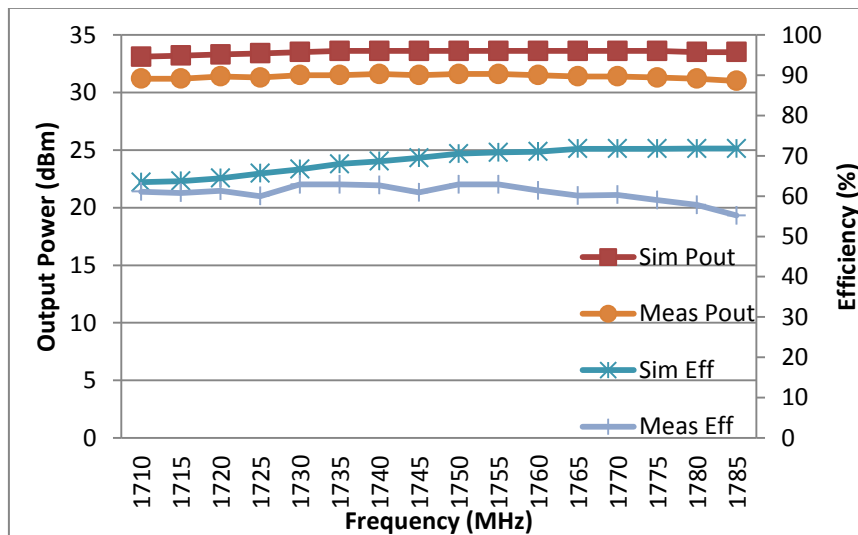
6.2 Fixed Matching Power Amplifier

A novel technique to design a switched-band PA was presented in the previous section and called SMPA. The SMPA showed the similar performances for both bands of operation in terms of output power and efficiency. However, the reported output performances decreased

compared to the dual-band Class-E PA, in Chapter 5. Another method of designing switched-band Class-E PA with fewer switches is presented here. The switch in the OMN will be eliminated and dual-band OMN will be used instead. The only switch in this design methodology is the switch for shunt capacitor as its effect on improving the efficiency has been proved in the previous chapter. This PA is called Fixed Matching PA (FMPA), as there is no switch in the OMN and just the shunt capacitance is switched.



(a)



(b)

Figure 6.6-Output power and efficiency of simulation and measurement of SMPA in (a) the lower and (b) the higher band

6.2.1 Theory

The FMPA has been designed with the dual-band OMN as described in Chapter 5 by aid of a transmission line (TL) and a stub (S), shown in Fig.6.7. The only switch in the FMPA is applied to the shunt capacitance across the transistor, method 2 of switching (Fig.6.2(b)). As it explained in section 6.1.1, the SW is ON for the lower band and OFF for the higher band of operation. The advantages of this method are that there are fewer switches, switching to ground to decrease the losses of the switch and also, that the switch is ON only in the lower band of operation.

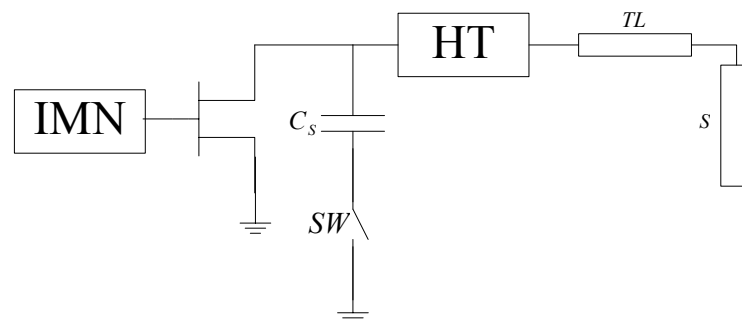


Figure 6.7- FMPA schematic

6.2.2 Simulation

The FMPA has been simulated in AWR for LTE application with the same GaN HEMT. The dual-band OMN has been designed based on the calculated lumped element component. The calculated shunt capacitance is 0.6 pF for the lower band. A 0.6 pF capacitor and a PIN diode are applied across the transistor. In the lower band the PIN diode is ON, connecting the capacitor to the ground, therefore, the shunt capacitor is introduced across the transistor. In the higher band of operation, the PIN diode is OFF and the capacitor is disconnected. Similar to the previous PAs, the second HT circuit and dual-band IMN are designed and applied for this PA. Class-E PA is a switched-mode PA and the transistor operates as a switch (ON and OFF state), which means that the transistor should be driven into compression by aid of an appropriate input power and gate voltage bias. The same gate voltage and input power (as

reported in 6.1.2) are applied for the FMPA. The performance of the FMPA is summarised in the Table 6.2. The efficiency and output power performances in both band of operation for ON and OFF state of the switch are presented in Fig 6.9. As shown in Fig.6.9, the efficiency stays constant for both band and above 70% and the output power is about 34 dBm. The current and voltage waveforms at the device plane are shown in Fig 6.8. These waveforms are presenting the acceptable Class-E waveforms condition.

Table 6.2-Dual-band OMN and switched shunt capacitance Class-E PA (FMPA) Performances

	Output Power	Drain Efficiency	PAE
First band	34 dBm	74.8%	67.4%
Second band	35.1 dBm	72.5%	67.2%

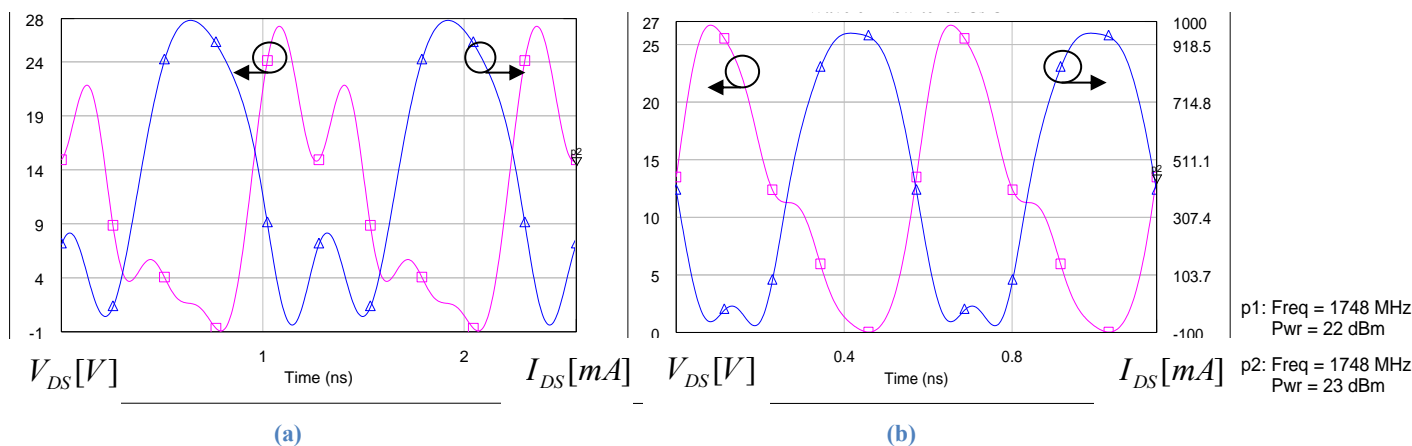
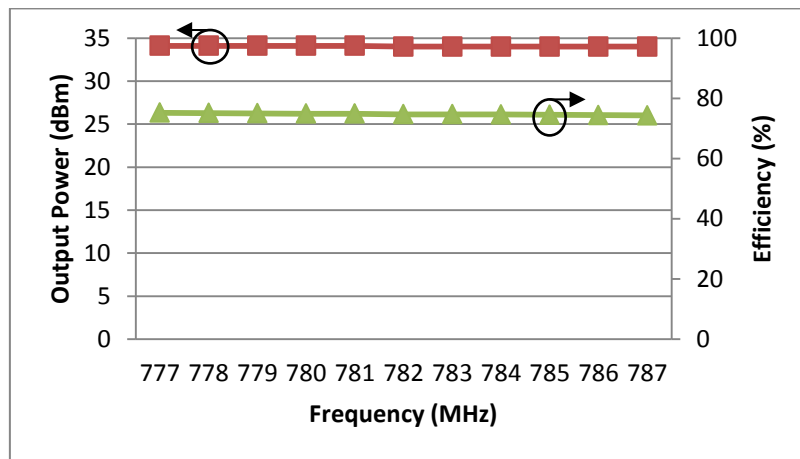
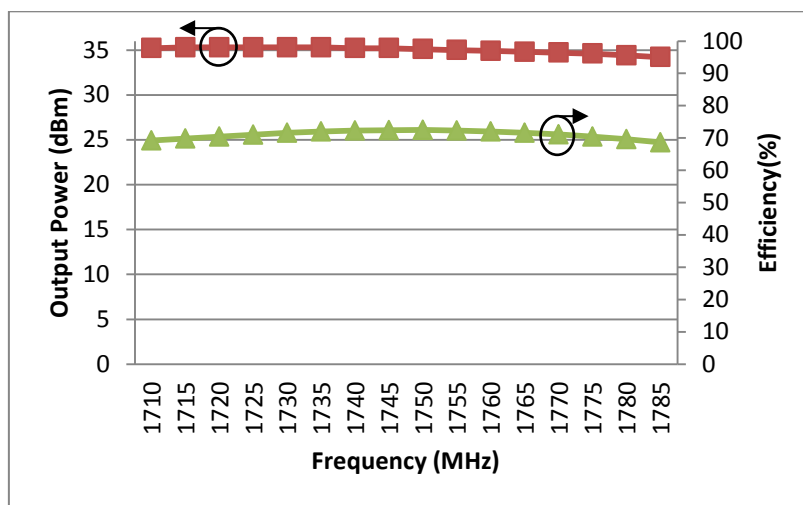


Figure 6.8-Voltage and current waveforms of FMPA in (a) ON and (b) OFF state



(a)



(b)

Figure 6.9-Output power and efficiency of FMPA over frequency in (a) OFF state and (b) ON state

The simulation result of the FMPA illustrates similar performances in both bands. This PA has not been fabricated due to lack of time but similar measured performances as the simulation result are expected as reasonable agreement between simulation and measurement was achieved in the previous switched-band Class-E PA.

6.3 Discussion

Providing the similar performances in all bands of multiband PAs is a challenge for PA designers. Two switched-band Class-E PAs have been analyzed in this chapter, SMPA and FMPA. Table 6.3 summarize performances of the reported switched-band Class-E PAs and the proposed PAs in this work. Techniques of these PAs ([81], [88]-[89]) are explained in Chapter 3. As shown in this Table, the proposed switched-band Class-E PAs (SMPA and FMPA) in this Chapter perform with higher efficiency compared to the existing SB-PAs in this class of operation.

The SMPA has two switches in the OMN and provides the efficiency of about 60% for the both bands. Only one switch has been applied in the FMPA to switch the shunt capacitor and provide efficiency of about 70% for both bands. The FMPA has following advantages:

- Only one switch is applied
- The switch is ON in the lower band of operation
- Similar and high performances in both bands
- About 10% improvement in efficiency compared to SMPA

Table 6.3-Switched-band Class-E PAs

References	Band of operation (GHz)	Output Power (dBm)	Drain Efficiency (%)	PAE (%)
[81]	0.9 and 1.8	20	38 and 26	N.A
[88]	1.9-2.3-2.6-3.5	24.2-23.8-23.4-20.5	48.2-44.3-40.9-35.6	N.A
[89]	1.7 and 2.5	28 and 27	N.A	57 and 61.5
This work (SMPA)	0.782 and 1.748	34.1 and 33.6	60 and 71	56.3 and 66.1
This work (FMPA)	0.782 and 1.748	34 and 35.1	74.8 and 72.5	67.4 and 67.2

Chapter 7

Conclusion

Fast growth in the number of users of the wireless communication systems attracts a lot of attention from researchers to improve the quality of this service by increasing battery life, improving reliability, reducing the size and weight, and lowering the cost of the devices, while providing internet connections for users everywhere and anytime without decreasing the speed and the quality of service. These requirements can be met by designing high efficiency and adaptive transmitters. The main concern of the presented research in this thesis was to study and discover a methodology for designing high efficiency frequency adaptive PA (the most challenging component of the transmitter) for wireless communication systems. Achievements during this study were:

- Designed SB-MNs and minimised losses of the switch and derived an original recursive analytical solution for all the proposed MNs.
- Developed an approach to the design of Class-E PA with distributed MNs based on reflection coefficient approach with high efficiency performances.
- Proposed design methodology of dual-band Class-E PA with high output performance, but higher efficiency obtained in the higher band of operation.
- Proposed and designed two switched-band Class-E PAs: Switchable Matching PA (SMPA) and Fixed Matching PA (FMPA), similar and high output performance was achieved. Both used switched shunt capacitor to maintain Class-E operation in the selected band.

- Discussed and compared the feasibility of dual-band and switched-band Class-E PAs, showing the trade-offs that need to be considered by designers of PAs for engineering multiband communication standards.

7.1 Thesis Summary

This research started with the background review on the important merits of the PAs and devices, as shown in **Chapter 2**. All the reported techniques of designing frequency adaptive PAs (multiband and switched-band) are discussed in **Chapter 3**. One approach to design a PA for multiband systems is designing a broadband PA; low efficiency and limited gain are drawbacks of this approach. The other approaches are MB-PAs and SB-PAs and Chapter 3 is mainly concentrated on these two approaches. This research proved that designing with MB-MN or SB-MN has better performances compare to utilizing parallel single-band PAs (with or without switches). This literature review on the current techniques clarified the need for research on discovering a methodology to design frequency adaptive PAs to perform with high PAE at all the frequency bands.

The design of high efficiency frequency adaptive PAs started with designing SB- MN with the purpose of reducing losses of the switches in the circuit and providing more accurate results in all the working bands. Three methods (detach- , short- and open- stub) to design SB-MN were presented in **Chapter 4**. The Open to Short stub (OTS) and Short to Stub (STS) methods are more compact compared with the detach stub [21], [73], [110] and methods involving switching between two individual MNs [86], [87]. OTS and STS address the thermal problem of PIN diodes by connecting one terminal to ground. In this contribution, for the first time, the feasibility of SB-MNs for different frequencies, by aid of the derived equations, has been shown. The proposed theoretical approach, based on the SB-MNs, provides a closed-form and recursive solution to design SB-MNs precisely, given any two

frequencies. Furthermore these methods can be applied not only for two but for several band MNs. Numerical and experimental results have been presented by this work and the results were compared to prove the validity of the algorithm. The presented MNs and derived algorithm could be applied to a wide range of multiband components, such as antennas, LNAs and PAs. These promising results encouraged further research on designing SB-MNs that take account of harmonic termination requirements, which are important in PA applications. The proposed method consists of two blocks, HT (Harmonic Termination Network) and MN.

Chapter 5 has presented the design methodology of high efficiency Class-E PA to work in single-band and multiband application. Dual-band Class-E PAs are presented to operate in an up-link band of the LTE system. Dual-band OMN is applied to achieve amplification in both bands without any switches (GaAs HFET has been used in this design) and measured high drain efficiency of 60% and 84.5% and output power of 22 and 27 dBm at 777-787 and 1718-1785 MHz, respectively. The same technique is applied with another transistor (GaN HEMT). This dual-band Class-E PA provides dual-band amplification with drain efficiency of 67.7% and output power of 34.2 dBm at first band and 81.3% drain efficiency and 35.8dBm output power at the second band. Both dual-band Class-E PAs perform with satisfying high efficiency and provide higher efficiency at the higher band of operation. The reason for the different efficiencies in the two bands was addressed and is due to the requirement of different shunt capacitance across the transistor in different operating frequencies.

The difference in efficiencies at both bands of operation is overcome in **Chapter 6** by applying SB-MNs in the circuit. Two switched-band Class-E PAs were proposed in this chapter. The first PA, SMPA, utilises a switch for OMN and another switch to change the

value of shunt capacitance for both bands. The measurement result of SMPA shows 30.7 and 31.5 dBm output power in the two bands with drain efficiency of 60% and 61%, respectively. The second SB-PA, FMPA, was designed with dual-band OMN and a switched shunt capacitor. Output power of 34 and 35.1 dBm and drain efficiency of 74.8% and 72.5% achieved from this PA at the lower and higher band of operation, respectively. The FMPA reduced the number of switches in the circuit and improved the efficiency about 10% compared to SMPA. The similar performances in both bands have been achieved in the SB-PAs at the cost of decreasing efficiency in the higher band.

7.2 Conclusion

For comparison purposes, performances of all the designed Class-E PA in this work are shown in the Table 7.1. This table shows the simulated result in each case in order to provide a consistent comparison. Confidence in the validity of the results has been demonstrated by building and testing several example designs.

Table 7.1-Simulation performance comparison between all the designed Class-E PAs

Band of Operation	Output Power (dBm)		Efficiency (%)		PAE (%)	
	f_1	f_2	f_1	f_2	f_1	f_2
Dual-band PA	34.2	35.8	67.6	81.3	61.4	76.8
SMPA	34.1	33.6	60	71	56.3	66.1
FMPA	34	35.1	74.8	72.5	67.4	67.2

The best obtained efficiency is from the dual-band PA at the second band. Efficiency of about 70% was obtained for both bands in FMPA. The key factor discovered here was the need to switch the parallel capacitor value. There is a trade off between providing highest possible efficiency in one band at the cost of degrading efficiency in the other band (dual-band PA) or obtaining similar performances for both bands (FMPA). In the dual-band PA and

FMPA, there is a limitation to the number of bands that can be covered, whereas SMPA is capable of covering more bands of frequency by applying more switches, although this results in introducing more losses.

7.3 Future Work

This thesis has advanced in the research area of high efficiency adaptive PA design. Like any research, lots of questions and ideas arise during the study, which some of them still remained unanswered and uncovered. Some of them are presented here as possible research works. This research was mainly focusing on improving the efficiency of frequency adaptive PAs. The chosen class of operation in this work (Class-E) is inherently nonlinear because the active device acts as a switch. Linearity of a PA is one of the important factors. By improving efficiency of a PA, linearity will normally be reduced and vice versa. Linearity of the proposed PAs in this work has not been investigated. Future work for the proposed high efficiency PAs is to linearize them with one of the current techniques; such as, pre-distortion [13] and Envelope Elimination and Restoration (EER) [111]-[112].

Another future work is to design a PA with ability of switching between broadband and narrow-band high efficiency PA (switching operation modes of PA). This design can use a Class-E highly efficient PA to work in a narrow band of frequencies and a Class-B PA to cover broader bandwidths when required.

References

1. B. A. Fette, *Cognitive Radio Technology*, 2nd edition, Elsevier, 2009.
2. T. S. Rappaport, “Wireless Communication: Principles and Practice”, 2nd Edition, Prentice Hall, 2001.
3. T. W. Rondeau, and C. W. Bostian, *Artificial Intelligence in Wireless Communication*, London: mobile communication series, 2009.
4. S. C. Cripps, *RF power amplifiers for wireless communications*, 2nd Edition, Artech House Publishers, 2006.
5. F. H. Raab, P. Asbeck, et al, “Power Amplifiers and Transmitters for RF and Microwave”, *IEEE Transaction on Microwave Theory and Techniques*, vol.50, no.3, March 2002.
6. Y. Chung, C. Y. Hang, S. Cai et al, “AlGaN/GaN HFET Power Amplifier Integrated With Microstrip Antenna for RF Front-End Applications”, *IEEE Transaction on Microwave Theory and Techniques*, vol.51, no.2, pp.653-659, February 2003.
7. N. O. Sokal, N.O. and A. D. Sokal, “Class E-A New Class of High-Efficiency Tuned Single-Ended Switching Power Amplifiers”, *IEEE Journal of Solid-State Circuits*, Vol. SC-10. No. 3, pp.168-176, 1975.
8. F. H. Raab, "Effects of circuit variations on the class E tuned power amplifier," *IEEE Journal of Solid-State Circuits*, vol.13, no.2, pp.239-247, April 1978.
9. Y. Qin, S. Gao, A. Sambell, “Broadband High-Efficiency Circularly Polarized Active Antenna and Array for RF Front-End Application”, *IEEE Transactions on Microwave Theory and Techniques*, Vol. 54, No. 7, pp. 2910-2916, 2006.
10. D. P. Kimber, *Class E Amplifiers and their Modulation Behaviour*, Thesis submitted at the University of Birmingham, 2005.

References

11. F. H. Raab, P. Asbeck, S. Cripps, P. B. Kenington, Z. B. Popovic, N. Pothecary, J. F. Sevic, N. O. Sokal, "RF and Microwave Power Amplifier and Transmitter Technologies", *High Frequency Electronics*, pp.22-54, May 2003- January 2004.
12. S. C. Cripps, *RF Power Amplifiers for Wireless Communications*, Norwood: Artech House, 2008.
13. S. C. Cripps, *RF Power Amplifiers for Wireless Communications*, Norwood: Artech House, 1999.
14. G. D. Vendelin, A. M. Pavio, and U. L. Rohde, *Microwave Circuit Design Using Linear and Nonlinear Techniques*, 2nd edition, Canada: Wiley Interscience, 2005.
15. P. Wright, J. Lees, J. Benedikt, P. J. Tasker, S. C. Cripps, "A Methodology for Realizing High Efficiency Class-J in Linear and Broadband PA", *IEEE Transaction on Microwave Theory and Techniques*, vol.57, no.12, pp.3196-3204, December 2009.
16. N. O. Sokal, "Class-E RF Power Amplifiers", *QEX*, No. 204, pp.9-20, January/February 2001.
17. T. B. Mader, E. W. Bryerton, M. Markovic, et al "Switched-Mode High-Efficiency Microwave Power Amplifiers in a Free-Space Power-Combiner Array", *IEEE Transactions on Microwave Theory and Techniques*, Vol. 46, No.10, pp.1391-1398, 1998.
18. A. Grebennikov and N. O. Sokal, *Switchmode RF Power Amplifiers*, Linacre House, Jordan Hill, Oxford OX2 8DP, UK, 2007.
19. A. M. Mohamed, S. Boumaiza, R. R. Mansour, "Novel Reconfigurable Fundamental/Harmonic Matching Network for Enhancing the Efficiency of Power Amplifiers", *40th European Microwave Conference*, 2010.
20. A. Sheikh, "High Power Waveform Engineering", PhD Thesis, University of Wales, Cardiff University, Cardiff, June 2009.

References

21. A. Fukuda, H. Okazaki, T. Hirota and Y. Yamao, "Novel 900 MHz/1.9 GHz Dual-Mode Power Amplifier Employing MEMS Switches for Optimum Matching", *IEEE Microwave and Wireless Components Letters*, vol.14, no.3, pp. 121-123, March 2004.
22. A. Fukuda, T. Furuta, H. Okazaki, S. Narahashi, "A 0.9-5-GHz Wide-Range 1 W-Class Reconfigurable Power Amplifier Employing RF-MEMS Switches", *IEEE*, pp. 1859-1862, 2006.
23. J. Kim, F. Mkadem, S. Boumaiza, "A High Efficiency and Multi-Band/Multi-Mode Power Amplifier using a Distributed Second Harmonic Termination", *40th European Microwave Conference*, pp 1662-1665, 2010.
24. M. Watertown, *The PIN Diode Circuit Designers' Handbook*, Massachusetts: Microsemi Corporation, 1998.
25. G. M. Rebeiz and J. B. Muldavin, "RF MEMS Switches and Switch Circuits", *IEEE Microwave Magazine*, pp. 59-71, 2001.
26. Y. Yashchyshyn, "Reconfigurable Antennas by RF Switches Technology", *MEMSTECH*, pp. 155-157, 2006.
27. Skyworks Solutions Inc, "Application Note: Varactor Diodes", *Skyworks*, 2008.
28. W. C. Edmund Neo, Y. Lin, X. D. Liu; L. C. N. De Vreede, L. E. Larson, M. Spirito, M. J. Pelk, K. Buisman, A. Akhnoukh, A. Anton de Graauw, L. K. Nanver, "Adaptive Multi-Band Multi-Mode Power Amplifier Using Integrated Varactor-Based Tunable Matching Networks," *IEEE Journal of Solid-State Circuits*, vol.41, no.9, pp.2166-2176, September 2006.
29. B. Doherty, and M. Watertown, "PIN Diode Fundamental", *MicroNote series 701*.
30. G. Hiller, "Design with PIN Diodes", *Application Notes*.

References

31. A. C. K. Mak, C. R. Rowell, R. D. Murch, and C. Mak, "Reconfigurable Multiband Antenna Designs for Wireless Communication Devices", *IEEE Transactions on Antennas and Propagation*, vol. 55, no. 7, pp. 1919-1928, 2007.
32. E. G. Jeckeln, F. M. Ghannouchi, F.M. and M. A. Sawan, "A New Adaptive Predistortion Technique Using Software-Defined Radio and DSP Technologies Suitable for Base Station 3G Power Amplifiers", *IEEE Transactions on Microwave Theory and Techniques*, Vol. 52, No. 9, pp.2139-2147, 2004.
33. S. Bruss, "Linearization Methods", pp.1-8, 2003.
34. J. C. Pedro, N. B. Carvalho, *Intermodulation Distortion in Microwave and Wireless Circuits*, Artech House, Norwood, 2003.
35. J. Yi, Y. Yang, M. Park, W. Kang, et al, "Analog predistortion linearizer for high-power RF amplifiers," *IEEE Transactions on Microwave Theory and Techniques*, vol.48, no.12, pp.2709-2713, December 2000.
36. F. H. Raab, P. Asbeck, S. Cripps, et al "RF and Microwave Power Amplifier and Transmitter Technologies-Part 4", *High Frequency Electronics*, pp.38-49, November 2003.
37. M. A. Briffa, *Linearization of RF Power Amplifiers*, Doctor of Philosophy thesis, Melbourne 1996.
38. J. H. Chen, K. U-yen, J. S. Kenney, "An envelope elimination and restoration power amplifier using a CMOS dynamic power supply circuit," *IEEE MTT-S International Microwave Symposium Digest*, vol.3, pp.1519-1522, 6-11 June 2004.
39. F. H. Raab, "Idealized Operation of the Class E Tuned Power Amplifier", *IEEE Transaction on Circuits and Systems*, pp.725-735, 1977.
40. D. M. Pozar, *Microwave Engineering*, University of Massachusetts, 2005.

References

41. R. Sorrentino, G. Bianchi, *Microwave and RF Engineering*, 1st edition, John Wiley & Sons, 2010.
42. S. C. Cripps, *Advanced Technique in RF Power Amplifier Design*, Artech House Publishers, 2002.
43. P. Savary, A. Girardot, G. Montoriol, F. Dupis, B. Thibaud, R. Jaoui, L. Chapoux, V. Esnault, L. Cornibert, O. Izumi, D. Hill, M. Sadaka, H. Henry, E. Yu, M. Tutt, M. Mejerus, R. Uscola, F. Clayton, C. Rampley, S. Klingbeil, K. Rajagopalan, A. Mitra, and A. Reyes, "Dual-band Multi-Mode Power Amplifier Module Using A Third Generation HBT Technology", *IEEE Gallium Arsenide Integrated Circuit Symp*, pp.71-74, 2001.
44. D. Kalim, R. Negra, "Concurrent planar multiharmonic dual-band load coupling network for switching-mode power amplifiers," *IEEE MTT-S International Microwave Symposium Digest (MTT)*, pp.1-4, 5-10 June 2011.
45. K. Uchida, Y. Takayama, T. Fujita, K. Maenaka, "Dual-Band GaAs FET Power Amplifier with Two-Frequency Matching Circuits", *Asia-Pacific Microwave Conference*, vol.1, 2005.
46. S. H. Ji, C. S. Cho, J. W. Lee, J. Kim, "Concurrent Dual-Band Class-E Power Amplifier Using Composite Right/Left-Handed Transmission Lines", *IEEE Transactions on Microwave Theory and Techniques*, vol. 55, no. 6, pp. 1341-1374, June 2007.
47. J. L. Jimenez-Martin, V. Gonzalez-Posadas, F. J. Arques, L. E. Garcia-Munoz, D. Secovia-Vargas, "Dual Band High Efficiency Power Amplifier Based on CRLH Lines", *RADIOENGINEERING*, vol.18, no.4, pp.567-578, December 2009.
48. J. Shi, T. Liu, Y. Ye, S. Ge, G. Xu, "Dual-Band Power Amplifier Using Composite Right/Left-Handed Transmission Line," *6th International Conference on Wireless Communications Networking and Mobile Computing (WiCOM)*, pp.1-4, 23-25 September 2010.

References

49. A. Fukuda, H. Okazaki, S. Narahashi, T. Nojima, "Concurrent multi-band power amplifier employing multi-section impedance transformer," *IEEE Topical Conference on Power Amplifiers for Wireless and Radio Applications (PAWR)*, pp.37-40, 16-19 January 2011.
50. A. Fukuda, H. Okazaki, S. Narahashi, T. Nojima, "A concurrent multi-band power amplifier with compact matching networks," *General Assembly and Scientific Symposium*, pp.1-4, August 2011.
51. A. Fukuda, H. Okazaki, S. Narahashi, "Novel multi-band matching scheme for highly efficient power amplifier," *European Microwave Conference, EuMC*, pp.1086-1089, 2009.
52. S. Pei, J. Nan, Y. Qu, "Two kinds of dual-band power amplifier matching networks using three-section microstrip line," *10th International Symposium on Antennas, Propagation & EM Theory (ISAPE)*, pp.702-705, 22-26 October 2012.
53. X. Fu, D. T. Bepalko, S. Boumaiza, "Novel Dual-Band Matching Network for Effective Design of Concurrent Dual-Band Power Amplifiers," *IEEE Transactions on Circuits and Systems I: Regular Papers*, vol.61, no.1, pp.293-301, January 2014.
54. K. Rawat, F. M. Ghannouchi, "Dual-band matching technique based on dual-characteristic impedance transformers for dual-band power amplifiers design," *Microwaves, Antennas & Propagation, IET*, vol.5, no.14, pp.1720-1729, November 2011.
55. Y. Ding, Y. X. Guo, F. L. Liu, "High-efficiency concurrent dual-band class-F and inverse class-F power amplifier," *Electronics Letters*, vol.47, no.15, pp.847-849, July 2011.
56. R. Liu, D. Schreurs, W. De Raedt, F. Vanaverbeke, R. Mertens, "Concurrent dual-band power amplifier with different operation modes," *IEEE MTT-S International Microwave Symposium Digest (MTT)*, pp.1-4, 5-10 June 2011.

References

57. P. Saad, P. Colantonio, M. Junghwan, L. Piazzon, F. Giannini, K. Andersson, B. Kim, C. Fager, "Concurrent dual-band GaN-HEMT power amplifier at 1.8 GHz and 2.4 GHz," *IEEE 13th Annual Wireless and Microwave Technology Conference (WAMICON)*, pp.1-5, 15-17 April 2012.
58. P. Saad, P. Colantonio, L. Piazzon, F. Giannini, K. Andersson, C. Fager, "Design of a Concurrent Dual-Band 1.8–2.4-GHz GaN-HEMT Doherty Power Amplifier," *IEEE Transactions on Microwave Theory and Techniques*, vol.60, no.6, pp.1840-1849, June 2012.
59. K. Rawat, F. M. Ghannouchi, "Design Methodology for Dual-Band Doherty Power Amplifier With Performance Enhancement Using Dual-Band Offset Lines," *IEEE Transactions on Industrial Electronics*, vol.59, no.12, pp.4831-4842, December 2012.
60. A. Cidronali, N. Giovannelli, I. Magrini, G. Manes, "Compact Concurrent Dual-Band Power Amplifier for 1.9GHz WCDMA and 3.5GHz OFDM Wireless Systems", *3rd European Microwave Integrated Circuits Conference*, Amsterdam, pp.518-521, 2008.
61. P. Colantonio, F. Giannini, R. Giofre, L. Piazzon, "A Design Technique for Concurrent Dual-Band Harmonic Tuned Power Amplifier", *IEEE Transactions on Microwave Theory and Techniques*, Vol. 56, No. 11, pp. 2545-2555, 2008.
62. M. R. Ghajar, S. Boumaiza, "Concurrent dual band 2.4/3.5GHz fully integrated power amplifier in 0.13 μ m CMOS technology," *Microwave Integrated Circuits Conference, 2009. EuMIC 2009. European*, pp.375-378, Rome, 28-29 September 2009.
63. D. T. Bespalko and S. Boumaiza, "Concurrent Dual-Band GaN Power Amplifier with Compact Microstrip Matching Network", *Microwave and Optical technology Letters*, vol.51, no.5, pp.1604-1607, 2009.
64. S. Gao, Z. Wang, C. W. Park, "Concurrent dual-band power amplifier with second harmonic controlled by gate and drain bias circuit," *IEEE International Conference*

References

- on *Microwave Technology & Computational Electromagnetics (ICMTCE)*, pp.309-312, 22-25 May 2011.
65. R. Negra, A. Sadeve, S. Bensmida, F. M. Ghannouchi, "Concurrent Dual-Band Class-F Load Coupling Network for Applications at 1.7 and 2.14 GHz," *IEEE Transactions on Circuits and Systems II: Express Briefs*, vol.55, no.3, pp.259-263, March 2008.
66. R. Zhang, M. Acar, M. Apostolidou, M. P. Heijden, D. M. W. Leenaerts, "Concurrent L- and S-Band Class-E Power Amplifier in 65nm CMOS", *IEEE Radio Frequency Integrated Circuits Symposium*, pp. 217-220, 2012.
67. Y. C. Lin, C. T. Chen, T. S. Horng, "High Efficiency Dual-Band Class-E Power Amplifier Design", *APMC*, pp.355-357, December 2012.
68. S. Wood, R. pengelly, J. Crescenzi, "A High Efficiency Doherty Amplifier with Digital Predistortion for WiMAX", *High Frequency Electronics*, pp. 18-28, 2008.
69. K. Yamamoto, S. Suzuki, K. Mori, T. Asada, T. Okuda, A. Inoue, T. Miura, K. Chomei, R. Hattori, M. Yamanouchi, T. Shimura, "A 3.2-V operation single-chip dual-band AlGaAs/GaAs HBT MMIC power amplifier with active feedback circuit technique," *IEEE Journal of Solid-State Circuits*, vol.35, no.8, pp.1109-1120, August 2000.
70. Y. Eo, K. Lee, "A 2.4GHz/5.2GHz CMOS power amplifier for dual-band applications," *Microwave Symposium Digest*, vol.3, pp.1539-1542, 6-11 June 2004.
71. K. Y. Kim, J. H. Kim, Y. S. Noh, C. S. Park, "Cellular/PCS dual-band MMIC power amplifier of a newly devised single-input single-chain network," *Gallium Arsenide Integrated Circuit (GaAs IC) Symposium*, pp.131-134, 9-12 November 2003.
72. A. Adar, J. DeMoura, H. Balshem, J. Lott, "A high efficiency single chain GaAs MESFET MMIC dual band power amplifier for GSM/DCS handsets," *Gallium Arsenide Integrated Circuit (GaAs IC) Symposium*, pp.69-72, 1-4 November 1998.

References

73. A. Fukuda, H. Okazaki, S. Narahashi, T. Hirota,; Y. Yamao, "A 900/1500/2000-MHz triple-band reconfigurable power amplifier employing RF-MEMS switches," *Microwave Symposium Digest, 2005 IEEE MTT-S International* , pp.657-660, 12-17 June 2005.
74. H. M. Nemati, J. Grahn and C. Fager, "Band-Reconfigurable LDMOS Power Amplifier", in *40th European Microwave Conference*, 2010, pp.978-981.
75. A. Fukuda, H. Okazaki and S. Narahashi, "A Novel Compact Reconfigurable Quad-band Power Amplifier Employing RF-MEMS switches", in *36th European Microwave Conference*, 2006, pp. 344-346.
76. H. Okazaki, A. Fukuda, K. Kawai, T. Furuta, S. Narahashi, "MEMS-based Reconfigurable RF Front-end Architecture for Future Band-free Mobile Terminals," *European Conference on Wireless Technologies*, pp.300-303, 8-10 October 2007.
77. Y. Lu, D. Peroulis, S. Mohammadi, L. P. B. Katehi, "A MEMS reconfigurable matching network for a class AB amplifier," *Microwave and Wireless Components Letters, IEEE*, vol.13, no.10, pp.437-439, October 2003.
78. D. Qiao, R. Molfino, S. M. Lardizabal, B. Pillans, P. M. Asbeck, G. Jerinic, "An intelligently controlled RF power amplifier with a reconfigurable MEMS-varactor tuner," *IEEE Transactions on Microwave Theory and Techniques*, vol.53, no.3, pp.1089-1095, March 2005.
79. H. Magnusson and H. Olsson, "A Compact Dual-Band Power Amplifier Driver for 2.4GHz and 5.2GHz WLAN Transmitters," *Radio Frequency Integrated Circuits (RFIC) Symposium*, pp.83-86, 3-5 June 2007.
80. F. Ali, E. Lourandakis, R. Gloeckler, et al, "Tunable Multiband Power Amplifier using Thin-Film BST Varactors for 4G Handheld Applications", *IEEE*, pp.236-239, 2010.

References

81. L. Larcher, R. Brama, M. Ganzerli, J. Iannacci, B. Margesin, M. Bedani, A. Gnudi, "A MEMS Reconfigurable Quad-Band Class-E Power Amplifier for GSM Standard", *IEEE*, pp.864-867, 2009.
82. J. Hur, O. Lee, C. H. Lee, et al, "A Multi-Level and Multi-Band Class-D CMOS Power Amplifier for the LINC System in the Cognitive Radio Application", *IEEE Microwave and Wireless Components Letters*, vol. 20, no. 6, pp.352-354, 2010.
83. J. Cui, K. Zhang, T. Tian, "A dual-level and dual-band class-D CMOS power amplifier for iot applications," *IEEE 11th International New Circuits and Systems Conference (NEWCAS)*, pp.1-4, 16-19 June 2013.
84. H. Zahng, H. Gao, G. Li, "Broad-Band Power Amplifier With a Novel Tunable Output Matching Network", *IEEE Transactions on Microwave Theory and Techniques*, vol. 53, no. 11, pp. 3606-3614, 2005.
85. H. Zhang, H. Gao, G. P. Li, "A novel tunable broadband power amplifier module operating from 0.8 GHz to 2.0 GHz," *Microwave Symposium Digest*, 12-17 June 2005.
86. C. Zhang, A. E. Fathy, "A Novel Reconfigurable Power Amplifier Structure for Multi-Band and Multi-Mode Portable Wireless Applications using a Reconfigurable Die and a Switchable Output Matching Network", *IEEE*, pp. 913-916, 2009.
87. U. Kim, K. Kim, J. Kim, Y. Kwon, "A Multi-Band Reconfigurable Power Amplifier for UMTS Handset Applications", *IEEE Radio Frequency Integrated Circuits Symposium*, pp. 175-178, 2010.
88. K. Y. Kim, W. Y. Kim, H. S. Son, I. Y. Oh, C. S. Park, "A Reconfigurable Quad-Band CMOS Class-E Power Amplifier for Mobile and Wireless Applications", *IEEE Microwave and Wireless Components Letters*, vol. 21, no. 7, pp. 380-382, July 2011.
89. D. Kalim, A. Fatemi, R. Negra, "Dual-Band 1.7GHz/2.5GHz Class-E Power Amplifier in 130nm CMOS Technology", *IEEE*, pp. 473-476, 2012.

References

90. A. Fukuda, K. Kawai, T. Furuta, H. Okazaki, S. Oka, S. Narahashi, A. Murase, "A high power and highly efficient multi-band power amplifier for mobile terminals," *Radio and Wireless Symposium (RWS)*, pp.45-48, 10-14 January 2010.
91. P. Sjoblom, H. Sjolund, "Measured CMOS Switched High-Quality Capacitors in a Reconfigurable Matching Network," *IEEE Transactions on Circuits and Systems II: Express Briefs*, vol.54, no.10, pp.858-862, October 2007.
92. H. T. Jeong, J. E. Kim, I. S. Chang, C. D. Kim, "Tunable Impedance Transformer Using a Transmission Line With Variable Characteristic Impedance," *IEEE Transactions on Microwave Theory and Techniques*, vol.53, no.8, pp.2587-2593, August 2005.
93. R. W. Vogel, "Effect of the T-Junction Discontinuity on the Design of Microstrip Directional Couplers", *IEEE Transaction on Microwave and Techniques*, pp. 145-146, 1972.
94. F. M. Ghanouchi, M. S. Hashmi, *Load-Pull Techniques with Applications to Power Amplifier Design*, Springer, 2013.
95. R. Garg, I. Bahl, M.Bozzi, *Microstrip Lines and Slotlines*, Artech House, 2013.
96. R. Giofre, P. Colantonio, F. Giannini, L. Piazzon, "A new design strategy for multi frequencies passive matching networks," *European Microwave Conference*, pp.838-841, 9-12 October 2007.
97. T. B. Mader and Z. Popovic, "The Transmission-Line High-Efficiency Class-E Amplifier", *IEEE Microwave Guided Wave Letter*, vol. 5, no. 9, pp.290-292, September 1995.
98. J. C. Pedro and N. B. Carvalho, *Intermodulation Distortion in Microwave and wireless Circuits*, Artech House, 2003.
99. A. Raffo, F. Scappaviva, G. Vannini, "A New Approach to Microwave Power Amplifier Design Based on the Experimental Characterization of the Intrinsic Electron Device Load

References

- Line", *IEEE Transaction on Microwave Theory and Techniques*, Vol. 57, Issue 7, pp. 1743-1752, July 2009.
- 100.Y. L. Chow, K. L. Wan, "A transformer of one-third wavelength in two sections - for a frequency and its first harmonic," *Microwave and Wireless Components Letters, IEEE* , vol.12, no.1, pp.22,23, January 2002.
- 101.X. Liu, Y. Liu, S. Li, F. Wu, "Design of dual-band amplifier using three-section dual-frequency matching structure," *IEEE International Conference on Communications Technology and Applications*, pp.775-779, 16-18 October 2009.
- 102.C. Monzon, "Analytical derivation of a two-section impedance transformer for a frequency and its first harmonic," *IEEE Microwave and Wireless Components Letters*, vol.12, no.10, pp.381-382, October 2002.
- 103.C. Monzon, "A small dual-frequency transformer in two sections," *IEEE Transactions on Microwave Theory and Techniques*, vol.51, no.4, pp.1157-1161, April 2003.
- 104.S. J. Orfanidis, "A two-section dual-band Chebyshev impedance transformer," *Microwave and Wireless Components Letters, IEEE*, vol.13, no.9, pp.382-384, September 2003.
- 105.P. Colantonio, F. Giannini, L. Scucchia, "A new approach to design matching networks with distributed elements," *15th International Conference on Microwaves, Radar and Wireless Communications*, vol.3, pp.811-814, 17-19 May 2004.
- 106.Y. Wu, Y. Liu, S. Li, "A Dual-Frequency Transformer for Complex Impedances With Two Unequal Sections," *Microwave and Wireless Components Letters, IEEE*, vol.19, no.2, pp.77-79, February 2009.
- 107.Y. Wu, Y. Liu, S. Li, C. Yu, X. Liu, "A Generalized Dual-Frequency Transformer for Two Arbitrary Complex Frequency-Dependent Impedances," *Microwave and Wireless Components Letters, IEEE*, vol.19, no.12, pp.792-794, December 2009.

References

- 108.M. L. Chuang, "Dual-Band Impedance Transformer Using Two-Section Shunt Stubs," *IEEE Transactions on Microwave Theory and Techniques*, vol.58, no.5, pp.1257-1263, May 2010.
- 109.F. G. S. Silva, R. N. De Lima, S. M. Nascimento, R. C. S. Freire, "A design methodology for concurrent impedance matching networks based on multiresonant circuits," *New Circuits and Systems Conference (NEWCAS)*, pp.386-389, 26-29 June 2011.
- 110.F. Norouzian, P. Gardner, "Analytical solution for switched band matching networks," *3rd Annual IET Seminar on Passive RF and Microwave Components*, pp.43-52, 26-26 March 2012.
111. L. Kahn, "Single-sideband transmission by envelope elimination and restoration," *Proc. IRE*, pp. 803-806, July 1952.
112. T. Rautio, S. Hietakangas, T. Rahkonen, "Development Environment for EER and Envelope Tracking RF transmitters," *Norchip Conference*, pp.151-154, November 2006.
- 113.M. Hiebel, *Fundamentals of Vector Network Analysis*, Rohde & Schwarz, fifth edition, 2011.
- 114.C. Rauscher, *Fundamentals of Spectrum Analysis*, Rohde & Schwarz, fifth edition, 2007.
115. M. T. Thompson, "Inductance Calculation Technique-Part II: Approximations and Handbook Methods", *Power Control and Intelligent Motion*, December 1999.

Appendix A

Components Data Sheets

Transistors:

- GaAs HFET: http://pdf.datasheetcatalog.com/datasheets2/46/462767_1.pdf
- GaN HEMT: http://www.propagation.gatech.edu/ECE6361/project/Project2_09/NPTB00004.pdf

Transistor Package:

http://www.amkor.co.kr/datasheets/psop_2_3.pdf

PIN Diodes:

- Infineon:
<http://www.infineon.com/dgdl/bar50series.pdf?folderId=db3a304314dca3890114fea780a30a91&fileId=db3a304314dca3890114fea7dd410a92>
- Skyworks: http://www.skyworksinc.com/uploads/documents/SMP1302_085PB.pdf

Capacitors-AVX:

<http://www.avx.com/docs/catalogs/accuf-p.pdf>

Inductors-Coil craft:

<http://www.coilcraft.com/pdfs/0603hp.pdf>

Resistors-Panasonic:

<http://industrial.panasonic.com/www-data/pdf/AOA0000/AOA0000CE1.pdf>

Appendix B

Measurement

B.1 Vector Network Analyser

Description of the behaviour of the microwave network can be represented by Scattering parameters or S-parameters. The basic definition of S-parameters is a relation between incident wave (travelling towards network) and reflecting wave (travelling from the network) at one port. S-parameters can be measured with Vector Network Analyser (VNA) [40], Fig B.1.



FigureB.1-Vector Network Analyser

The VNA generates and applies a sinusoidal signal to the Device Under Test (DUT), and measure response of the DUT. VNA calculates S-parameters by measuring amplitude and phase of the wave quantities [113].

B.2 Spectrum Analyser

The PA measurement setup is shown in Fig. B.2. The signal generator has been used to produce input RF signal. This device can generate the signal maximum of 10dBm. This level of signal is not sufficient for switch-mode PAs. A pre-amplifier which is a linear and high gain PA has been used between the signal generator and a main PA to provide the sufficient input RF signal. Spectrum analyser has been used to measure the output response of the PA. Spectrum analyser, Fig B.3, measures the amplitude of electrical signals in the frequency domain [114]. An attenuator is applied between the output of the PA and input of spectrum analyser as the PA's output is higher than the maximum permissible input of the spectrum analyser.

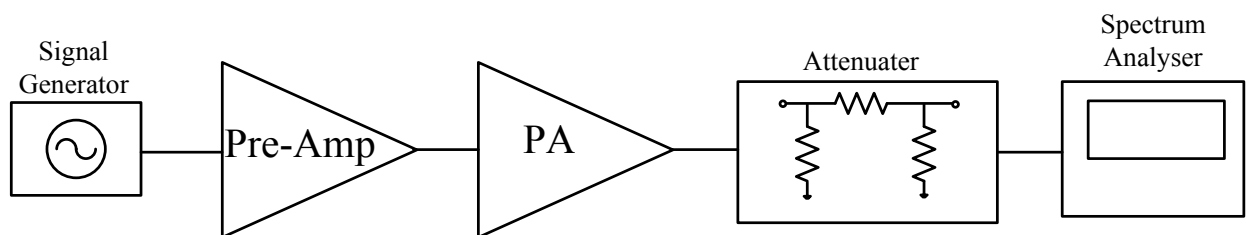


Figure B.2-Measurement Setup



Figure B.3-Spectrum Analyser

Appendix C

Paper 1

“Analytical Solution for Switched Band Matching Networks”

F.Norouzian and P.Gardner

3rd Annual IET Seminar on Passive RF and Microwave Components, 2012

Analytical Solution for Switched Band Matching Networks

Norouzian, F. and Gardner, P.
School of Electronic, Electrical and Computer Engineering
University of Birmingham
Birmingham, UK
FXN837@bham.ac.uk

Abstract — In this paper, an analytical solution is presented for a dual band switched matching network. By means of a detachable stub it provides the required matching impedances for different frequencies. The analytical solution enables an investigation of range of frequencies and impedances achievable. This solution provides values for the lengths of the transmission lines and stubs to give more precise results and shorten the design stage. The solution is tested analytically and shown to work for several different ranges of frequencies and impedances. Based on this solution, an example switched matching network is designed, fabricated and tested. This analytical solution can be applied to the design of switched band matching networks for many applications (e.g. PAs, LNAs, Antennas etc).

Keywords — Analytical model, dual band, impedance matching, Transmission lines

I. INTRODUCTION

The significant increase in demand for wireless communication systems and the proliferation of communication standards has created interest in more efficient ways of sharing the spectrum in the last few years. Software Defined Radio (SDR) provides an adaptable technology with the potential to improve use of spectrum holes efficiently. At RF and microwave component level, one of the resulting challenges is the design of multiband matching networks (MN). In [1], a technique for dual band MN was introduced using an output-matching to provide first frequency and a shunted switchable stub to produce second frequency. The same technique was used in [2] and [3] with additional stubs to provide three bands of operation. In [4] and [5], the designers tried to make the transmission line shorter and compact the circuits even more. This aim was achieved by implementing a reconfigurable stub for the first matching network consisting of two stubs and a transmission line between them, and a series of transmission lines with switches. However there is a trade off between compactness and extra insertion loss in the MN due to number of switches.

The MNs mentioned above provide a promising approach for multiband problems, but there are issues about the achievable frequency ranges. To address this

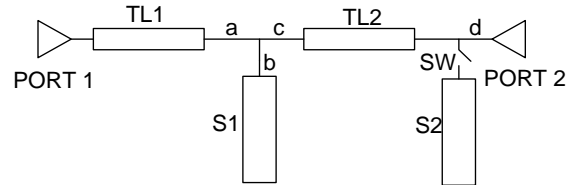


Fig. 1. Detached stub matching network

issue, an analytical solution is required. Furthermore, such a solution will help circuit designers to arrive at optimum multiband MNs in a shorter time.

The present paper is divided into three sections. Equations to design dual band MN are proposed in section II, followed by numerical examples and performance obtained by simulation in the next section. An experimental example based on the derived analytical solution, is discussed in section IV along with measurement results.

II. ANALYTICAL SOLUTION

The employed MN is based on the concept which is used in [1]. The first stub is fixed and the second one is connected by a switch. With the switch OFF, the MN provides a required impedance at the first required frequency (f_1) and in ON state of the switch, the desired impedance at the second frequency (f_2) is met.

The analytical solution is derived from MN shown in Fig. 1. The equations are derived for ideal and physical transmission lines with effective dielectric constant (ϵ_r).

A. Ideal Transmission line

The ideal transmission line is utilised to prove the possibility of using analytical solution. The whole idea of this method is to match by aid of a designated transmission line and a stub for each frequency. The transmission line TL1 of length l provides $Y_0 + jB$ at point a and jB is eliminated by introducing the susceptance of an open stub, equal to $-jB$ by S1. The required impedance looking into TL1 at port 1 at the

first frequency is Z_{L1} and defined as $R_{L1} + jX_{L1}$. At point a, admittance (Y_1) can be written as:

$$Y_1 = Y_0 \frac{Z_0 - X_{L1} \tan \theta_{L1} + jR_{L1} \tan \theta_{L1}}{R_{L1} + j(X_{L1} + Z_0 \tan \theta_{L1})} \quad (1)$$

where Z_0 and θ_{L1} are the characteristic impedance and the electrical length of TL1, respectively.

Splitting Y_1 into real part and imaginary part yields (2) and (3) respectively.

$$Re(Y_1) = \frac{R_{L1}(1 + \tan^2 \theta_{L1})}{R_{L1}^2 + (-X_{L1} + Z_0 \tan \theta_{L1})^2} \quad (2)$$

$$Im(Y_1) = \frac{R_{L1}^2 \tan \theta_{L1} - (Z_0 + X_{L1} \tan \theta_{L1})(-X_{L1} + Z_0 \tan \theta_{L1})}{Z_0 [R_{L1}^2 + (-X_{L1} + Z_0 \tan \theta_{L1})^2]} \quad (3)$$

Given that the real part of Y_1 is equal to the characteristic admittance of the system, Y_0 , the electrical length of the transmission line can be obtained by the following equation.

$$\theta_{L1} = \tan^{-1} \left(\frac{-X_{L1} - \sqrt{R_{L1} [(Z_0 - R_{L1})^2 + X_{L1}^2] / Z_0}}{R_{L1} - Z_0} \right) \quad (4)$$

By substituting θ_{L1} value back into (3), the susceptance part of Y_1 , B , can be obtained. The value of B can be eliminated by the open stub $S1$. The admittance at b in Fig. 1 is $jY_0 \tan \theta_{S1}$ and should be equal to $-jB$. So the electrical length of the stub can be calculated by

$$\theta_{S1} = -\tan^{-1} \left(\frac{B}{Y_0} \right) \quad (5)$$

To provide the desired impedance $Z_{L2} = R_{L2} + jX_{L2}$ at f_2 , the second stub is introduced into the circuit by turning the switch ON. To calculate the length of the second transmission line and stub (TL2 and S2 respectively), the admittance at c (Y_3) is calculated by (6).

$$Y_3 = \frac{Z_0 + X_{L2} \tan(\theta'_{L1}) + jR_{L2} \tan(\theta'_{L1})}{R_{L2} + j(Z_0 \tan(\theta'_{L1}) - X_{L2})} + jY_0 \tan(\theta'_{S1}) \quad (6)$$

The physical length of TL_1 and S_1 are fixed but their electrical lengths vary as the frequency changes; therefore, θ'_{L1} and θ'_{S1} are introduced which are electrical length of first transmission line and stub at f_2 , respectively. Following the same procedure by applying

$1/Y_3$ instead of Z_{L1}^* , we can calculate the electrical lengths of TL_2 and S_2 .

The derived analytical solution is applicable for multiband MNs. This can be done by adding additional switched stubs, position relative to S_1 , by repeated application of (6) and back to (3)-(5).

B. Physical Transmission line

For practical applications, the above introduced algorithm needs to be implemented in a physical transmission line medium such as microstrip. To find the lengths of transmission lines in microstrip, the physical lengths need to be divided by $\sqrt{\epsilon_e}$ yielding (7) where ϵ_e denotes effective dielectric constant.

$$l = \frac{\theta \cdot c}{\sqrt{\epsilon_e} 2\pi f} \quad (7)$$

III. NUMERICAL EXAMPLES

To verify the presented approach, the equations have been applied to several different numerical values in different ranges of frequencies and one of them is presented in this section. A Gallium Nitride (GaN) HEMT from Nitronex is chosen as an example. Two different frequencies are selected and appropriate impedances are obtained from load pull information in the device datasheet. The required impedances are $0.49 + j0.366$ and $1.052 + j0.456$ at 1800 and 900 MHz, respectively. The MN has been designed so that the required impedance for the higher frequency is provided by the OFF state of the switch, since the amount of loss in switch in its ON state increases at higher frequency. Similar to previous section, appropriate lengths for the transmission lines and stubs are calculated in two different versions, ideal and physical transmission lines.

A. Ideal Transmission line

Using (3-5) the value of B , θ_{L1} and θ_{S1} are calculated respectively. In next step Y_3 is obtained using (6). Using the same procedure θ_{L2} and θ_{S2} are calculated. These results are used in the simulations and the simulation outputs are shown Fig. 2 (a), confirming good agreement with the required impedances taken from the device datasheet.

In the first frequency, one transmission line and one stub is used to match to the required impedance. The second desired impedance is converted to Y_3 at point c in

Fig. 1. The second line and stub parameters are calculated to transform Y_3 at the second frequency to Y_0 at points c and d, respectively. No further iteration of the first line and stub are required to achieve this. The presented method proves that there is no forbidden region to match any dual frequencies by this MN, because whatever the value of Y_3 , it can, in principle, be matched using a single line and stub.

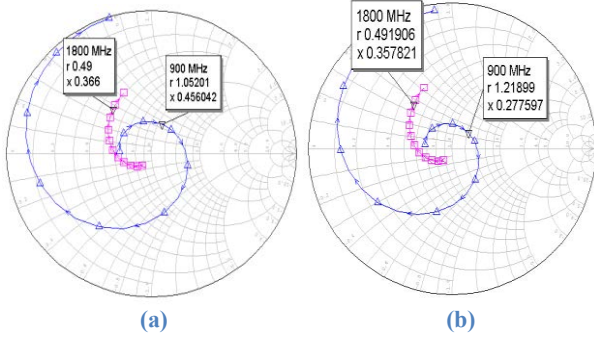


Fig. 2. Simulation result (a) ideal transmission line (b) physical transmission line

B. Physical Transmission line

The electrical lengths of the transmission lines in this case are evaluated as before and their physical lengths are found by use of (7). Fig. 2(b) shows the simulation results based on the calculated lengths.

The results show a perfect match at 1800MHz and a reasonably close match at 900MHz. The reason for the difference observed in second frequency is the discontinuity of the T-junction. One solution to resolve this issue is to optimize the MN to compensate the discontinuity effect of the T-junction. Taking into account the discontinuity and fine tuning the simulation will give the result presented in Fig. 3 that shows good agreement at 900 MHz.

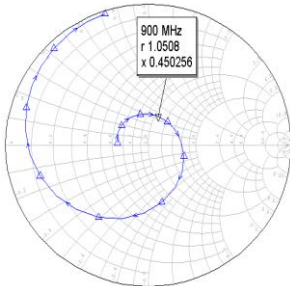


Fig. 3. Simulation result after adjustments

VI. EXPERIMENTAL

The MN based on the calculation in the last part was built, to prove the validation of the algorithm. It was fabricated on microstrip substrate of thickness of 0.76 mm and relative dielectric constant of 3.5. A PIN diode was used as the switch because of its advantages such as low insertion loss, high isolation, high switching speed and excellent power handling at microwave frequencies [6]. The PIN diode was type BAR50 from Infineon.

The simulation and measurement results are compared and plotted by their magnitude (Fig. 4) and on the Smith Chart (Fig. 5). The markers on Fig. 5 ((a) and (b)) indicate the reflection coefficient at the intended frequencies for the ON and OFF state (1800 and 900 MHz, respectively). Both graphs are shown good agreement between simulation and measurement. The small differences are due to real components and their tolerances.

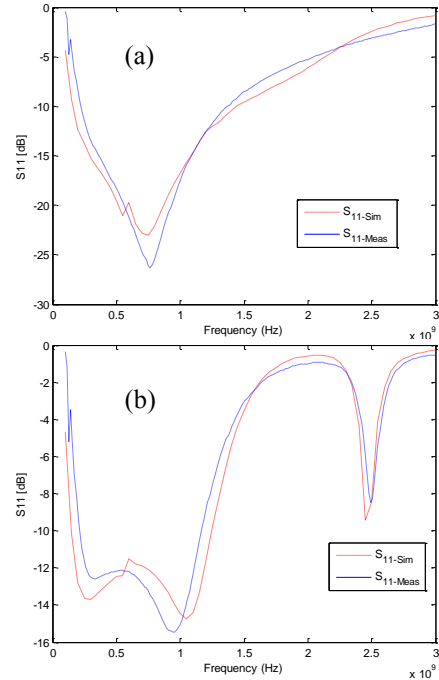


Fig. 4. Simulated and measured S11 in (a) OFF and (b) ON state

V. CONCLUSION

In this contribution, for the first time, the feasibility of multiband MNs for different frequencies, by aid of derived equation, has been shown. The proposed theoretical approach, based on the detached stub MN, provides a closed-form and recursive solution to design dual-band MNs precisely, given any two frequencies. Furthermore this method can be applied not only for two

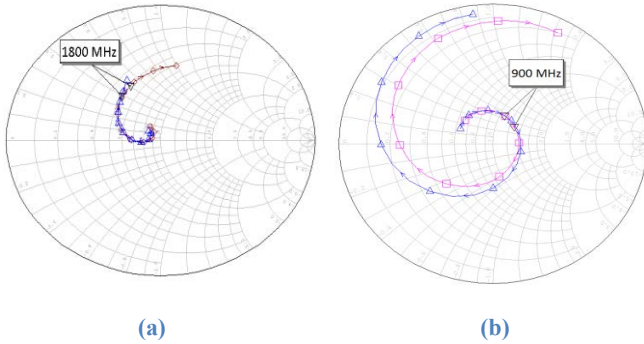


Fig. 5. Simulated and measured input impedance of MN (a) OFF state and (b) On state

but for several band MNs. Numerical and experimental results have been presented by this work and the results were compared to prove the validity of the algorithm. The presented MNs and derived algorithm could be applied to a wide range of multiband components, such as antennas, LNAs and PAs. These promising results encourage further research on designing multiband MNs that take account of harmonic termination requirements, which are important in power amplifier applications. Investigation of nonlinearity caused by a PIN diode is also a matter of interest.

VI. REFERENCE

- [1] A. Fukuda, H. Okazaki, T. Hirota and Y. Yamao, "Novel 900 MHz/1.9 GHz Dual-Mode Power Amplifier Employing MEMS Switches for Optimum Matching", *IEEE Microwave and Wireless Components Letters*, vol.14, no.3, pp. 121-123, March 2004.
- [2] A. Fukuda, H. Okazaki, S. Narahashi, T. Hirota and Y. Yamao, "A 900/1500/200-MHz Triple-Band Reconfigurable Power Amplifier Employing RF-MEMS Switches", *IEEE*, pp. 657-660, 2005.
- [3] H. M. Nemat, J. Grahn and C. Fager, "Band-Reconfigurable LDMOS Power Amplifier", in *40th European Microwave Conference*, 2010, pp.978-981.
- [4] A. Fukuda, H. Okazaki and S. Narahashi, "A Novel Compact Reconfigurable Quad-band Power Amplifier Employing RF-MEMS switches", in *36th European Microwave Conference*, 2006, pp. 344-346.
- [5] A. Fukuda, T. Furuta, H. Okazaki, S. Narahashi, "A 0.9-5-GHz Wide-Range 1 W-Class Reconfigurable Power Amplifier Employing RF-MEMS Switches", *IEEE*, pp. 1859-1862, 2006.
- [6] M. Watertown, *The PIN Diode Circuit Designers' Handbook*, Massachusetts: Microsemi Corporation, 1998.

Paper 2

“Concurrent Dual-Band High Efficiency Class-E Power Amplifier”

F.Norouzian and P.Gardner

2013 European [Microwave Integrated Circuits Conference \(EuMIC\)](#),

Concurrent Dual-Band High Efficiency Class-E Power Amplifier

Fatemeh Norouzian

School of Electronic, Electrical and Computer Engineering
University of Birmingham
Birmingham, UK
FXN837@bham.ac.uk

Peter Gardner

School of Electronic, Electrical and Computer Engineering
University of Birmingham
Birmingham, UK
gardnerp@adf.bham.ac.uk

Abstract— In this paper, a concurrent dual-band class-E power amplifier is proposed. A distributed matching network is designed without any switch to achieve dual-mode operation. The power amplifier works in the 777-787 MHz and 1710-1785 MHz bands for LTE system. The measured results show 22 and 27 dBm output power at first and second band, respectively. This power amplifier obtains efficiency of 60% in lower bandwidth and 84.5 % in higher bandwidth. A novel matching network is also presented to switch between two different optimum operations for class-E design to improve the efficiency in the lower band.

Keywords—class-E; dual-band; high efficiency; power amplifier

I. INTRODUCTION

The significant increase in demand for wireless communication systems and the proliferation of communication standards has created interest in more efficient ways of sharing the spectrum in the last few years. Software Defined Radio (SDR) provides an adaptable technology with the potential to improve use of spectrum holes efficiently. The Power Amplifier (PA) is the most power consuming part in transmitters. Designing high efficiency multiband PAs is a critical research area.

Different multiband class-E PAs have been reported. Some of their features are summarized in table 1, [1]-[6]. Composite right/left-handed transmission lines (CRLH TLs) are used in [1] to provide dual-band amplification. In [2], MEMS are used to switch between two frequencies. A quad-band class-E PA is proposed in [3] which consists of four transistors and a single input/output matching network (MN). It works in one of the frequency bands at a time and is switched between bands by controlling the gate bias. Sub-optimum class-E operation is assumed in [4] with element values evaluated for a compromise between two bands. A multi-level switching resistance model is incorporated to switch between two frequencies in [5]. A dual-band class-E with finite DC-feed inductance is presented in [6]. A switch is applied to achieve optimum performance in the selected band, while the inductors are constant.

Class-E has highly frequency dependent characteristics. Therefore, designing a dual-band class-E PA is challenging

Table 1. Multiband class-E PAs

Reference	Frequency band (GHz)	Output power (dBm)	Efficiency (%)	PAE (%)
[1]	0.836 /1.95	27	N.A	42
[2]	0.9/1.8	20	38/26	N.A
[3]	1.9/2.3/ 2.6/3.5	24.2/23.8/ 23.4/20.5	48/44/40/35	N.A
[4]	L-/S-band	30/28	61/42	50/30
[5]	1.95/2.6	29/28	N.A	65/63
[6]	1.7/2.5	27	N.A	57
This work	0.782/1.748	22/27	60/84.5	55/72

because optimum output matching and harmonic elimination have to be achieved in both bands at the same time with a single output matching network (OMN) to satisfy the required efficiency and output power in both operating bands. In this paper, a dual-band class-E PA with high efficiency in both bands is presented. This PA is designed without switches to minimize the number of components and reduce the losses introduced by switches. The effect of the shunt capacitor across the transistor on efficiency is studied and a switched band MN is proposed to enable the OMN to switch between two optimum modes and improve efficiency further.

II. DUAL-BAND CLASS-E POWER AMPLIFIER

The class-E PA was invented by Nathan and Alan Sokal in the 1970s [7]. The active device in class-E PA is operating as a switch; when the transistor is off, current flows through the shunt capacitance and in the on duration, current flows through the transistor. The OMN plays a crucial role in designing a highly efficient class-E PA. OMN includes a set of specific valued components at fundamental frequency to avoid any overlap between voltage and current waveforms; resulting in 100% efficiency, ideally. In practice some of the delivered power will appear in second and third harmonic frequencies. To maximize the efficiency, all harmonics should be open circuit. The transistor should be biased at pinch off and driven into compression, so the transistor will be on for the forward cycle of sinusoidal input RF waveform and for all of the reverse cycle the transistor is switched off.

The first stage of designing a class-E PA is to calculate optimum parameters of OMN. Equations (3) to (6), taken from [7], are applied to provide values of components (i.e. load resistance R , shunt capacitance C , series capacitance and

inductance, C_0 and L_0 respectively). These equations are derived from a time domain equation, according to required voltage and current assumption across the transistor, in OFF and On state, respectively, (1) and (2).

$$V_D(t)|_{t=T} = 0 \quad (1)$$

$$\frac{dV_D(t)}{dt}|_{t=T} = 0 \quad (2)$$

These components are calculated based on specific supply voltage V_D and required output power P_{out} . Loaded quality factor (Q_L) is a free choice variable and chosen by designers based on a tradeoff between operating bandwidth and rejection of harmonics. For having duty ratio of a usual choice, 50%, the minimum value of Q_L is 1.7879. The most desirable range to provide acceptable efficiency and linearity is between 5 and 10.

$$R = 0.5768 \left(\frac{V_D^2}{P_{out}} \right) \left(1 - \frac{0.451759}{Q_L} - \frac{0.402444}{Q_L^2} \right) \quad (3)$$

$$C = \frac{1}{5.44668\omega R} \left(1 + \frac{0.91424}{Q_L} - \frac{1.03175}{Q_L^2} \right) + \frac{0.6}{\omega^2 L_D} \quad (4)$$

$$C_0 = \frac{1}{\omega R} \left(\frac{1}{Q_L - 0.104823} \right) \left(1 + \frac{1.101468}{Q_L - 1.7879} \right) - \frac{0.2}{\omega^2 L_D} \quad (5)$$

$$L_0 = \frac{Q_L R}{\omega} \quad (6)$$

The dual-band class-E PA presented in this work is designed with a transmission line OMN based on two lumped element networks. Each lumped element network is designed to operate in one of the desired frequencies. As it is understandable from equations, the value of components will be different for each band of frequency, hence a simple lumped element matching network would require a switch. For that reason, a distributed OMN which works simultaneously in two different frequencies without switches has been proposed here to avoid losses of switch. Generally, transmission line MNs are preferred over using lumped elements as their practical implementation is more convenient and they have more reliable performances as well as less insertion loss. To fulfill the requirements of the two lumped element network using a single transmission line and stub, a required reflection coefficient has to be obtained from the two lumped element MN in the two operation frequency bands. A single transmission line and a single stub, tuned by width and length, have been used in the OMN to provide the same reflection coefficient as the lumped element networks at desired frequencies, Fig.1. Having only a single transmission line and a stub will enable working simultaneously in two frequencies and make the design more compact than substituting each component with their equivalent transmission line.

It has been shown that second harmonic termination is sufficient to have class-E performance to a reasonable approximation [8]. The second harmonic termination (HT)

is designed to behave as open circuit at drain of the transistor at both frequencies. The basic idea to terminate the harmonic frequencies is using a transmission line and

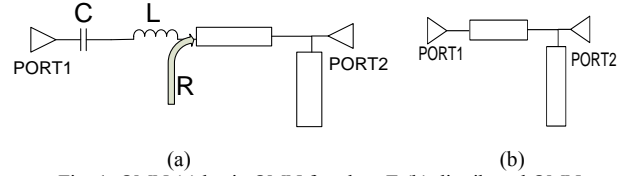


Fig. 1. OMN (a) basic OMN for class-E (b) distributed OMN

an open stub both with electrical length of $\lambda/4$, Fig. 2. Thus this block is composed of a transmission line and a stub which is $\lambda/4$ at the second harmonic of the higher frequency. To terminate the second harmonic of the lower frequency, a second $\lambda/4$ stub is required. Then another $\lambda/4$ transmission line is required to convert the short circuit to open circuit at port 1. This requirement is satisfied by the aid of the first transmission line, the first stub and an added transmission line (TL). By adjusting the length of TL, the cascaded line-stub-line combination can be made equivalent to an impedance inverter at that specific frequency. This harmonic termination circuit concept could be extended for terminating n harmonics with n transmission lines and stubs. The OMN and HT circuits are implemented together to provide the required performances for class-E operation.

The dual-band input matching network (IMN) is designed to have promising return loss in both desired bands.

III. SIMULATION AND MEASUREMENT

This dual-band PA is designed for the LTE system to cover two bands, 777-787 MHz and 1710-1785 MHz and output power of 23 dBm in both bands.

A. Simulation

Components are calculated for both bands, based on desired output power and voltage supply (Q_L set as 10). The calculated values are illustrated in table 2. A transmission line and stub are used to transform the 50Ω impedance of the transmitting antenna to the calculated load impedance, 62.45Ω . Then calculated capacitance and inductance for both bands are simulated to find out their reflection coefficient at the required frequencies to be used in designing the equivalent distributed version, Fig. 3.

In order to design this OMN practically, termination of the second harmonic frequencies is considered. Thus, the introduced HT circuit aims to provide open circuit at second harmonic frequencies of operating frequencies, 782 and 1748 MHz. The designed HT circuit is implemented with OMN. IMN is modeled to provide reasonable match at both frequency bands, by the aid of a transmission line and two stubs.

Table 2. Calculated components for both bands

	R	C	C_0	L_0
First band	62.45 Ω	0.6 pF	0.4 pF	127 nH
Second band	62.45 Ω	0.3 pF	0.2 pF	56 nH

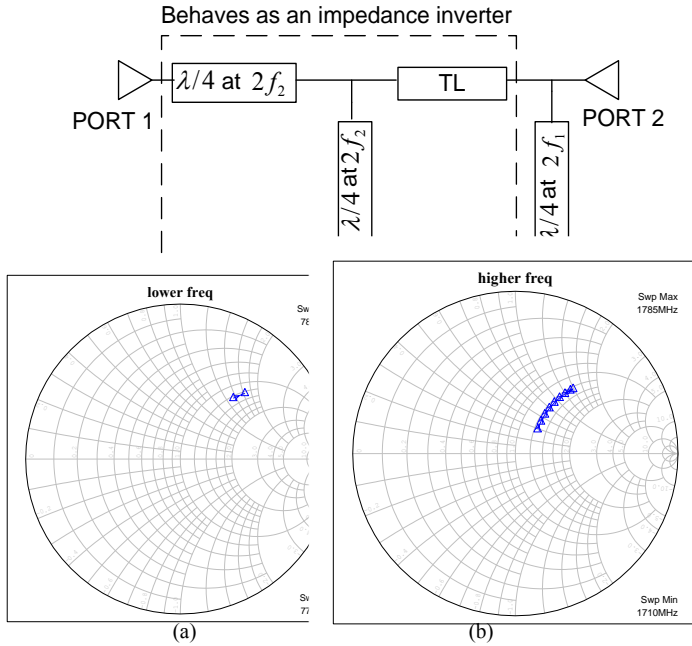


Fig. 3. Load reflection coefficient data for OMN in (a) first band and (b) second band

B. Measurement

To verify this method, the PA is fabricated on a microstrip substrate with thickness of 0.76 mm and relative dielectric constant of 3.5 using a HFET from TriQuint as a power device. Fig. 4 shows the image of the manufactured PA. In class-E operation, the transistor should be biased close to pinch off and driven into compression. To find the desired gate voltage and RF input power, to make the transistor switch, a few measurements are required. The pinch off value was obtained from the device datasheet which is -2.1v. Then, the PA was driven with different input RF power to find the required input power to make the performance of the PA independent of gate voltage. Input power more than 10 dBm is appropriate for both bands.

The PA performance using the obtained parameters from the above measurements is presented in table 3 in terms of output power and efficiency. Fig. 5 shows efficiency and output power of the PA with varying input power in both bands. In the higher band, efficiency of 94% at 18 dBm input power is obtained. In the case of operating the PA as a concurrent dual-band PA, both bands should be driven with the same input power. In table 3, the power and efficiency figures given are for 16 dBm input power. The obtained efficiency is the highest reported efficiency for dual-band class-E with such a big difference of frequency bands.

Table 3. PA performance

	Output Power	Drain Efficiency	PAE
First band	22 dBm	60 %	55 %
Second band	27 dBm	84.5 %	72.6 %

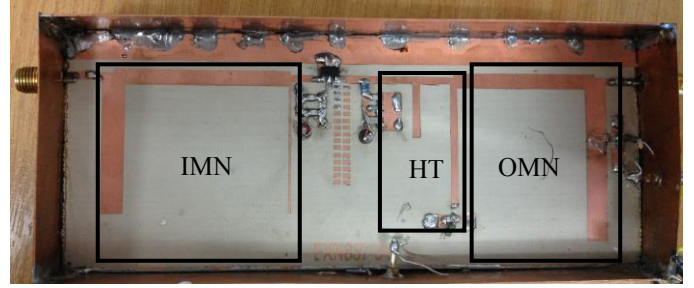


Fig. 4. Fabricated prototype of dual-band class-E PA

C. Discussion

This design has demonstrated that having a concurrent dual-band class-E PA in two different and widely separated bands is feasible at the cost of having a lower efficiency in one of the band. The measurements show higher efficiency at the higher band of frequency and more output power. Although the efficiency of the lower working frequency is good among reported efficiencies, the big gap introduced between efficiencies of two working frequency bands is due to the required shunt capacitor across the transistor. The value of shunt capacitor across the transistor is an important component to produce desired efficiency and output power and its ideal value is different for different frequencies. In the higher band, the required shunt capacitance is calculated to be 0.3 pF and internal capacitance of transistor is close to 0.3 pF which fulfills the required capacitance. To have the same performance in lower band, a shunt capacitance of 0.6 pF is required. Setting the value of capacitance close to one of the operation frequencies using a shunt capacitor will yield a high performance in that particular frequency and relatively lower performance in the other frequency. One option could be using a capacitance in between which would degrade the performance of both bands from their ideal result. Therefore, to have high efficiency in both bands, it is required to have different shunt capacitance which could be done using a switch. This option is explored further in the next section.

IV. SWITCHED-BAND MATCHING NETWORK

A switched-band OMN is proposed to design a switched-band class-E PA with high efficiency in both bands. In dual-band OMN case, a transmission line and a stub are used to provide desired performance at both bands. Performance will be improved by applying a switch to have more accurate result. The OMN is proposed in this work called Stub to Short switching (STS), which is composed of one transmission line and one stub and utilizes a switch somewhere in the middle of the stub to connect it to the ground, Fig.6. Placing the switch between stub and ground to open or short the stubs can provide different impedances in different operating frequencies and help to minimize losses which are introduced by the switch. When the switch is ON, the stub is shorter and is grounded. The longer and open stub is provided in the OFF state of the switch. Typically, the higher frequency needs a shorter stub than the lower frequency; therefore ON state of the switch is applied at higher frequency. As a result, there is a

better match between lumped element and distributed OMN. Simulation and measurement results are plotted in the Smith chart in Fig. 7 in lower and higher band of operation.

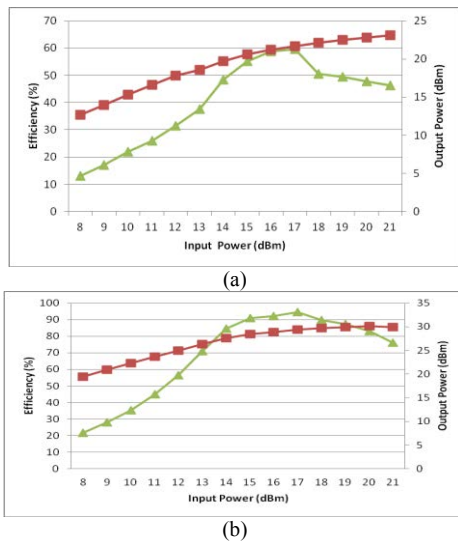


Fig. 5. Measured efficiency and output power vs input power for concurrent design. (a) first band (b) second band

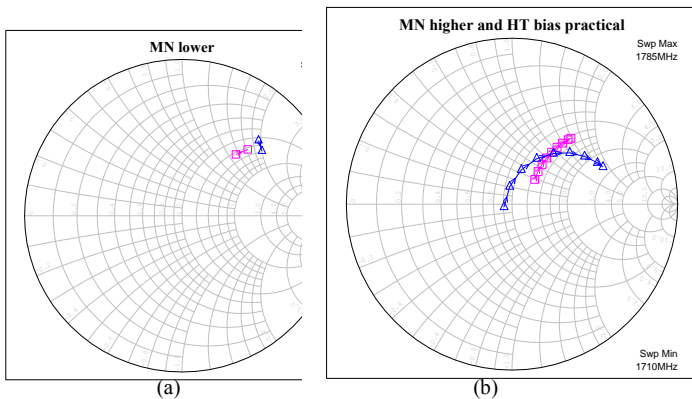
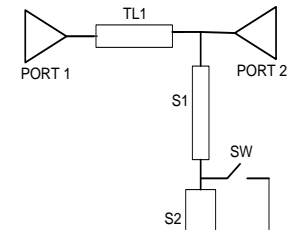


Fig. 7. Simulation and measurement result of switched-band OMN (a) lower band (b) higher band of operation

The PA design shows that to achieve a high efficiency in both bands, the shunt capacitor across the transistor also has to be variable. To make this possible, two switching capacitance methods are presented here. In most cases the internal capacitance of the transistor is high enough. In this case for lower band, another 0.3 pF needs to be connected to the transistor. Fig. 8 (a) illustrates the first method. When the switch is ON, a stub is introduced to the circuit and provides shunt capacitance of 0.3 pF. Appropriate length and width are chosen for the stub to provide the required capacitance. In

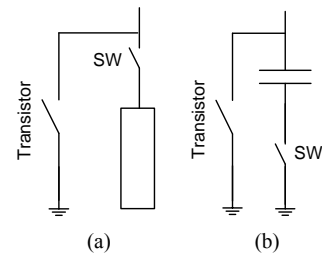


Fig. 8. Proposed method for shunt capacitance (a) with a stub (b) with a capacitor

higher frequency, the switch is OFF but it leaves a small residual capacitance of about 0.007 pF, resulting from the series combination of the switch in its OFF state and the stub. Method 2 uses a capacitor with a switch to ground, Fig. 8 (b).

V. CONCLUSION

A concurrent dual-band class-E PA is presented in this paper to operate in up-link band of LTE system. Dual-band transmission line OMN is applied to achieve amplification in both bands without any switches, with high drain efficiency of 60% and 84.5% and output power of 22 and 27 dBm at 777-787 and 1718-1785 MHz, respectively. The proposed OMN is based on tuning of the characteristic impedance and electrical length of transmission line and stub. The high efficiency of this PA encourages further study on the effect of shunt capacitance on the efficiency of class-E operation. The novel switched-band OMN is presented and fabricated to improve the efficiency. In future work, a switched-band class-E PA based on the proposed OMN will be designed.

ACKNOWLEDGMENT

The authors thank Mr. A. Yates, technician at EECE, the University of Birmingham for his practical support.

REFERENCES

- [1] S.H.Ji, C.S.Cho, J.W.Lee, J.Kim, "Concurrent Dual-Band Class-E Power Amplifier Using Composite Right/Left-Handed Transmission Lines", *IEEE Transactions on Microwave Theory and Techniques*, vol. 55, no. 6, pp. 1341-1374, June 2007.
- [2] L. Larcher, R. Brama, M. Ganzerli, J. Iannacci, B. Margesin, M. Bedani, A. Gnudi, "A MEMS Reconfigurable Quad-Band Class-E Power Amplifier for GSM Standard", *IEEE*, pp.864-867, 2009.
- [3] K.Y.Kim, W.Y.Kim, H.S.Son, I.Y.Oh, C.S.Park, "A Reconfigurable Quad-Band CMOS Class-E Power Amplifier for Mobile and Wireless Applications", *IEEE Microwave and Wireless Components Letters*, vol. 21, no. 7, pp. 380-382, July 2011.
- [4] R.Zhang, M.Acar, M.Apostolidou, M.P.Heijden, D.M.W.Lenaerts, "Concurrent L- and S-Band Class-E Power Amplifier in 65nm CMOS", *IEEE Radio Frequency Integrated Circuits Symposium*, pp. 217-220, 2012.
- [5] Y.C.Lin, C.T.Chen, T.S.Hornng, "high Efficiency Dual-Band Class-E Power Amplifier Design", *APMC*, pp.355-357, DEC 2012.
- [6] D.Kalim, A.Fatemi, R.Negra, "Dual-Band 1.7GHz/2.5GHz Class-E Power Amplifier in 130nm CMOS Technology", *IEEE*, pp. 473-476, 2012.
- [7] N.O. Sokal, "Class-E RF Power Amplifiers", *QEX*, Jan/Feb 2001, pp.9-19.
- [8] T.B. Mader and Z. Popovic, "The Transmission-Line High-Efficiency Class-E Amplifier", *IEEE Microwave Guided Wave Letter*, vol. 5, no. 9, pp.290-292, Sep. 1995.